The Role of CD44 in the Induction of Myeloid-Derived Suppressor Cells by Hepatic Stellate Cells

Dissertation

zur Erlangung des akademischen Grades eines

Doktors der Medizin (Dr. med.)

an der

Medizinischen Fakultät der Universität Hamburg.

vorgelegt von

Simon Christian Burkhardt

aus

Pforzheim

2025

Betreuerin/Gutachterin der Dissertation: Prof. Dr. Linda Diehl

Gutachterin der Dissertation: Prof. Dr. Sabine Windhorst

Vorsitz der Prüfungskommission: Prof. Dr. Sabine Windhorst
Mitglied der Prüfungskommission: PD Dr. Katrin Neumann
Mitglied der Prüfungskommission: Prof. Dr. Johannes Herkel

Datum der mündlichen Prüfung: 23.04.2026

CONTENTS

1 INTRODUCTION

1.1 Myeloid-Derived Suppressor Cells

1.1.1 Introduction

The term "myeloid-derived suppressor cells" (MDSC) was introduced about 20 years ago, labeling the emerging heterogeneous discoveries of myeloid cells that displayed immunosuppressive functions (Gabrilovich et al. 2007). Early discoveries linked to our current understanding of MDSC were made three to four decades ago in murine models of cancer (Tamadaho et al. 2018). MDSC were linked to poorer prognosis and tumor progression and therefore became more and more fundamental to understanding the tumor microenvironment (Talmadge & Gabrilovich 2013). Since then, they emerged as universal regulators of the immune system in various pathological conditions, such as cancer, infections, traumata, sepsis and autoimmune disorders. Today, MDSC are defined as a heterogeneous group of myeloid cell progenitors and precursors, that can exert immunosuppressive functions (Nepal et al. 2024; Veglia, Perego & Gabrilovich 2018a; Hsieh et al. 2019). In the liver, they exert key functions - proinflammatory and antiinflammatory - in various pathological states, such as hepatitis B and C, autoimmune liver disease, non-alcoholic fatty liver disease (NAFLD), liver fibrosis and liver cancer (Q. Sun et al. 2023). MDSC came to the forefront of therapeutic research not only limited to cancer. For instance, targeting MDSC for therapeutic strategies in AIDS and tuberculosis is subject of recent research (Dorhoi & Plessis 2018; Fleming et al. 2018). MDSC-targeting therapies, e.g. signal transducer and activator of transcription 3 (STAT3) inhibitors may provide new treatments for liver diseases. Given the complex nature of MDSC, refining comprehension of MDSC biology is fundamental to new perceptions of various pathologies as well as providing targets for improved future clinical management of global health burdens (Q. Sun et al. 2023).

1.1.2 Phenotyping Myeloid-Derived Suppressor Cells

MDSC share morphological and phenotypical features with neutrophils and monocytes, which makes identifying MDSC still a challenging algorithm. Moreover, MDSC phenotypes differ according to the microenvironment, anatomical location and type of pathological condition, in which they expand (Tamadaho et al. 2018; Brandau et al. 2016). Despite the increasing relevance of MDSC, there is still a lack of harmonized specific surface markers, so valid identification of MDSC still relies on a consecutive proof of their immunosuppressive traits in suppression assays (Mandruzzato et al. 2015; Veglia, Perego & Gabrilovich 2018b).

Moreover, MDSC subsets differ in mice and man. Originally, murine MDSC were identified using co-expression of CD11b and Gr-1. Since 20-30% of normal murine bone marrow cells bear this phenotype but only 2-4% of them were suppressive, it became clear that these markers display a vast heterogenicity and uncertainty, unsuitable for proper identification. Anti-Gr-1 antibodies bind to two separated epitopes, namely Ly6C and Ly6G, that opened up a more detailed description of MDSC. $CD11b^+$ cells were further divided into either monocytic (mMDSC) or granulocytic/polymorphonuclear (gMDSC) according to their expression pattern of Ly6C and Ly6G, referring to their precursors and myeloid lineages (Tamadaho et al. 2018; Brandau et al. 2016; Lim et al. 2020). mMDSC and gMDSC differ distinctively on a molecular level as well as in their origin, morphology and suppressive functions (see 1.1.3 and 1.1.4). Phenotyping human MDSC is further complicated by the fact that Gr-1 is not expressed on human myeloid cells. Therefore, naming human MDSC is based on a different approach. As in mice, there are two major classes of human MDSC, $CD14^+$ monocytic (mMDSC) and $CD15^+$ polymorphonuclear/granulocytic MDSC (gMDSC). Additionally, an early-stage lineage marker negative (Lin^-) immature MDSC (iMDSC) phenotype was described, where Lin comprises CD3, CD14, CD15, CD19 and CD56 (Veglia, Perego & Gabrilovich 2018b). Human MDSC either do not express or downregulate surface HLA-DR during development, which is an essential hallmark of their immature phenotype and deployed for identification. Common myeloid markers like CD33 and CD11b are generally expressed by human MDSC. There are additional markers, that are not part of the common definition but help to facilitate the distinction towards other cell types. For instance, dendritic cell–specific intercellular adhesion molecule-3-grabbing non-integrin (DC-SIGN) is used to discriminate immature dendritic cells from mMDSC (Obermajer & Kalinski 2018; An et al. 2018).

For both, murine and human MDSC many markers were described, but none of them displayed the necessary specificity or were linked to certain experimental settings only. Therefore, proposed minimal characteristics of MDSC with an adequate amount of specificity are commonly used today to facilitate comparability of MDSC research (Tamadaho et al. 2018; Brandau et al. 2016; Mandruzzato et al. 2015).

Taken together, murine gMDSC are phenotyped as $CD11b^{+}Ly6G^{+}Ly6C^{lo}$ cells, whilst mMDSC have a $CD11b^{+}Ly6G^{-}Ly6C^{hi}$ phenotype (Illustration 1). The three human MDSC subsets are phenotyped as $CD15^{+}HLA\text{-}DR^{-/lo}$ gMDSC, $CD14^{+}HLA\text{-}DR^{-/lo}$ mMDSC and $Lin^{-}HLA\text{-}DR^{-/lo}$ iMDSC (Brandau et al. 2016; Hoechst et al. 2013; Lim et al. 2020).

Illustration 1: Phenotypes of mMDSC and gMDSC in Mice and Humans
In mice, MDSC express CD11b and are subdivided based on their expression patterns of Ly6C and Ly6G. Human MDSC downregulate HLA-DR and are phenotyped by their expression of either CD14 or CD15. An additional lineage-negative ($CD14^{-}$ and $CD15^{-}$) immature subtype exists in humans (not shown). There are additional facultative markers of MDSC in both mice and humans; however, the markers presented here are the most commonly used and form the basis of the classification applied in this work.

1.1.3 Biology and Functions of Myeloid-Derived Suppressor Cells

The source of MDSC are immature myeloid cells that ultimately originate from the bone marrow. Hematopoietic stem cells give rise to myeloid progenitors and precursors that eventually migrate to lymphoid tissue, the spleen or sites of infection and disease, where they rapidly differentiate into mature granulocytes, dendritic cells and macrophages. After successfully resolving inflammational triggers and pathogens, the balance of myeloid cells is restored to steady state (Kumar et al. 2016; Lim et al. 2020). Classical activation of myeloid cells by toll-like receptor (TLR) ligands, pathogen-associated molecular patterns (PAMPs) and damage-associated molecular pattern (DAMPs) leads to rapid mobilization, increase of proinflammatory cytokines, respiratory bursts, MHC II upregulation and phagocytosis (Illustration 2). While this acute immunological response is usually of short duration and driven by relatively strong signals, unresolved chronic inflammation is characterized by relatively weak but persistent signaling (Shi & Pamer 2011; Umansky et al. 2016; Veglia, Perego & Gabrilovich 2018b). Sustained inflammatory states present in chronic infections, cancer, autoimmune diseases and trauma lead to a partial block of myeloid maturation and expansion of MDSC (Illustration 2). This deviant myeloid activation program is characterized by expansion of immature phenotypes, low phagocytosis, production of anti-inflammatory cytokines and low MHCII expression levels. Ultimately, this state favors inhibition of host defense mechanisms instead of elimination of the actual threat. In a healthy steady state MDSC are usually not detectable, but in chronic inflammation they expand and correlate with disease severity as well as lower survival rates (Hsieh et al. 2019; Veglia, Perego & Gabrilovich 2018b; Brandau et al. 2016).

Differentiation, Expansion & Recruitment of MDSC

The precise development of MDSC from hematopoietic stem cells remain unclear but is proposed to be governed by two general signals driving initial expansion and then activation of their suppressive traits. Factors of expansion and accumulation of MDSC coincide with the ones of normal myelopoiesis. STAT3 is considered to be a master transcription factor of the MDSC expansion pathway, since most of the pathways mentioned below converge on it (Dysthe & Parihar 2020). GM-CSF was repeatedly shown to be the main driver of MDSC expansion *in vitro* and *in vivo* (Gabrilovich & Nagaraj 2009; Lechner et al. 2010; Obermajer & Kalinski 2018). The key role of GM-CSF is among rather early findings of MDSC research as immature dendritic cells

generated using low-dose GM-CSF were found to facilitate allograft protection *in vivo* (Lutz et al. 2000). Immunosuppressive effects were found to be dose-dependent in clinical trials using GM-CSF as cancer vaccination adjuvant (Parmiani et al. 2007). Also, GM-CSF signaling blockade contributes to inhibition of MDSC function *in vitro* and locally applied anti-GM-CSF antibodies, or knockdown of the GM-CSF gene, prevented tumor growth and reduced MDSC infiltration (Gargett et al. 2018). For *in vitro* generation of murine and human MDSC, usually a combination of GM-CSF and

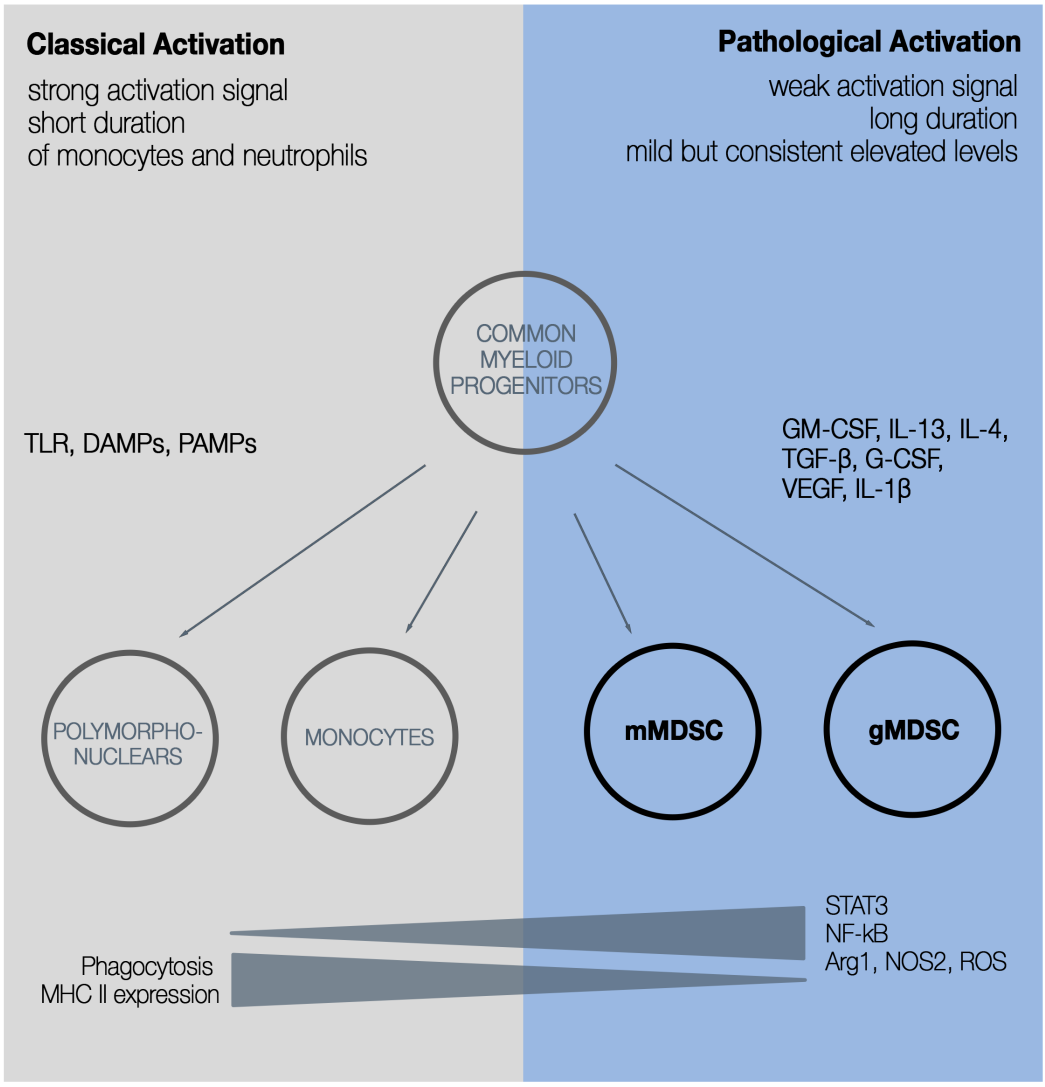

Illustration 2: Expansion of Myeloid-Derived Suppressor Cells (MDSC)
The nature of the immunological stimulus determines whether common myeloid progenitors differentiate into pro-inflammatory monocytes and polymorphonuclear cells, or into immunosuppressive MDSC. Classical activation involves a strong but short-lived activating stimulus, while pathological activation driving MDSC expansion, relies on weak but prolonged stimuli, associated with immunosuppessive effectors & transcription factors. Danger- or pathogen-associated molecular patterns (DAMPs/PAMPs) and TLR signaling are strong inducers of classical activation increasing phagocytosis functions and MHC II expressions. GM-CSF, IL-13, IL-4, TGF-β, G-CSF, VEGF, and IL-1β are key mediators in the pathological activation model. g/m-MDSC: granulocytic/monocytic MDSC.

cytokines, also associated with MDSC expansion, are used (Lechner et al. 2010; Highfill et al. 2010). Interleukin-4 receptor α (IL-4Rα) is a common biomarker for immunosuppressive MDSC and serves as receptor for IL-13. GM-CSF combined with IL-13 or IL-4 facilitates MDSC development from murine BMC and human peripheral blood monocytes (PBMC) respectively (Highfill et al. 2010; Heine et al. 2017; Obermajer & Kalinski 2018). TGF-β is deeply involved in mediating MDSC suppression mechanisms, but has also been shown to effectively expand MDSC *in vitro* when combined with GM-CSF (Casacuberta Serra et al. 2017; C.-R. Lee et al. 2018). TGF-β increases the proportion of mMDSC at the expense of gMDSC. While mMDSC require GM-CSF for accumulation, gMDSC are preferentially influenced by G-CSF (Tamadaho et al. 2018; C.-R. Lee et al. 2018). Some studies demonstrated that GM-CSF treatment solely is sufficient for generating MDSC from murine BMC and human PBMC (Greifenberg et al. 2009; Lechner et al. 2010). Furthermore, vascular endothelial growth factor (VEGF), a key mediator of angiogenesis and expressed by many cancer types, was identified as potent MDSC expander *in vivo* and *in vitro* (Lechner et al. 2010; Dysthe & Parihar 2020). Certain chemokines, like CCL2, CCL3, CXCL2, CXCL4 and CXCL12, are part of the recruitment mechanisms, attracting MDSC to inflammation and tumor sites (Dolcetti et al. 2010; Tcyganov et al. 2018). The presence of specific chemokines also affects the MDSC phenotype that is generated. For instance, tumor models using CCL2 demonstrated MDSC accumulation restricted to mMDSC (Lim et al. 2020). Inflammatory mediators S100A8 and S100A9 also act as MDSC attractants and their overexpression is associated with MDSC accumulation (Dysthe & Parihar 2020; Greifenberg et al. 2009).

Following expansion and accumulation, an activation signal endows MDSC with their characteristic suppressive functionality. Among these are proinflammatory cytokines such as IL-1β, IL-6, PGE_2, TNFα, IFNy and LPS. MDSC activating signaling is mainly carried out through signaling via the transcription factor NF-κB (Dysthe & Parihar 2020; Bunt et al. 2017). IL-1β and IL-6 in combination with GM-CSF, respectively, are potent generators of suppressive MDSC (Lechner et al. 2010; Obermajer & Kalinski 2018; Yaddanapudi et al. 2016). Moreover, treatment of mMDSC with the eicosanoid PGE_2 results in an increased suppressive function in MDSC. Conversely, blocking PGE_2 production via COX-2 inhibition is associated with a decreased MDSC count (Dysthe & Parihar 2020). PGE_2 together with GM-CSF was shown to be an effective combination for generating immunosuppressive human MDSC *in vitro* and murine

MDSC *ex vivo* (Lechner et al. 2010; Obermajer & Kalinski 2018; Casacuberta Serra et al. 2017). LPS and IFNy injections into healthy mice led to expansion of splenic myeloid precursors, dampening dendritic cell (DC) maturation and activation of MDSC suppression (Greifenberg et al. 2009).

Thus, mediators capable of affecting MDSC induction, expansion and function, make up a large network with complex interactions. These shape the many facets of MDSC and contribute to the vast heterogeneity of MDSC complicating MDSC research.

Suppressive Functions of MDSC

Immunosuppressive capacity is the main feature of MDSC, allowing reliable functional distinction against monocytes and neutrophils. They inhibit various innate and adaptive components of the immune system. Among these, T cells are the most documented targets. MDSC use a variety of antigen-dependent or non-dependent mechanisms, that depend on microenvironment, state of T cell activation, organ and context of the pathological condition. In essence, MDSC establish an immunosuppressive

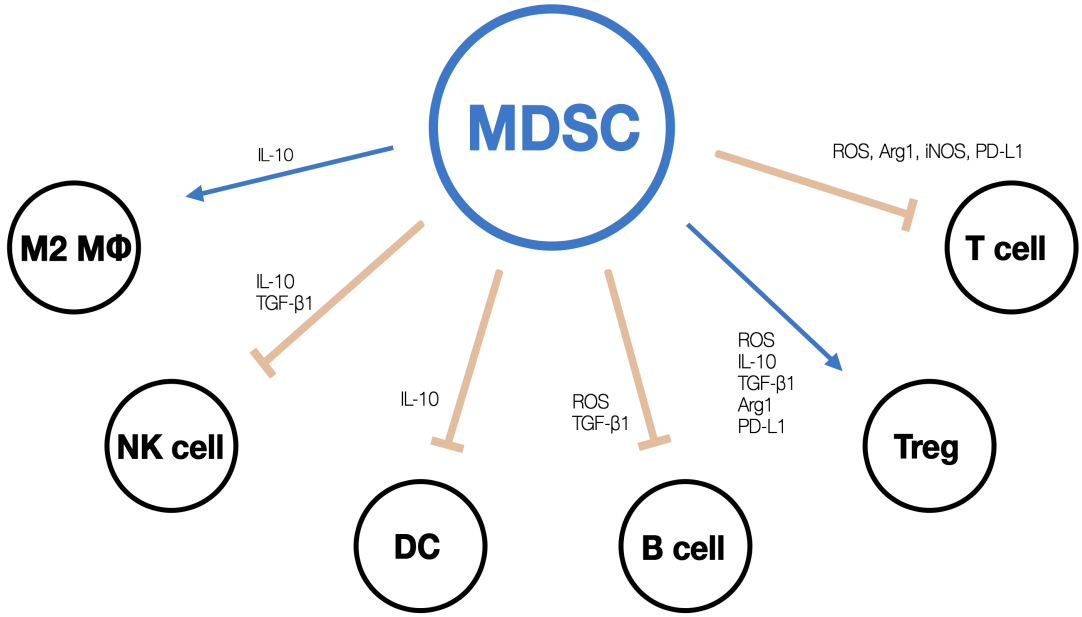

Illustration 3: Suppression Mechanisms of MDSC
Myeloid-derived suppressor cells (MDSC) utilize a variety of mechanisms to regulate the activity of diverse immune cells, including macrophages (MΦ), natural killer cells (NK cells), dendritic cells (DC), B cells, T regulatory cells (Treg) and T cells. The main suppression mechanisms are nutrient depletetion by metabolizing arginine via arginase-1 (Arg1), generating reactive oxygen species (ROS), secreting immunosuppressive cytokines such as IL-10 & TGF-β1, and expressing programmed death-ligand 1 (PD-L1). In addition, MDSC mediate nitration and nitrosylation of T cell components (CD3, TCR) via inducible nitric oxide synthase (iNOS).Indirect effects comprise the induction of suppressive Tregs and the promotion of macrophage polarization toward regulatory M2 phenotypes.

microenvironment by nutrient depletion, oxidative stress, anti-inflammatory cytokines, T regulatory cell (Treg) induction and specific cell-to-cell interactions (Illustration 3) (Dorhoi & Plessis 2018; Veglia, Perego & Gabrilovich 2018b).

Nutrient depletion of inflammatory effector cells is a major aspect of MDSC suppression mechanisms. Proliferation and effector functions of T cells rely on protein synthesis. Upon activation their amino acid uptake is substantially increased. MDSC interfere with several amino acid metabolisms, depriving T cells. Shortage of specific amino acids, e.g. arginine, blocks T cells proliferation, downregulates T cell receptor components – such as CD3ζ – and arrests T cells cell cycle in G0 (Vanhaver et al. 2021). MDSC express the enzyme arginase-1 that converts the non-essential amino acid arginine to urea and ornithine and thereby decreasing extra cellular arginase levels. Moreover, arginine is consumed by MDSC to produce nitric oxide (NO) via the inducible nitric oxide synthase (iNOS) and further downstream metabolites (such as spermine) known to modulate T cell differentiation (Ibáñez-Vea 2018; Carriche et al. 2021). High arginine levels correlate with higher survival rates and anti-tumor activity in cancer (Geiger et al. 2016). Tryptophan deprivation is another method utilized by MDSC to enhance their suppressive capacity. Indoleamine 2,3-dioxygenase 1 (IDO) is the first enzyme in the tryptophan degradation and overexpressed in MDSC. Low levels of tryptophan causes T cell anergy, arrest of protein synthesis, triggers Treg differentiation and even enhances Treg suppressive activity (Platten et al. 2012; Belladonna et al. 2009). Coherently, cysteine depletion by MDSC was demonstrated to block T cell activation and arrests their proliferation (Srivastava et al. 2010).

Additionally, MDSC exert suppressive function via oxidative stress, generating highly reactive oxygen species (ROS). These molecules damage nucleic acids, proteins and lipids, thus impairing cellular functions (Vanhaver et al. 2021). MDSC subspecies substantially differ in their ROS generation mechanisms. mMDSC predominantly express iNOS and arginase-1 to produce NO, while gMDSC are characterized by NADPH oxidase (NOX2) usage for generating superoxide radicals (Ibáñez-Vea 2018). Oxidative stress affects T cell receptor (TCR) signaling components, such as lymphocyte-specific protein tyrosine kinase (LCK) and CD3ζ, via inducing post-translational modifications or downregulation, eventually causing T cell hyporesponsiveness and anergy (Vanhaver et al. 2021; Cemerski et al. 2002; Cemerski et al. 2003). NO in particular demonstrated nitrosylation of the T cell receptor and induction of conformational changes abolishing antigen-specific recognition as

well as nitrosylation of important mediations of the T cell sustaining IL-2 pathway (Gabrilovich & Nagaraj 2009; Mazzoni et al. 2002). It was shown to exert an inhibitory effect on MHC II expression and impairing Fc receptor-mediated functions of natural killer cells (NK) (Stiff et al. 2018; Grimm et al. 2002). Furthermore, CCL2 nitration by NO dampens the influx of T cells into inflammatory sites (Molon et al. 2011). Effector T cells are more prone to ROS damage than Tregs, therefore the balance of suppressive and activated T cells is also affected by oxidative stress caused by MDSC (Takahashi et al. 2005; Mougiakakos et al. 2009). S100A8 and S100A9 are not only involved in MDSC accumulation (see above) but also enhance their suppressive power by potentiating ROS relevant enzymes (J. Yang et al. 2018).

Anti-inflammatory cytokines, such as TGF-β, IL-10 and PGE_2, are secreted by MDSC and crucially contribute to the immunosuppressive microenvironment. As a key cytokine in MDSC expansion, TGF-β was also found to be an essential part of their suppression mechanism. Tregs are induced by MDSC in a TGF-β-dependent manner and expand MDSC suppression mechanisms are well as promote their expansion via TGF-β, forming a positive feedback loop (Dysthe & Parihar 2020). TGF-β impairs effector T cell function by affecting IL-2 production and can directly suppress expression of genes essential for T cell cytotoxicity (Thomas & Massagué 2005; Brabletz et al. 1993). mMDSC were also found to use membrane-bound TGF-β to inhibit cytotoxic activity and cytokine production of NK cells (Dorhoi & Plessis 2018). MDSC-related immunosuppressive molecules iNOS, arginase, IL-10, and TGF-β itself are increased by TGF-β (C.-R. Lee et al. 2018). TGF-β and IL-10 drive expansion of the suppressive M2 Macrophage phenotype and negatively regulate NK cells (Lim et al. 2020). IL-10 facilitates the impairment of $CD8^+$ T cells, is involved in Treg expansion and inversely correlates with proinflammatory cytokine IL-12, that promotes anti-tumor immunity (Krishnamoorthy et al. 2021; Groth et al. 2019). PGE_2 is a common inflammatory regulator and implicated in MDSC expansion within a positive feedback loop between COX-2 and PGE_2. COX-2 expressed by MDSC is associated with increased levels of suppressive mediators, like IDO, IL-10, arginase and iNOS. Likewise, PGE_2 was reported to perpetuate many factors involved in MDSC-associated suppression mechanisms as well as to dampen IFNγ secretion and suppress T cells IL-2-dependently (Krishnamoorthy et al. 2021; Obermajer & Kalinski 2018; Obermajer et al. 2011). Treg induction was found to be conducted in a MDSC-T cell contact-dependent manner through CD40 and CD40L. MDSC upregulate several co-

stimulatory molecules (CD86, PD-L1) additionally promoting Treg formation (Vanhaver et al. 2021; Dysthe & Parihar 2020). In murine mouse models, the induction of tumor specific Tregs was found to be facilitated via tumor-associated antigen uptake and presentation by MDSC (Serafini et al. 2008). Hoechst et al demonstrated the transdifferentiation of T helper 17 cells (Th17) into Tregs induced by MDSC (Hoechst et al. 2011). Treg depletion reduced the immunosuppressive capacity of MDSC by decreasing their PD-L1 and IL-10 expression, illustrating their reciprocal interplay (Z. Yang et al. 2010). Several other cell types of the microenvironment are crucially affected by MDSC. Maturation, migration and antigen uptake by DC are dampened by MDSC leading to reprogramming of DC towards an anti-inflammatory phenotype (Chou et al. 2012; Chou et al. 2011).

The manifold and diverse immunosuppressive mechanisms of MDSC shape their immediate microenvironment, regulating immune responses and determining various pathological conditions.

1.2 The Liver: A Manifold Immunoregulatory Organ

1.2.1 Liver Anatomy and Physiology

The liver is one of the bodies biggest glands and is involved in diverse vital functions including metabolism, degradation, detoxification, digestion, immune reaction, immunotolerance, endo- and exocrine secretion. Its pivotal role is emphasized by the fact that the liver receives 25% of the cardiac output and consumes 20% of the total oxygen although making up only around 2% of the human body weight (Robinson et al. 2019; Vollmar & Menger 2009; Lautt 2009).

Anatomically, the liver is resided subdiaphragmatically in the upper right quadrant of the abdomen. Macroscopically it is separated into four main lobes - right, left, quadrant and caudate lobe - and can be further subdivided by its arterial branching pattern into eight segments (Cotoi & Quaglia 2016). The liver receives dual blood supply: about one third via the hepatic artery providing oxygen rich blood and two thirds via the portal vein system, that drains the gastrointestinal organs transporting assimilated nutrients (Vollmar & Menger 2009). On a cellular level the liver comprises of 80% parenchymal hepatocytes and 20% non-parenchymal cells, among which are sinusoidal endothelial

cells (LSEC), Kupffer cells (KC), hepatic stellate cells (HSC), biliary cells, resident DC and lymphocytes (Racanelli & Rehermann 2006).

Microscopically, the parenchyma is arranged in a complex and highly functional hepatic lobule, consisting of mainly hepatocytes arranged around a small central vein (Illustration 4). Central veins unite into the inferior vena cava. Peripherally the central vein and emerging bile ducts are connected to a portal triad, containing a portal venule, an arteriole and bile ducts. Portal venules and arterioles fuse to form the liver sinusoids draining into the central vein. These sinusoids are surrounded by a special fenestrated LSEC monolayer, enabling direct plasma contact with hepatocytes. The KC reside within the sinusoidal lumen scanning the blood for pathogens and debris (Meschner & Junqueira 2013; Böttcher et al. 2011). The perisinusoidal space between LSEC and hepatocytes is termed space of Disse, and it is where HSC are located. Quiescent HSC store around 80% of the body's vitamin A within lipid droplets, activated HSC produce components of the extra cellular matrix (ECM) and exert immunogenic functions. Bile ducts are formed between hepatocytes and bile acids are exocrinely secreted to support fat digestion within the intestine (Meschner & Junqueira 2013). Among non-parenchymal cells, lymphocytes are a large group present in the liver, contributing to the unique function of the liver in terms of immunology (Racanelli & Rehermann 2006).

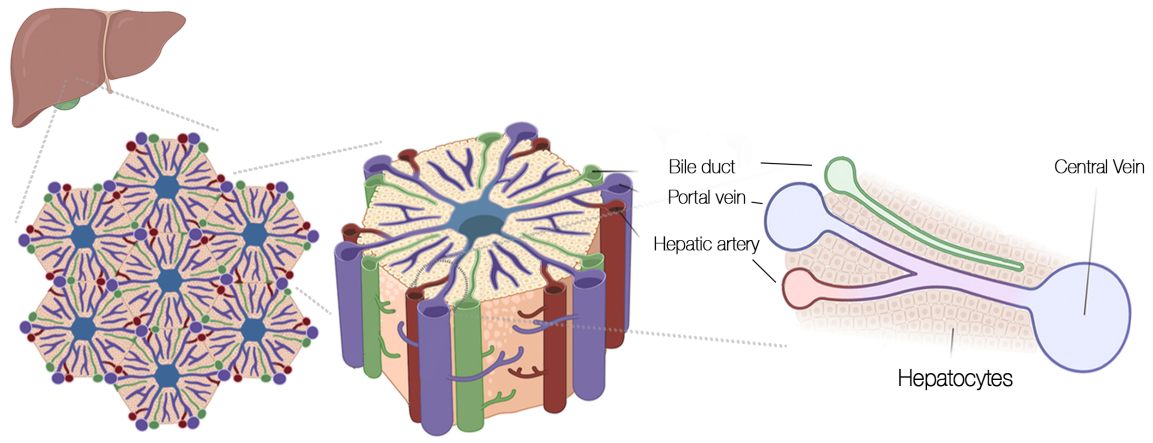

Illustration 4: Anatomic Microstructure of the Liver
The liver parenchyma is composed of hexagonally-shaped hepatic lobules. At its periphery, the portal triad is located, consisting of oxygen-transporting arterioles, nutrient-enriched portal venules, and bile ducts. Portal venules and arterioles merge into hepatic sinusoids, which drain into the central veins. The fenestrated hepatic sinusoids run between hepatocytes. Bile ducts are formed that drain into the portal triad.

modified from Roman, G. et al., 2023. "iPSC-derived liver organoids and inherited bleeding disorders: Potential and future perspectives." Frontiers in Physiology, 14, p.1094249. herited. Creative Commons licence, CC BY 4.0.

1.2.2 The Liver as an Immunotolerogenic Organ

The liver exerts an extraordinary immunological function, due to its constant exposure to non-self proteins derived from nutrients and commensal or transient microbiota (Illustration 5). Therefore, its role in inducing specific mechanisms of immunogenic tolerance is vital to prevent immune activation by harmless antigens. Hepatocytes, liver DC, LSEC, HSC and KC are capable of antigen presentation via MHC II as well as cytokine production, rendering them to be key players in facilitating tolerance (Heymann & Tacke 2016). Initial filter and scavenger functions are fulfilled by LSEC, DC, KC and HSC detecting PAMPs, such as lipopolysaccharide (LPS) via by pattern-recognition receptors, such as TLR (Illustration 5) (Thomson & Knolle 2010). Constant low-level exposure to LPS leads to an “endotoxin tolerance” via secretion of IL-10, TGF-β, hepatocyte growth factor, prostaglandins or HSC-derived retinoic acid (Takeuchi & Akira 2010). Higher amounts of PAMPs, alarmins or DAMPs trigger a cytokine response recruiting other immune cells like monocytes into the liver, eventually leading to inflammation (Heymann & Tacke 2016). Tregs are another population critical to the tolerogenic microenvironment. They induce antigen-specific tolerance and are expanded by various liver resident cells, like hepatocytes, HSC and KC (Böttcher et al. 2011; Heymann et al. 2015). Moreover, LSEC - unlike ordinary endothelial cells - induce tolerance upon interaction with T cells by expanding Treg and counteracting DC dependent T cell activation (Böttcher et al. 2011). Liver resident DC are less potent T cell activators. Additionally, high levels of IL-10 and prostaglandins lead to downregulation of co-stimulatory molecules, preventing T cell activation (Robinson et al. 2019). Another part of maintaining the tolerogenic liver environment are in fact MDSC. They originate from immature myeloid bone marrow cells but can also be transdifferentiated locally when transmigrating through the LSEC layer (Robinson et al. 2019; Gabrilovich & Nagaraj 2009; Heymann et al. 2015). It was shown that HSC are capable of inducing MDSC from PBMC (Hoechst et al. 2013). First evidence of the liver as a tolerance-inducing organ originated from transplantation studies, in which rejection of allogeneic liver transplantation was significantly lower compared to others organs (Tiegs & Lohse 2010). This pivotal immunotolerogenic trait of the liver is reflected by the lower immunosuppression therapies needed to maintain organ acceptance within transplant patients (Lerut & Sanchez-Fueyo 2006). This function does come with disadvantages as far as effective clearing of pathogens from

the liver is concerned. The immunosuppressive environment of the liver is therefore prone to sustained chronic inflammation (Robinson et al. 2019).

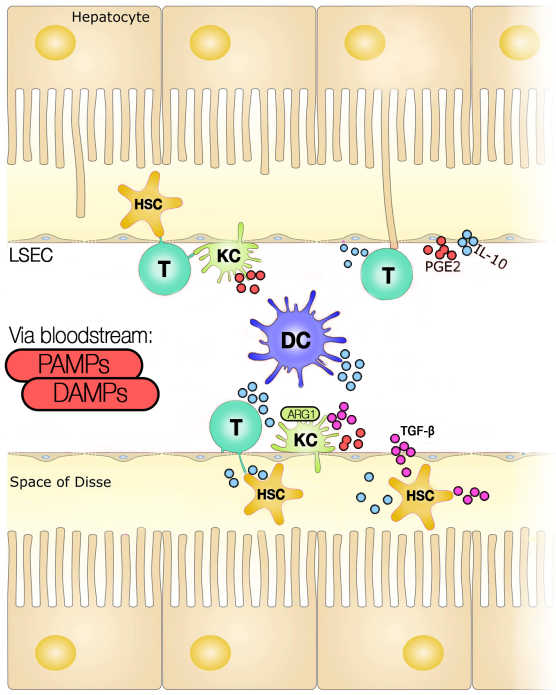

Illustration 5: Key Player Cells Involved in Immune Tolerance of the Liver
Anatomy of the liver sinusoid and its harboring cells: via the portal vein, pathogen-associated molecular patterns (PAMPs) and damage-associated molecular patterns (DAMPs) within the nutrient-rich blood are delivered into the liver sinusoids. Lining cells are liver sinusoidal endothelial cells (LSEC), which separate hepatocytes and hepatic stellate cells (HSC) from leukocytes circulating through the liver in the blood. Fenestrations in the LSEC allow direct molecular exchange between the perisinusoidal space and hepatocytes. Moreover, direct contact of lymphocytes via microvilli occurs. The liver interstitium is highly enriched with various cell populations capable of antigen presentation: dendritic cells, Kupffer cells, T cells, LSEC, hepatocytes, and HSC. Upon low levels of PAMPs, such as lipopolysaccharide, these cells secrete various mediators. IL-10, TGF-β, arginase, and prostaglandins shape the immunosuppressive microenvironment — a prerequisite for immunogenic tolerance.

modified from Jiang Y, Que W, Zhu P, Li XK. The Role of Diverse Liver Cells in Liver Transplantation Tolerance. Front Immunol. 2020 Jun 12;11:1203. doi: 10.3389/fimmu.2020.01203. PMID: 32595648; PMCID: PMC7304488. Creative Commons Attribution License (CC BY).

1.2.3 Biology of Chronic Liver Inflammation

Chronic liver disease is among the major health burdens worldwide. Hepatic fibrosis consequently to chronic liver inflammation affects over 800 million people and causing over two million deaths annually. Most frequent underlying diseases are hepatitis B, hepatitis C and – especially in Europe and the United States – alcoholic liver disease (AFLD). Within western countries the rise in obesity contributes to a massive increase (up to 46%) in non-alcoholic fatty liver disease (NAFLD). Less common diseases connected to chronic liver inflammation are autoimmune hepatitis, hemochromatosis, Wilson's disease and biliary cholangitis (Marcellin & Kutala 2018; Y. A. Lee & Friedman 2020). Progressive fibrosis leads to cirrhosis, eventually causing liver failure and ultimately hepatocellular carcinoma (HCC). The mortality and abundance render HCC to be the third leading cause of cancer related death worldwide (Y. A. Lee & Friedman 2020).

Although under homeostasis the liver is highly tolerogenic (see 1.2.2.), it can employ rapid immune mechanisms in response to harmful tissue damage or inflammation (Heymann & Tacke 2016). Although the liver has outstanding regenerative capabilities, sustained inflammatory triggers and cellular stress eventually derails its wound healing response leading to the development of fibrosis and functional impairment (Y. A. Lee & Friedman 2020). Among the triggers inducing such inflammation are DAMPs, PAMPs, bile acids, complement factors and classical alarmins, such as IL-33 and high mobility group protein B1 (HMGB1) (Heymann & Tacke 2016). Threshold-exceeding amounts of inflammatory stimuli leads to activation of KC, hepatocytes, LSEC, lymphocytes and HSC. This initiates the switch from a tolerogenic microenvironment, shaped by IL-10, IL-13 and TGF-β, to a pro-inflammatory one. Inflammatory cytokines, like IL-1β, IL-2, IL-6, IL-7, IL-12, IL-15 and IFNγ increase substantially and propagate inflammation. Moreover, acute phase proteins produced by hepatocytes and chemokines cause massive immune cell infiltration and exert direct effector functions (Robinson et al. 2019). 90% of the total body macrophages reside in the liver, which include the resident liver KC. They carry out immune effector functions by releasing cytokines, ROS, complement induction and activation of $CD4^+$ and $CD8^+$ T cells (Böttcher et al. 2011). Furthermore, DC prime T cells and danger signal guided neutrophils mediate pathogen clearance and further activate KC and LSEC (Heymann & Tacke 2016; Böttcher et al. 2013). LSEC express TLR detecting PAMPs and have also been described to prime T cells in context of inflammatory responses (Böttcher et al. 2011). Hepatic inflammation recruits and activates various innate (innate lymphoid cells, NKT cells, NK cells) and adaptive lymphocyte populations ($CD4^+$ T cells, $CD8^+$ T cells, B cells) that are potent cytokine producers, further influencing innate and adaptive immune responses (Robinson et al. 2019).

HSC express various TLR and scavenger receptors, complementing KC tasks in detection and clearing of pathogens (Robinson et al. 2019). Additionally, they are able to prime $CD8^+$ T cells (Böttcher et al. 2011). They show phagocytic traits and express MHC I, MHCII and lipid-presenting molecules (Thomson & Knolle 2010). In a chronic inflammatory environment, HSC are activated and gain a myofibroblast-like phenotype, initiating wound healing processes. Activated HSC produce inflammatory signals and deposit excessive amounts of the ECM, making them the key fibrogenic cell type within the liver. TGF-β is one of the main drivers of HSC activation and fibrotic remodeling of liver, and is produced by KC, LSEC and hepatocytes (Y. A. Lee &

Friedman 2020; Hu et al. 2018). Persistent inflammatory signals also cause the expansion of MDSC within the liver, counteracting ongoing sustained inflammation (Gabrilovich & Nagaraj 2009; Hammerich & Tacke 2015; Pallett et al. 2015). While MDSC are part of a mechanism to prevent extreme damage to the liver parenchyma, persistent inflammation with attenuation of pathogen clearance on the other hand may also promote secondary infections, which may ultimately contribute to liver fibrosis and failure (Bernsmeier & Antoniades 2017; Sehgal et al. 2021). Multiple reports show that activated HSC are capable of inducing MDSC in humans and mice and contribute to establishing an immunosuppressive environment (Hoechst et al. 2013; Chou et al. 2011; Hsieh 2015a). Since HSC are main contributors to control liver fibrogenesis and are involved in regulating chronic inflammation by MDSC induction, they represent a crucial, but maybe underestimated, cell population in liver immunology.

1.2.4 Hepatic Stellate Cells – Fibrogenic and Immunogenic Cells

General Functions and Activation of HSC

HSC were initially discovered by Kupffer as star-shaped “Sternzellen” in the late 19th century. 80 years later, Ito described a population of lipid-containing perisinusoidal cells (hence their pseudonym “Ito-cells”). It was Wake in the 1980s, who identified Ito cells to be same as the ones Kupffer had described and therefore ending the enigmatic nature of HSC (Senoo et al. 2010; Y. A. Lee & Friedman 2020). Since then HSC have been shown to be remarkably versatile cells vital to liver homeostasis, especially in orchestrating the response to liver injury (Friedman 2008).

HSC are of mesenchymal origin, make up one third of non-parenchymal and 8-14% of all liver cells. They reside within the perisinusoidal space of Disse at the interface of hepatocytes and the fenestrated LSEC monolayer. Their characteristic long dendritic projections create cellular contacts to LSEC, KC and hepatocytes facilitating functional intercellular cross-talk (Kitto & Henderson 2021). HSC contribute to hepatic development, liver regeneration and angiogenesis (Y. A. Lee & Friedman 2020). Under homeostasis, HSC are present in a quiescent non-proliferating state and store 90% of the body’s vitamin A in small cytoplasmic retinoid droplets (Friedman 2008). Furthermore, HSC regulate the sinusoidal tone, remodeling, blood flow and ECM turnover by controlling synthesis and degradation via matrix metalloproteinases. They

ensure tissue homeostasis and cellular integrity by excreting a broad range of growth factors and cytokines, such as hepatocyte growth factor (HGF) and VEGF, mediating the proliferation of hepatocytes and LSEC, respectively (Kitto & Henderson 2021). Following liver injury, HSC transdifferentiate from their quiescent state into an activated myofibroblast-like phenotype. Upon this activation, they become highly secretory, chemotactic, proliferative and increasingly responsive to local stimuli. They dramatically upscale the deposition of ECM proteins (collagen, laminin, proteoglycans), rendering them to be the main contributor of fibrotic liver remodeling (Y. A. Lee & Friedman 2020; Tsuchida & Friedman 2017). Interestingly, but not fully understood, HSC activation is accompanied by the loss of their retinoid droplets (Friedman 2008). Among the main drivers of HSC activation are hepatocyte secreted platelet-derived growth factor (PDGF), LSEC produced VEGF and wound healing key mediator TGF-β. Following liver injury, HSC themselves can secrete latent TGF-β, essentially driving the ECM production by HSC and promoting angiogenesis (Kitto & Henderson 2021; Kallis et al. 2011; Friedman 2008). Besides liver resident cells and soluble mediators, the complex activation process of HSC is further perpetuated by the influx of immune cells (Y. A. Lee & Friedman 2020). While immune cells shape the activation process, activated HSC gain capacity of controlling various immune cells within the response to liver inflammation. Within the last decade many findings showed activated HSC to be capable of influencing both innate and adaptive immunity. This imposes a new understanding of HSC as crucial immunogenic cells in a before unexpected magnitude (Hsieh 2015a).

HSC as Immune Regulators and MDSC Inductors

In recent years, HSC gained increasing attention as immunoregulatory cells. Activated HSC build up a negative immune network providing the basis for immune escape mechanisms driving HCC progression, facilitating protection of allografts and counter-balancing ongoing immune events in chronic liver inflammation. Among the key mechanisms shaping this immunosuppressive microenvironment are HSC-dependent induction of T cell apoptosis, tolerogenic DC, Tregs and MDSC (Xu et al. 2020; Hsieh 2015a). Cotransplanting HSC with allogenic islets effectively prolonged survival of the allografts without the requirement of immunosuppression. Elevated numbers of Tregs and MDSC were found to be critical to achieve long-term survival of the grafts (H.-R. Yang et al. 2009; C.-H. Chen et al. 2006; Chou et al. 2011). Many essential mediators

leading to MDSC induction and expansion are produced by HSC, such as complement factor C3, PGE_2, GM-CSF, macrophage colony-stimulating factor (M-CSF), IL-6 and VEGF (Xu et al. 2020; Arakawa et al. 2014; Lu & Hsieh 2013). Moreover, PD-L1 found to be essential for the immunomodulatory activity of murine and human HSC (Hsieh 2015a). HSC-induced MDSC in transplant tolerance is based on IFNγ signaling pathway in HSC (Chou et al. 2011). Moreover, Chou et al also showed that MDSC can be propagated from murine bone marrow cells (BMC) using activated HSC *in vitro* (Chou et al. 2011).

Most tumors arise from chronic inflammatory events, tolerogenic properties of HSC-mediated MDSC eventually promoting the development of HCC in context of chronical hepatitis B and C (Bowen & Walker 2005; Hsieh et al. 2019). Several studies revealed an importance of MDSC in tumor progression. MDSC are upregulated within HCC patients (Hoechst et al. 2008) and HSC are key factors to create an immunosuppressive environment enabling HCC progression *in vivo* and *in vitro* (W. Zhao et al. 2013; Xu et al. 2020). Hoechst et al. proved that the induction of MDSC from PBMC by primary human HSC is mediated by CD44 and is cell-cell contact dependent (Hoechst et al. 2013).

1.3 CD44

CD44 is a widely expressed, polymorphic transmembrane glycoprotein and was initially discovered as the hyaluronic acid (HA) receptor (Ponta et al. 2003). Since then, CD44 was found to be involved in countless functions. Among these are mediation of cell-cell adhesion, cell-matrix interactions, cellular homing, proliferation, angiogenesis, cellular motility and lymphocyte rolling (Knutson et al. 1996; Weber et al. 1996; Ponta et al. 2003)(Julia Schumann 2015). While HA is its main and most specific ligand, CD44 also interacts with several other molecules, such as osteopontin, laminin, serglycin, fibrin, MMP9, fibronectin and collagen (Weber et al. 1996; C. Chen et al. 2018; Govindaraju et al. 2019). Although CD44 does not possess signaling capacity itself, it can function as a co-receptor for various receptor tyrosine kinases, for instance Met, Ron, VEGFR, EGFR and CD74 (Govindaraju et al. 2019; Yoo et al. 2016). CD44 is encoded by single gene only. In humans, it is comprised of nineteen exons, nine of which are variably expressed. In mice, it consists of twenty exons with ten being variably expressed (Naor et al. 2008) (Ponta et al. 2003). Its broad functional range of

CD44 is expanded by post-translational modifications like glycosylation and alternative splicing (Brazil et al. 2013; Teye et al. 2016; Screaton et al. 1993; Johnson & Ruffell 2009). The most widely expressed form is the CD44 standard (CD44s), whereas the larger variant isoforms (CD44v) are expressed in only a few tissues but are typically overexpressed in multiple cancer entities (Naor et al. 2008)(Orian-Rousseau 2015). CD44v3-v6 isoforms were shown to exert platform-like functions by trapping growth factors and serving as coreceptors to various tyrosine kinases, ultimately enhancing cellular migration, adhesion and oncogenic invasion (Ponta et al. 2003). Hence, CD44 can serve as an interpreter of the extracellular environment, switching between promoting and restricting invasiveness (Ponta et al. 2003). In cancer, CD44 was found to be involved in the epithelial to mesenchymal transition, invasion and metastasis of cancer cells, and has been identified as a surface marker for cancer stem cells (C. Chen et al. 2018; Chikamatsu et al. 2011). Its crucial role in tumorigenesis and invasiveness is being addressed in targeted therapies in clinical trials (C. Chen et al. 2018). Recent pan-cancer analyses have demonstrated that CD44 expression correlates with prognosis and immunotherapy response across various cancer types, suggesting its potential as a prognostic biomarker and therapeutic target in oncology (Chen *et al.*, 2023).

Given its broad functional spectrum, CD44 is also profoundly involved in numerous pathways of pro- and anti-inflammatory nature (Johnson & Ruffell 2009). For instance, CD44 is known to form the signaling component of the macrophage migration inhibitory factor receptor (MIF-receptor) CD74. MIF is an upstream activator of innate immunity and a proinflammatory cytokine produced by various immune cells, endothelial cells, macrophages and some parenchymal cells upon stress stimulation (Calandra & Roger 2003; Schober et al. 2008). In liver inflammation both MIF and CD74 deficient mice were prone to exacerbated inflammation and increased HSC activation. Contrary, daily application of recombinant MIF inhibited fibrogenic responses in a murine toxic liver fibrosis model and reduced HSC activation *in vivo* (Wasmuth & Heinrichs 2017). MIF signaling sustained survival and activation of monocytes as well as dose-dependently upregulated and increased alternative splicing of CD44 (Yoo et al. 2016). MIF promotes differentiation of myeloid cells into $CD14^{+}HLA\text{-}DR^{low/-}$ mMDSC resulting in a higher amount of MDSC and metastasis in tumors (Simpson et al. 2012). MDSC generated from bone marrows of MIF deficient mice were significantly less suppressive compared to the ones generated in wild type mice (Yaddanapudi et al. 2016).

Besides impairments in the distribution of myeloid progenitors and thymus migration of lymphocytes, CD44 deficient mice develop largely aphenotypically (Protin et al. 1999; Schmits, Filmus, Gerwin, Senaldi, Kiefer, Kundig, Wakeham, Shahinian, Catzavelos, Rak, Furlonger, Zakarian, Simard, Ohashi, Paige, Gutierrez-Ramos & Mak 1997a). This might be due to partly compensation by other hyaladherins in terms of molecular redundancy, such as the receptor for hyaluronan-mediated motility (RHAMM) (Nedvetzki et al. 2004). CD44 deficiency in mice showed increased inflammatory and reduced fibrogenic responses (Govindaraju et al. 2019). The majority of these mice died due to an unremitting state of inflammation, which is linked to a lack of CD44-dependent upregulation of TGF-β1 (Johnson & Ruffell 2009; Ouhtit et al. 2013). Blocking CD44 resulted in elevated levels of proinflammatory mediators such as IL-1β, IL-6, COX-2, NFkB and MMP (Wu et al. 2019). These findings demonstrate various antiinflammatory aspects of CD44.

On the other hand, CD44 was shown to be involved in pathways of proinflammatory impact. Crosslinking CD44 was found to induce COX-2 and interactions between CD44 and HA, displaying crucial proinflammatory effects (L. K. Sun et al. 2001; McKee et al. 1996). In CD44 KO mice, reduced lymphocyte migration to inflamed tissues or infection sites is observed, impairing the immune response to injuries or infections and also disrupting the resolution phase of inflammation (Jordan et al. 2015). CD44 blocking antibodies reduced inflammation in various pathological conditions like arthritis, allergic encephalomyelitis and pulmonary eosinophilia, underlining this complex duality (Mikecz et al. 1995; Brocke et al. 1999; Katoh et al. 2003).

CD44 displays a crucial role in context of liver pathologies. Compared to in other organs CD44 expression is relatively low but in response to liver damage is significantly increased (Han et al. 2024). In a murine concanavalin A mediated model of human autoimmune hepatitis, CD44 deficient mice exhibited more severe manifestations (D. Chen et al. 2001; McKallip et al. 2005). Murine *in vivo* studies have shown, that upon tissue injury CD44 is upregulated (Govindaraju et al. 2019; W. Zhao et al. 2011). In humans, patients with chronic liver inflammation showed elevated hepatic CD44 expression (Urashima et al. 2000). As well as it was found to be upregulated in livers of HCC patients and even correlated with higher histological grades and poor differentiation (Endo & Terada 2000; Dhar et al. 2018). In early phases of toxic liver injury in CD44 deficient mice, inflammatory events were suppressed due to the reduced CD44-mediated migration of lymphocytes, neutrophils and

macrophages (Kimura et al. 2008). Despite initial suppressive effects, late phases showed an even exacerbated inflammational state in CD44 deficient mice (Wang et al. 2002; Teder et al. 2002; Kimura et al. 2009). Elevated levels of CD44, both at mRNA and protein levels, have been associated with hepatocyte ballooning and increased alanine aminotransferase concentrations in patients diagnosed with hepatic steatosis, metabolic dysfunction-associated steatohepatitis (MASH), or HBV infection (Han et al. 2024).

In HSC CD44 plays a critical role in their activation. The progression of liver fibrosis is marked by CD44 upregulation, which coincides with increased S100A4 expression, thereby promoting further HSC activation and fibrotic processes. CD44 has been implicated in the activation of the Wnt/B-catenin pathway via the S100A4 promoter to induce its expression. Both activated HSC and quiescent HSC express multiple CD44 variants (Kikuchi et al. 2005). While under steady state conditions the level of surface CD44 on HSC is only marginally, upon activation CD44 is upregulated in mice and human cells (Hoechst et al. 2013; De Minicis et al. 2007; Satoh et al. 2000; Kim & Seki 2023). Upregulation of CD44 further drives HSC activation by upregulating profibrotic genes and therefore contributing to the acquisition of fibrogenic, proliferative, and invasive phenotypes in HSC (Han et al. 2024). Activated primary human HSC upregulated CD44 upon which they gain the capacity to transdifferentiate $CD14^+$ PBMC into suppressive mMDSC (Hoechst et al. 2013). Together this shows a strong implication of CD44 and liver injury, especially in context of MDSC induction by HSC.

1.4 Previous Work

In previous work, it was shown that activated human HSC can induce suppressive mMDSC from $CD14^+HLA\text{-}DR^+$ PBMC in a CD44-dependent manner *in vitro* (Hoechst et al. 2013). Human $CD14^+HLA\text{-}DR^+$ were cocultured with primary HSC from healthy donors or the HSC cell-line LX2 resulted in an efficient HLA-DR downregulation. This effect was found to be exclusively in HSC presence. For this HSC needed to be in an activated state upon which CD44 was found to be upregulated. Cocultures in transwell settings did not affect HLA-DR expression, thus rendering it to be cell-cell-contact dependent. Phenotypically the transdifferentiated cells resembled mMDSC. Moreover, the induction process was found to be restricted to mMDSC-like phenotype only. PBMC cultured in presence of HSC showed upregulated mRNA levels of MDSC-

related genes (*IL-4a*, *S100A12* and *Arg-I).* HSC induced CD14^{+}HLA-DR$^{-/low}$ cells suppressed CD8^{+} proliferation. Their suppressive function was exerted via arginase-I. Adding CD44-blocking antibodies into cocultures reduced mMDSC induction and dose-dependently abrogated their suppression. CD44 knock down within LX2 cells revoked the capacity of inducing HLA-DR downregulation, thus mMDSC Induction, and rendered this process to be dependent to CD44 expressed on HSC (Hoechst et al. 2013).

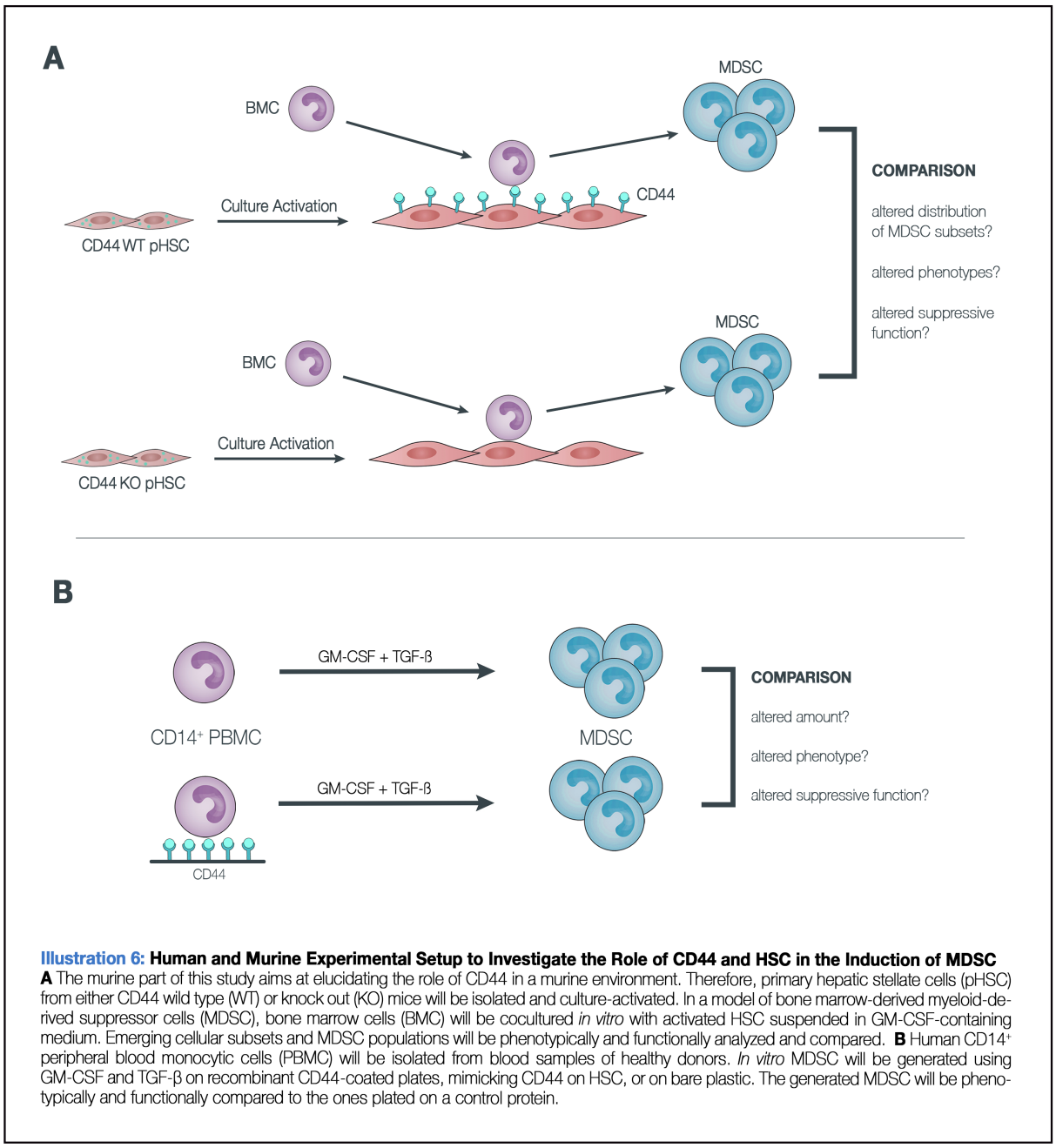

Illustration 6: Human and Murine Experimental Setup to Investigate the Role of CD44 and HSC in the Induction of MDSC
A The murine part of this study aims at elucidating the role of CD44 in a murine environment. Therefore, primary hepatic stellate cells (pHSC) from either CD44 wild type (WT) or knock out (KO) mice will be isolated and culture-activated. In a model of bone marrow-derived myeloid-derived suppressor cells (MDSC), bone marrow cells (BMC) will be cocultured *in vitro* with activated HSC suspended in GM-CSF-containing medium. Emerging cellular subsets and MDSC populations will be phenotypically and functionally analyzed and compared. **B** Human CD14^{+} peripheral blood monocytic cells (PBMC) will be isolated from blood samples of healthy donors. *In vitro* MDSC will be generated using GM-CSF and TGF-β on recombinant CD44-coated plates, mimicking CD44 on HSC, or on bare plastic. The generated MDSC will be phenotypically and functionally compared to the ones plated on a control protein.

1.5 Aims of This Study

MDSC crucially affect the microenvironment of chronic inflammation. HSC were shown to induce mMDSC from human PBMC in a CD44-dependent manner, suggesting that CD44 on HSC plays a new substantial role in orchestrating inflammatory processes within the liver by taking part in MDSC induction. However, the underlying mechanisms are still poorly understood. This study aims to further elucidate the role of CD44 in the induction of MDSC by HSC.

The first part focuses on whether the attributed role of CD44 upholds in a murine model of MDSC induction. Therefore, primary HSC of CD44-WT and CD44-KO mice will be isolated and used in a model of *in vitro* generation of MDSC. The HSC derived MDSC, generated in this way, will be phenotypically and functionally analyzed (Illustration 6A).

The second part focusses on the role of CD44 in induction of MDSC from human $CD14^+$ PBMC. We will investigate if CD44 is needed in a cell-dependent manner, or whether CD44 without cellular context can act on its own to induced MDSC. To this end, we establish an *in vitro* model of MDSC generation from $CD14^+$ PBMC using GM-CSF and TGF-β. We then transfer this model on CD44 coated plates and assess its effects on phenotype and suppressive capacity of resulting mMDSC (Illustration 6B).

2 MATERIALS & METHODS

2.1 Materials

2.1.1 Technical Equipment

TABLE 1: Technical Equipment

TECHNICAL EQUIPMENT	SUPPLIER
FACSCanto II	BD Bioscience, Franklin Lakes, USA
BD FACSAria III Cell Sorter	BD Bioscience, Franklin Lakes, USA
Centrifuge 5810 R	Eppendorf, Hamburg, Germany
Centrifuge 5430 R	Eppendorf, Hamburg, Germany
Eppendorf Research Plus Pipettes	Eppendorf, Hamburg, Germany
FACS AriaFusion Cell Sorter	BD Bioscience, Franklin Lakes, USA
Flow Cytometer Tubes	Sarstedt, Nümbrecht, Germany
HandyStep® Electronic	BRAND GmbH, Wertheim, Germany
Galaxy 170R CO_2 Incubator	New Brunswick Scientific, Nürtingen, Germany
ThermoScientific MAXISAFE 2030i	Thermo Fisher Scientific, Waltham, USA
Olympus CKX41 Microscope	Olympus Europa, Hamburg, Germany
GFL Water Bath 1068 and 1083	LAUDA-GFL, Lauda-Königshofen, Germany
Masterflex L/S Pump	Cole-Parmer, Wertheim, Germany
Neubauer Improved Chamber	Roth, Karlsruhe, Germany
Pipetboy	Integra Bioscience, Huston, USA
VWR Mixer Mini Vortex 230V EU	VWR, Darmstadt, Germany
LSRFortessa Cell Analyzer	BD Bioscience, Franklin Lakes, USA
QuantStudio 5 Real-Time PCR System	Thermo Fisher Scientific, Waltham, USA

T Professional Trio Thermocycler	Analytik Jena, Jena, Germany
NanoDrop Photometer ND-1000	PEQLAB Biotechnologie GmbH, Erlangen, Germany
AxioCam MRc	Carl ZEISS, Dresden, Germany
Axiocert 25 Inverted Microscope	Carl ZEISS, Dresden, Germany

2.1.2 Reagents & Kits

TABLE 2: Reagents & Kits

REAGENTS AND KITS	SUPPLIER
Dynabeads Mouse T-Activator CD3/CD28	GIBCO, Thermo Fisher Scientific, Waltham, USA
Dynabeads Human T-Activator CD3/CD28	GIBCO, Thermo Fisher Scientific, Waltham, USA
Fetal Bovine Serum (FCS)	Sigma-Aldrich, Munich, Germany
Fetal Bovine Serum (cFCS), Charcoal Stripped	Sigma-Aldrich, Munich, Germany
CD4+ T cell isolation Kit, Murine	Miltenyi Biotec, Bergisch Gladbach, Germany
CD14 Microbeads, Human	Miltenyi Biotec, Bergisch Gladbach, Germany
CD8+ T Cell Isolation Kit, Human	Miltenyi Biotec, Bergisch Gladbach, Germany
Dulbecco's Phosphate Buffered Saline (DPBS) (1x)	GIBCO, Thermo Fisher Scientific, Waltham, USA
L-Glutamine Solution, 200mM	Sigma-Aldrich, Munich, Germany
Hepes Solution (1M)	Sigma-Aldrich, Munich, Germany
Sodium Pyruvate (100mM)	Sigma-Aldrich, Munich, Germany
Recombinant Mouse TGF-β1	R&D Systems, Minneapolis, USA

Penicillin-Streptomycin (10000 U/mL Penicillin)/ (10 mg/mL Streptomycin)	Sigma-Aldrich, Munich, Germany
Recombinant Human IgG1-Fc Protein	R&D Systems, Minneapolis, USA
Recombinant Human CD44-Fc Chimera Protein	R&D Systems, Minneapolis, USA
RPMI-1640, With L-glutamine and Sodium Bicarbonate	Sigma-Aldrich, Munich, Germany
Dulbecco's Modified Eagle Medium DMEM, Low Glucose	Sigma-Aldrich, Munich, Germany
HISTOPAQUE-1077	Sigma-Aldrich, Munich, Germany
Recombinant Human GM-CSF (E. coli)	PeproTech, Hamburg, Germany
Recombinant Human TGF-β1 (CHO Derived)	PeproTech, Hamburg, Germany
Pronase E (0,25 U/mg) (from Clostridium histolyticum)	Merck, Darmstadt, Germany
Collagenase D (0,25 U/mg)	Roche, Grenzach-Wyhlen, Germany
DNase I	Roche, Grenzach-Wyhlen, Germany
Nycodenz	Axis-Shield, Dundee, Scotland
EGTA	Carl Roth, Karlsruhe, Germany
NaCl	Carl Roth, Karlsruhe, Germany
KCl	Carl Roth, Karlsruhe, Germany
NaH_2PO_4. H_2O	Carl Roth, Karlsruhe, Germany
Na_2HPO_4	Carl Roth, Karlsruhe, Germany
HEPES	Carl Roth, Karlsruhe, Germany
$NaHCO_3$	Carl Roth, Karlsruhe, Germany
Glucose	Carl Roth, Karlsruhe, Germany
$CaCl_2$. $2H_2O$	Carl Roth, Karlsruhe, Germany
$MgCl_2$. $6H_2O$	Carl Roth, Karlsruhe, Germany
$MgSO_4$. $7H_2O$	Carl Roth, Karlsruhe, Germany

CFSE Proliferation Dye	eBioscience (Thermofisher), San Diego, California
LIVE/DEAD Fixable Aqua Dead Cell Stain Kit (used in 1:1000 with FACS buffer)	Thermo Fisher Scientific, Waltham, USA
High-Capacity cDNA Reverse Transcription Kit	Thermo Fisher Scientific, Waltham, USA
RNeasy Plus Micro Kit	Qiagen, Düsseldorf, Germany
Ethanol 99%	TH. Geyer, Renningen, Germany
2-Mercaptoethanol 50mM	GIBCO, Thermo Fisher Scientific, Waltham, USA
EDTA	Carl Roth, Karlsruhe, Germany
Geneticin (G418)	GIBCO, Thermo Fisher Scientific, Waltham, USA
Iscove's Modified Dulbecco's Medium (IMDM)	GIBCO, Thermo Fisher Scientific, Waltham, USA

2.1.3 Buffers, Solutions & Culture Media

TABLE 3: Buffers, Solutions & Culture Media

SOLUTION	COMPOSITION
FACS Buffer	PBS (5x) 2% FCS 0,02% Sodium Azide pH: 7.2
Hanks' Balanced Salt Solution (HBSS), Sigma-Aldrich, Munich, Germany	5.4 mM KCl 0.3 mM Na2HPO4 x 7 H2O 4.2 mM NaHCO3 1.3 mM CaCl2 0.5 mM MgCl2 x 6 H2O 0.6 mM MgSO4 x 7 H2O

	137 mM NaCl 5.6 mM D-Glucose pH 7.4
MACS Buffer	PBS (5x) 2% FCS 2 mM EDTA pH: 7.2
PBS	137.9 mM NaCl 6.5 mM Na2HPO4 x 2 H2O 1.5 mM KH2PO4 2.7 mM KCl pH 7.4
RPMI Medium	RPMI-1640 8% cFCS 2% L-Glutamine Solution 1% Penicillin-Streptomycin
H-MDSC Medium	RPMI-1640 8% cFCS 2% L-Glutamine Solution 1% Penicillin-Streptomycin 10ng/ml Human Recombinant GM-CSF
HSC Medium	DMEM, 10% FCS, 1% Penicillin-Streptomycin, 1% Sodium-Pyruvate, 2,5% Hepes
IMDM Cell Line Medium	IMDM, 8% cFCS 2% L-Glutamine Solution 1% Penicillin-Streptomycin 50µM β-mercaptoethanol

AG Medium	IMEM, 8% FCS, 1% Penicillin-Streptomycin, 1% Sodium-Pyruvate, 2,5% Hepes 30% Cell line Ag 8653 Supernatant
EGTA-Solution	8000mg/L NaCl 400mg/L KCl 88.17mg/L NaH_2PO_4. H_2O 120.45mg/L Na_2HPO_4 2380mg/L HEPES 350mg/L $NaHCO_3$ 190mg/L EGTA 900mg/L Glucose pH: 7,35-7,4
Enzyme Solution	8000mg/L NaCl 400mg/L KCl 88.17mg/L NaH_2PO_4. H_2O 120.45mg/L Na_2HPO_4 2380mg/L HEPES 350mg/L $NaHCO_3$ 560mg/L $CaCl_2$. $2H_2O$ pH: 7,35-7,4
GBSS-A	370mg/L KCl 210mg/L $MgCl_2$. $6H_2O$ 70mg/L $MgSO_4$. $7H_2O$ 59,6mg/L Na_2HPO_4 30mg/L KH_2PO_4 991mg/L Glucose 227mg/L $NaHCO_3$ 225mg/L $CaCl_2$. $2H_2O$ pH: 7,35
GBSS-B	8000mg/L NaCl 370mg/L KCl

	210mg/L $MgCl_2$. $6H_2O$ 70mg/L $MgSO_4$. $7H_2O$ 59,6mg/L Na_2HPO_4 30mg/L KH_2PO_4 991mg/L Glucose 227mg/L $NaHCO_3$ 225mg/L $CaCl_2$. $2H_2O$ pH: 7,35
Nycodenz Solution	0,29g Nycodenz/ml GBSS-A
DNase Solution	0,05mg DNase I/ml GBSS-B
Enzyme Mix Solution	Enzyme Solution containing: 0,5mg/ml Pronase E, 0,0083mg/ml DNase I, 0,0625mg/ml Collagenase D
Pronase E Solution	0,4mg Pronase E/ml Enzyme-Solution
Collagenase D Solution	0,375mg Collagenase D/ ml Enzyme Solution
ACK Lysis Buffer	1000ml ddH_20 8.29g NH_4Cl 1g $KHCO_3$ 37.2mg Na_2EDTA

2.1.4 Antibodies

TABLE 4: Human FACS Antibodies

NAME/TARGET	CLONE	CONJATED FLUORESCENCE	ISO-TYPE	DILU-TION	SUPPLIER
FcX TrueStain	-	PUR	-	1:200	BioLegend, San Diego, USA
CD14	M5E2	PE	Mouse IgG2a, κ	1:200	BioLegend, San Diego, USA

HLA-DR	L244	Pacific Blue	Mouse IgG2a, κ	1:200	BioLegend, San Diego, USA
DCSIGN (CD209)	9E9A8	APC	Mouse IgG2a, κ	1:200	BioLegend, San Diego, USA
CD3	SK7	PerCP-Cy5.5	Mouse IgG2a, κ	1:200	BioLegend, San Diego, USA

TABLE 5: Murine FACS Antibodies

NAME/TARGET	CLONE	CONJATED FLUORESCENCE	ISO-TYPE	DILU-TION	SUPPLIER
CD16/32	-	PUR	Rat IgG2a, λ	1:200	BioLegend, San Diego, USA
CD11b	M1/70	PerCP-Cy5.5	Rat IgG2b, κ	1:200	eBioscience, San Diego, USA
CD11c	N418	APC	Armenian Hamster IgG	1:200	BioLegend, San Diego, USA
Ly6C	HK1.4	PE	Rat IgG2c, κ	1:500	BioLegend, San Diego, USA
Ly6G	1A8	FITC	Rat IgG2c, κ	1:100	BioLegend, San Diego, USA
MHC II/I-A/I-E	M5/11 4.15.2	APC-Cy7	Rat IgG2c, κ	1:200	BioLegend, San Diego, USA
CD44	IM7	PE-Cy7	Rat IgG2c, κ	1:200	BioLegend, San Diego, USA

2.1.5 Software

TABLE 6: Software

SOFTWARE	SUPPLIER
FACSDiva Software	BD Bioscience, Franklin Lakes, USA
FlowJo 10.5.0	FlowJo LLC, Ashland, USA
GraphPad Prism V.7.0a	GraphPad Software Inc., San Diego, USA
Illustrator CC (24.1.2)	Adobe Systems Software, Dublin, Ireland
Microsoft Office 2020	Microsoft GmbH, Washington, USA

2.1.6 Consumables

TABLE 7: Consumables

CONSUMABLES	SUPPLIER
Tubes (15 ml and 50 ml)	Sarstedt, Nümbrecht, Germany
Falcon Polystyrene 5 ml FACS tubes	BD Bioscience, Franklin Lakes, USA
TC-Plate Suspension R, 96 Wells	Sarstedt, Nümbrecht, Germany
Bemis Parafilm M Laboratory	Amcor, Zürich, Swiss
Pipette Tips (10µl, 100µl, 200µl, 1000µl)	Sarstedt, Nümbrecht, Germany
Pipette tips with and without filter (10µl, 100 µl and 1000 µl)	Sarstedt, Nümbrecht, Germany
Serological Plastic Pipettes (5ml, 10ml and 25ml)	Sarstedt, Nümbrecht, Germany
Syringes 5/10ml	Braun Melsungen AG, Melsungen, Germany
Introcan Safety, 22G	Braun Melsungen AG, Melsungen, Germany
Corning Cell Strainer 70µm Nylon	Corning Incorporate, Corning, New York, USA

40µm Polyamid Mesh	TH. Geyer, Renningen, Germany
TC-Plate Suspension F, 48/24/12/6 Wells	Sarstedt, Nümbrecht, Germany
S-Monovette 9ml	Sarstedt, Nümbrecht, Germany
SafteyMultifly 21G, 80mm Tube	Sarstedt, Nümbrecht, Germany
SUPRA Disposable Needle 2x100mm	Transcodent/Sulzer, Kiel, Germany
Reaction tubes (0.2ml, 0.5ml, 1.5ml, 2ml)	Sarstedt, Nümbrecht, Germany
Multiply PCR Tubes	Sarstedt, Nümbrecht, Germany
MicroAmp Optical 384-Well Plate	Life Technologies, Thermo Fisher Scientific, Waltham, USA
Petri dish 10cm & 15cm	Sarstedt, Nümbrecht, Germany
TC Flask T175 and T75, Standard	Sarstedt, Nümbrecht, Germany
Steritop (0.2µm Filter)	Merck, Darmstadt, Germany

2.1.7 qRT-PCR Primers

TABLE 8: qRT-PCR Primers

TARGET	PRIMER SEQUENCE (F/R)	AMP-LICON LENGTH	ANNEALING TEMPERATURE
GAPDH	5’ TGAAGGTCGGTGTGAACGG-3’ 3’-AGGCCATGAGGTCCACC-5‘	978	62°C
ALB	5’-GTTCGCTACACCCAGAAAGC-3’ 3’-AGCAGACACACACGGTTCAG-5‘	164	60°C
ACTA2	5’-TCCAGAGTCCAGCACAATACCAGT-3’ 3’-TGACAGAGGCACCACTGAACC-5‘	155	62°C

2.2 Methods

2.2.1 Mice

2.2.1.1 Mice Strains

Mice strains used in this experimental work were C57BL/6J, B6.129(Cg)-Cd44^{tm1Hbg}/J (CD44$^{-/-}$), female Mdr2$^{-/-}$ (FVB.129P2-Abcb4^{tm1Bor}) and B6 ACTb-EGFP (C57BL/6-Tg(CAG-EGFP)1Osb/J). All of them were bred in the animal facilities of the University Medical Center Hamburg-Eppendorf. All mice used for HSC isolation were at least 11 weeks old, while mice used for BMC were 2-8 weeks old.

2.2.1.2 Housing

Mice received humane care according to the guidelines of the National Institute of Health as well as to the legal requirements in Germany. Mice were held in individually ventilated cages with maximum 5 animals per cage under controlled conditions (20°C ± 2°C, 50% ± 5% humidity) in a 12-hour-day-night rhythm and were provided with autoclaved standard laboratory chow and water ad libitum.

2.2.2 Ag 8653 Cell Line

Cells were thawed and cultured in IMDM cell line medium for one single day, then 1mg/ml G418 was added. Non adherent cells were discarded and cells were split 1:5. 1.5x10^6 were harvested using PBS with 2mM EDTA, washed three times and plated in 15cm Petri dishes withing 15ml IMDM cell line medium and incubated for four days. Supernatant containing GM-CSF was collected and filtered through 0.2µm filter and finally stored -20°C.

2.2.3 Isolation of Cell Populations

2.2.3.1 Isolation of Primary Murine Hepatic Stellate Cells

Our isolation protocol of primary murine HSC consisted of a retrograde *in situ* perfusion, an *in vitro* digestion with a subsequent density-gradient purification followed

by a FACS-sort. All used mice were at least 11 weeks old, since older age is associated with higher HSC yield. If not otherwise stated experimental settings were performed using male and female mice (cells were pooled) of the C57BL/6J strain. Due to low HSC yields, a group of four to ten mice were used for one experiment. Initially, GBSS-A, GBSS-B, EGTA solution, enzyme-solution, Nycodenz-solution, Collagenase D solution, Pronase E solution were prepared under sterile conditions and filtered through a 0.2µm filter. The tube of the Masterflex pump was flushed with ddH_2O, 80% ethanol and PBS and then filled with the EGTA solution. The EGTA, Pronase E and Collagenase D solution were put in a water bath at 42°C.

In Situ perfusion.

Mice used for HSC isolation were sacrificed by exposure to a mixture of CO_2/O_2. The abdomen and thorax were opened and the thoracal inferior vena cava was pinched off using fine thread. Inferior vena cava was catheterized with a Introcan Safety 22G catheter connected to the pump's tube. The liver perfusion was started with EGTA solution at 5ml/min. After the liver was visibly pale and distended, the portal vein was cut allowing the solution to drain. After two minutes of EGTA solution, perfusion was carried on by 5min of Pronase E solution and 7 min of Collagenase D solution.

In vitro digestion.

Livers were obtained and after gall bladder removal kept in a petri dish filled with 15ml enzyme solution until all livers of the experimental group were obtained. Organs were taken, minced to 2x2x2mm sizes using sterile scissors, put into 15ml enzyme mix solution and then divided equally to three 50ml tubes. To each tube 40ml of enzyme mix solution was added and mixed with serological pipettes. Tubes were placed in a shaking water bath (low level, 40°C) for 25min. The digested solutions were filtered through a 70µm cell strainer, centrifuged (4°C, 580g, 10min) and pellets pooled in one 50ml tube of 5ml DNase solution. The suspension was centrifuged and washed with 50ml GBSS-B.

Density gradient.

The pellet was resuspended in 5ml GBSS-B and 5ml DNase solution was added. We added another 22ml GBSS-B and subsequently 16ml of nycodenz solution. After mixing, the suspension was divided equally to four 15ml tubes à 12ml. A 26G cannula

was used to carefully overlay 2ml of GBSS-B. Tubes were centrifuged (1380g, 17min, Dec=0, 4°C). The white interphase was collected using a serological pipette. Cells were washed with 50ml GBSS-B, then with MACS buffer and prepared for FACS-sort (see 2.2.5.2).

2.2.3.2 Isolation of Primary Murine Bone Marrow Cells

For isolation of primary murine bone marrow cells (BMC), mice were anesthetized by exposure to a mixture of CO_2/O_2. By checking the loss of pedal withdrawal reflex of the hind limb, level of anesthesia was estimated and subsequently mice were killed by cervical dislocation. Femurs and tibias were obtained and opened by cutting a small proximal and distal part of the bone under sterile conditions. Opened bones were placed in a 0.2ml tube, perforated multiple times by a small, sterile needle. The 0.2ml tube was placed within a 1.5ml tube, closed and centrifuged (800g, RT, 30s). The centripetal force accelerated the bone marrow out of the bone, through the perforations into the 1.5ml tube. Cells were washed using PBS + 2% FCS and the pellet was resuspended in 500µl ACK lysis buffer for two minutes for erythrocyte removal. Cells were washed two times with PBS + 2% FCS and counted.

2.2.3.3 Isolation of Primary Human PBMC

All human experiments were approved by the ethic commission of Ärztekammer Hamburg (Bearb.-Nr.: PV5377). 80ml of human peripheral blood was drawn from a single healthy donor using SafteyMultifly needles and S-Monovettes and pooled into 50ml tubes with a maximum of 20ml Blood per tube and 10ml of prewarmed (37°C) HBSS was added consecutively. 15ml HISTOPAQUE-1077 was sub layered and centrifuged at 500g room temperature (RT) for 30 minutes with an acceleration of 7 and deceleration of 1. Afterwards, the white PBMC containing interphase was obtained using a 5ml serological pipette and transferred in new 50ml tubes and filled up with HBSS. Tubes were centrifuged at 500g and RT for 7 minutes. Pellets were resuspended in 50 ml HBSS, centrifuged and resuspended in 1ml ACK lysis buffer, to lyse erythrocytes. After one minute, 45ml HBSS was added and tubes were centrifuged, yielding a pellet of adequately pure PBMC ready for Magnetic-activated Cell Sorting (MACS).

2.2.3.4 Isolation of Splenic T Cells

Murine spleen was transferred in 5ml PBS and minced through a 300µm steel sieve into a 50ml using a syringe plunger. The sieve was washed with 20ml PBS and centrifuged for 10 minutes at 500g (RT). Cells were resuspended in 4.5ml RPMI medium and added onto a nylon wool filled 5ml syringe, prefilled with warm medium (37°C). The nylon wool column was then incubated for 45 minutes at 37°C. By adding 5ml Medium on top, non-adherent cells were eluted, centrifuged (10 min, 500g, RT) and resuspended in 3ml ACK lysis buffer. After one minute, cells were washed using MACS buffer and prepared for MACS-Sort (see 2.2.3.7).

2.2.3.5 Mechanism of Magnetic-activated Cell Sorting (MACS-Sort)

Magnetic-activated Cell Sorting (MACS-Sort) allows separation of a cell fraction by using magnetic forces and deploying magnetic microbeads. They can be directly coupled to a specific surface antigen or indirectly via coupling to a preceding applied antibody. Magnetically labeled cells are passed through a magnetic column, retaining only labeled cells. The column is then washed to obtain the labeled cell fraction (positive selection) or the unlabeled cell fraction cleared from cells with the target antigen can be collected (negative selection).

2.2.3.6 MACS-Sort of Human $CD8^+$/$CD14^+$ Cells

Human PBMC were isolated as described (see 2.2.3.3), suspended in 3ml MACS buffer, filtered through a 40µm mesh and counted using the Neubauer Improved Chamber. Cells were centrifuged for 10 minutes at 300g (RT). According to cell count, the pellet was resuspended in 40µl/10^7 cells MACS buffer together with either 10µl/10^7 cells of human CD8 or CD14 microbeads cells and then incubated for 15 minutes (4°C). Afterwards, cells were washed with 10ml MACS buffer and resuspended in 0,5ml MACS buffer. Magnetic columns (MS) were attached to the magnetic stand, rinsed with 0,5ml MACS buffer and the cell suspension was added via a 40µm mesh. The column was washed three times with 0.5ml MACS buffer and then taken out of the magnetic stand. Plunging the column with 1ml MACS buffer yields the MACS-sorted pure $CD8^+$ or $CD14^+$ PBMC.

2.2.3.7 MACS-Sort of Murine $CD4^+$ Cells

Murine splenic T cells were isolated as described above (see 2.2.3.4) suspended in 3ml MACS buffer, filtered through a 40µm mesh and counted using the Neubauer Improved Chamber. According to cell count, the pellet was resuspended in 40µl/10^7 cells MACS buffer together with 10µl/10^7 cells of the kit's antibody cocktail and then incubated for 5 minutes (4°C). Cells were washed and then incubated in 30µl/10^7 cells MACS buffer and 20µl/10^7 cells anti-biotin beads for 10 minutes (4°C). Afterwards, cells were washed with 10ml MACS buffer and resuspended in 0,5ml MACS buffer. Magnetic columns (MS) were attached to the magnetic stand, rinsed with 0,5ml MACS buffer and the cell suspension was added via a 40µm mesh. The column was washed three times with 0.5ml MACS buffer and then taken out of the magnetic stand. Plunging the column with 1ml MACS buffer yields the MACS-sorted pure $CD4^+$ T cells.

2.2.4 *In vitro* Cell Culture

2.2.4.1 BMC HSC Coculture

Primary HSC were isolated (see 2.2.3.1) and culture activated by plating and incubating them (37°C) on bare plastic culture dishes (24-well TC-Plate Suspension F) at $4x10^4$ HSC/cm^2 for seven days in HSC medium. Cultured HSC tightly adhered to the plates bottoms and spreading to 80% confluency. On day seven murine BMC from same genetic background were isolated as described above (see 2.2.3.2) and $5x10^5$ BMC were added on top of the confluent HSC cell layer. The coculture was kept in AG medium, containing 30% supernatant of GM-CSF-producing cell line Ag 8653, that was shown to maturate BMC to DC within 7 days (Klotz et al. 2007). After four days BMC were obtained, while the tightly adherent HSC remain on the well bottom. BMC were washed and either prepared for suppression assay (see 2.2.4.3) or FACS analysis (2.2.5.1).

2.2.4.2 Generation of Human mMDSC *in vitro*

For generating human mMDSC *in vitro*, we plated $5x10^5$ freshly isolated $CD14^+$ PBMC (see 2.2.3.3 and 2.2.3.6) in a 24-well TC-Plate Suspension F. Cells were suspended in 1.2ml per well of either H-MDSC medium containing 2ng/ml TGF-β1 or H-MDSC

medium only. Regarding experiments comparing the effects of CD44 on human mMDSC (3.2.4 and 3.2.5), culture plates were preincubated with 500µl PBS containing 1µg/ml recombinant CD44 Fc or recombinant IgG1 Fc respectively. After 24 hours of incubation (4°C) the coating solution was carefully aspirated, and wells were washed with 1ml PBS. For this experimental setting, each approach contained three wells assigned to FACS analysis resembling triplicates and one well explicitly for the suppression assay.

Cells were harvested at day 6 of incubation by taking floating cells and incubate the remaining attached cells with 1ml MACS buffer at 4°C for 20 minutes. Afterwards, wells were gently rinsed with MACS buffer and cells were collected in 15ml tubes. Cells were counted and prepared for flow cytometry analysis (see 2.2.5.1) or suppression assay (see 2.2.4.3) respectively.

2.2.4.3 Suppression Assays

In human experiments, suppression assays were performed by using MACS-sorted $CD8^+$ T cells from human PBMC (see 2.2.3.3 and 2.2.3.7). Murine suppression assays deployed $CD4^+$ T cells from bone marrow cells of mice matching the genetic background of the ones used for BMC cocultured with HSC (see 2.2.4.1).

T cells were labeled with carboxyfluorescein succinimidyl ester (CFSE) by suspending the cells in 1ml PBS per 10^7 T cells and 0.1µl CFSE per ml PBS. After 10 minutes in water bath (37°C), CFSE was blocked by adding pure FCS into a 1:10 (CFSE:FCS) ratio. Subsequently, cells were washed twice with RPMI medium. Besides a distinct number of cells serving for negative control, CFSE labeled T cells were activated by adding Dynabeads T-Activator CD3/CD28 in a 1:0.8 ratio in human settings or a 1:1 ratio in murine settings (T cells:Dynabeads). Dynabeads were washed with RPMI medium before application. 10^5 T cells in 100µl RPMI medium were pipetted into the wells of a 96-well TC-Plate Suspension R in triplicates or quadruplicates per experimental approach.

Harvested human mMDSC at d6 (see 2.2.4.2) or harvested murine cocultured BMC on day four (see 2.2.4.1) were added corresponding to experimental layout in 1:1/1:2/1:3/1:4/1:8 ratios (MDSC:T cell). The culture plate was then centrifuged for one minute at 300g and incubated for 72h. After 72h cells were prepared for FACS analysis deploying the fluorescent activity of CFSE in the FITC channel. By each T cell mitosis,

the amount of CFSE within the cell is split in half resulting in reduced brightness in the FITC channel and therefore quantifiable proliferation by FACS.

2.2.5 Flow Cytometry & Fluorescent Activated Cell Sorting

2.2.5.1 Detection of Surface Proteins Using Flow Cytometry

For assessing surface expression of proteins and proliferation of CFSE labeled T cells, flow cytometry was used. Up to $4x10^5$ cells were prepared by being washed with FACS buffer and transferred into 96-well TC-Plate Suspension R. To prevent unspecific binding of staining antibodies, murine cells were incubated with Fc block anti-CD16/CD32 and human cells with FcX Truestain respectively, contained in 70µl FACS buffer for 10 minutes (4°C). Cells were washed two times using FACS buffer and resuspended with the staining antibody master mix for 24h (4°C). Cells from suppression assays were stained for 15min (4°C). After staining, cells were washed two times with FACS buffer and transferred into FACS tubes. All measurements and data were collected using the FACSCanto II or LSRFortessa flow cytometer and the FACSDiva software. Data was analyzed using FlowJo 10.5.0.

2.2.5.2 Fluorescent Activated Cell Sorting of HSC

To further purify density-gradient-purified primary HSC (see 2.2.3.1), we performed fluorescent activated cell sorting (FACS). We deployed the autofluorescence of the HSC retinoids and used a 405nm laser for excitation and a 450/50nm bandpass filter. Therefore, cells were resuspended in pure FCS with a maximum $1x10^6$ cells/ml and kept on ice. The FACS-sort took approximately 1-1.5 hours. Nozzle size was 100µm. FACS-sort was done using the BD FACSAria III Cell Sorter and FACSDiva Software.

2.2.6 mRNA Expression Analysis

RNA was isolated from $5x10^5$ or more cells using the RNeasy Plus Micro kit according to the manufacturer's description. Using the High-Capacity cDNA Reverse Transcription kit in accordance with the manufacturer's instruction, 1µg of RNA was transcribed into cDNA. T Professional Trio Thermocycler was programmed as followed: 10min at 25°C, 120min at 37°C, 5min at 85°C, cooldown to 4°C. qRT-PCR

was performed based on SYBR Green dye using the QuantStudio 5 Real-Time System programmed according to the primers used. We used 384-well MicroAmp Optical plates, with 5µl of total volume (2.5µl maxima SYBR green/ROX qPCR Master Mix, 0.25µl forward primer, 0.25µl reverse primer, 1.5µl ddH_2O, 0.5µl cDNA). The relative mRNA levels were calculated using the ΔCT method after normalization to the housekeeping gene glyceraldehyde 3-phosphate dehydrogenase (GAPDH).

2.2.7 Statistical Analysis

Statistical significance was assessed using ANOVA and t-test depending on the experimental setting. All data was analyzed using Graphpad 5 (Prism). P-value of <0.05 was considered significant.

3 RESULTS

3.1 The Role of CD44 on Primary Murine Hepatic Stellate Cells in Myeloid-derived Suppressor Cell Induction

3.1.1 Introduction

It has been shown that activated human HSC are capable of transdifferentiating mature $CD14^+$ PBMC into suppressive $CD14^+HLA\text{-}DR^{-/low}$ mMDSC. The human HSC cell line LX2 as well as primary human HSC were able to generate these mMDSC in a CD44-dependent fashion (Hoechst et al. 2013). However, primary human HSC were not able to induce MDSC *ex vivo*. Only after 7 days of culture activation and upregulation of CD44, HSC gained the ability to transduce human $CD14^+$ PBMC into mMDSC (Hoechst et al. 2013). Since HSC activation is required for MDSC induction, and murine liver MDSC are markedly increased after 14 days in *in vivo* models of liver inflammation induced by bile duct ligation (BDL) (Höchst et al. 2015), we hypothesized that primary murine HSC must also undergo proper activation to induce MDSC. Therefore, we analyzed whether primary murine HSC analogically upregulate surface CD44 upon activation and whether CD44 analogically relevant for MDSC induction by HSC.

3.1.2 Establishment of Isolation and Culture Activation of Primary Murine HSC

To study the activation and MDSC induction by primary murine HSC, we first established a HSC isolation protocol. We adapted the HSC isolation protocol from the work of Mederacke et al. (Mederacke et al. 2015). Livers of old (>11 weeks) mice were perfused *in situ* via the inferior vena cava (IVC). Before the perfusion was started the IVC above the liver was clamped and the portal vein cut allowing retrograde perfusion with first pronase and then collagenase solutions. The livers were then taken out and *in vitro* digested, after which HSC were purified by a subsequent nycodenz-based density gradient. To achieve sufficient yields of HSC, cells from 6-10 animals were pooled. By using size (SSC) and the autofluorescence signal of HSC in flow cytometric analysis, we monitored HSC purity. After the nycodenz-based gradient our HSC purity

levels were approximately 60% to 70% (Figure 1A). In order to enhance the HSC purity,

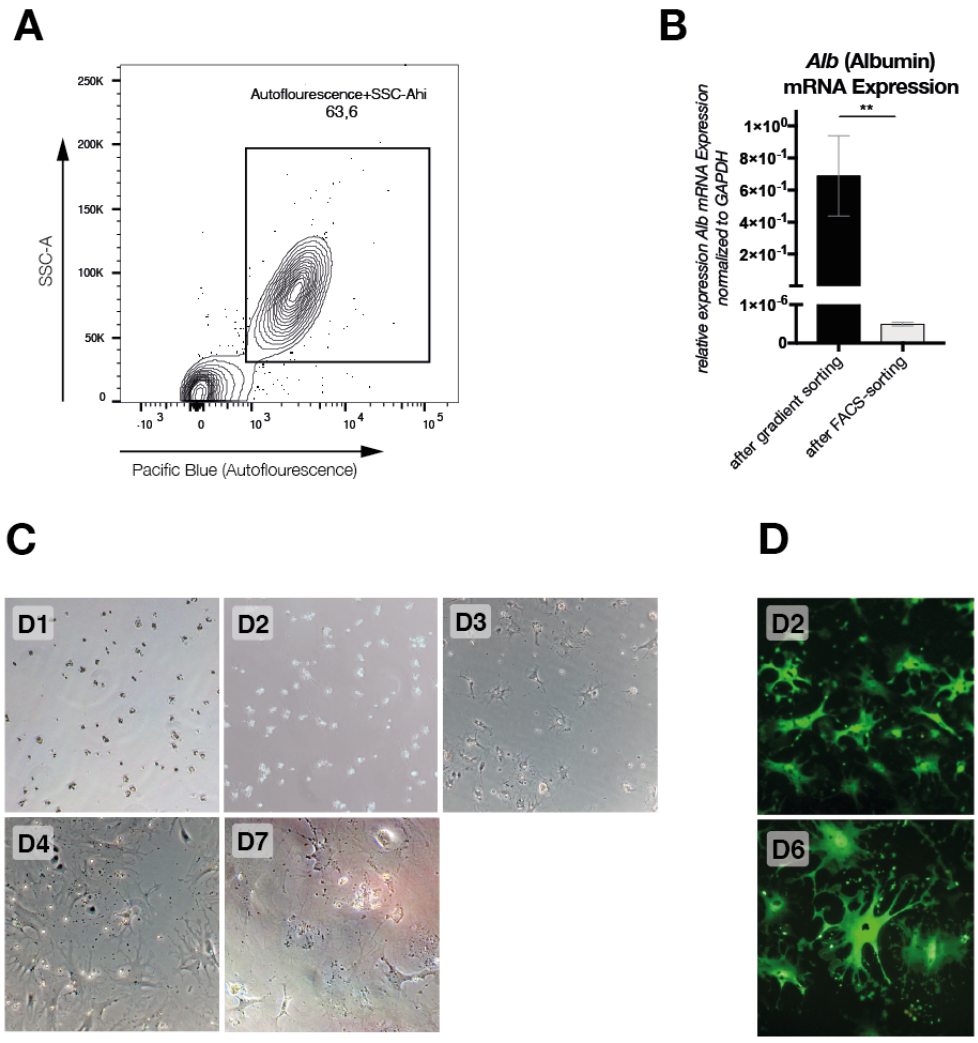

FIGURE 1: Establishment of the Isolation and Culture Activation of Primary Murine Hepatic Stellate Cells

(A) Gating strategy for FACS-based purification of primary isolated and density gradient presorted hepatic stellate cells (HSC). A 405nm laser for excitation and a 450/50-nm bandpass filter (Pacific Blue) were used for the detection of the HSC autofluorescence. **(B)** *Alb* mRNA expression was determined by RT-PCR. Glyceraldehyde 3-phosphate dehydrogenase (GAPDH) was used as a housekeeping gene. Cells were lysed after density-gradient separation of our isolation protocol and compared to FACS-based sorted HSC that were lysed after six days in culture. Data stems from one experiment only. Unpaired t-test; **p<0.01. **(C)** Phase contrast microscopy pictures of isolated and FACS-based purified HSC were taken on the indicated days in cell culture. **(D)** HSCs were isolated from transgenic mice expressing green fluorescent protein (GFP). Fluorescent microscopy images of HSC were taken at day 2 (D2) and day 6 (D6) of culture activation. **(E)** *Acta2* mRNA expression was determined by RT-PCR. GAPDH was used as a housekeeping gene. All HSC were FACS-based purified. Quiescent HSC were taken from MDR2$^{-/-}$ mice and lysed after 20 hours of cell culture. Acta2-mRNA levels shown compare MDR2$^{-/-}$ HSC and wild type (WT) HSC, both at D7 of culture. These data are from a single experiment and lack direct comparability due to different mouse genotypes. They serve as supportive data only.

we sorted the gradient-purified cells by flow cytometry employing the endogenous retinoid fluorescence of HSC (Mederacke et al. 2015) and their size reflected in their high side scatter (Geerts et al. 1998). After sorting, we performed a quantitative RT-PCR (qPCR) to assess HSC purity on a mRNA level. Contaminating hepatocytes were detected via Albumin mRNA expression (coding gene: *Alb*). After FACS-base sorting, contaminating hepatocytes were largely lost, as the level of detectable Alb mRNA was significantly reduced (Figure 1B) and we did not detect relevant amounts of hepatocytes in phase contrast microscopy. We did further exclude Kupffer cell contamination by lack of F4/80 mRNA (data not shown).

We plated $4x10^4$ HSC/cm^2 in bare plastic culture dishes. During culture on bare plastic HSC tightly adhere and spread into their typical eponymous star-like morphology (Figure 1C) (Winau et al. 2007). First, small cellular protrusions can be observed on D2. At D3 over 80% of cultured HSC are already tightly adhered, spreading and growing throughout D7 (Figure 1C). For better visualization and estimation of HSC confluency, we isolated HSC from green fluorescent protein (GFP) expressing mice (Figure 1D). Our seeding density of $4x10^4$ HSC/cm^2 resulted in reliable 80% confluency at D7. Culturing HSC on bare plastic is a well-established model for activating HSC *in vitro* (Weiskirchen & Gressner 2018; Hoechst et al. 2013). Upon activation HSC gain a contractile and highly proliferative myofibroblast-like phenotype (Sancho-Bru et al. 2005; De Minicis et al. 2007) and produce various ECM components, such as collagen, thus representing key players in liver fibrogenesis (U. E. Lee & Friedman 2011). Expression of smooth muscle alpha actin (coding gene: *Acta2)* is increased in this myofibroblast state and serves as an activation marker for HSC (Troeger et al. 2012) (Mederacke et al. 2015; Friedman 2008; Brenner et al. 2012). To confirm HSC activation in our culture settings, we analyzed *Acta2* mRNA expression by qPCR after 7 days of HSC culture. As a control, HSC were cultured for 20 hours, which constitutes an inactivated quiescent state (De Minicis et al. 2007). Even though we used HSC of $Mdr2^{-/-}$ mice in this particular experiment, which due to chronic liver inflammation are reported to yield larger amounts of HSC (Dropmann et al. 2020) (Mederacke et al. 2015) - but also due to this chronic inflammation may already yield preactivated HSC - we were still able to detect elevated *Acta2* mRNA expression in D7 HSC compared to their quiescent counter parts (Figure 1E). Although direct comparability was not given due to different mouse strains and it represents data of only experiment, this data can support that our isolated primary HSC are adequately activated during culture

on bare plastic in accordance with common literature (De Minicis et al. 2007). Taken together, we conclude that after 7 days in culture, the confluent cell layer of activated HSC can be used for further analysis and coculture experiments.

3.1.3 *In vitro* Cultured HSC Upregulate CD44 Upon Activation

We next sought to confirm whether CD44 expression is similarly regulated in murine HSC as compared to human HSC described in Hoechst's work (Hoechst et al. 2013). As it has already been reported that primary murine HSC after activation in culture show elevated levels of CD44 mRNA compared to quiescent HSC (De Minicis et al. 2007), we analyzed CD44 surface expression by flow cytometry of HSC comparing *ex vivo* (D0) and culture activated HSC (D7). Figure 2A shows the gating strategies, gating culture activated HSC based on their size (FSC-A) and their granularity (SSC-A) (Figure 2A). Single cells were then analyzed for CD44 expression (PE-Cy7) (Figure 2A). Only 4% of *ex vivo* isolated primary HSC expressed CD44 on their surface (Figure

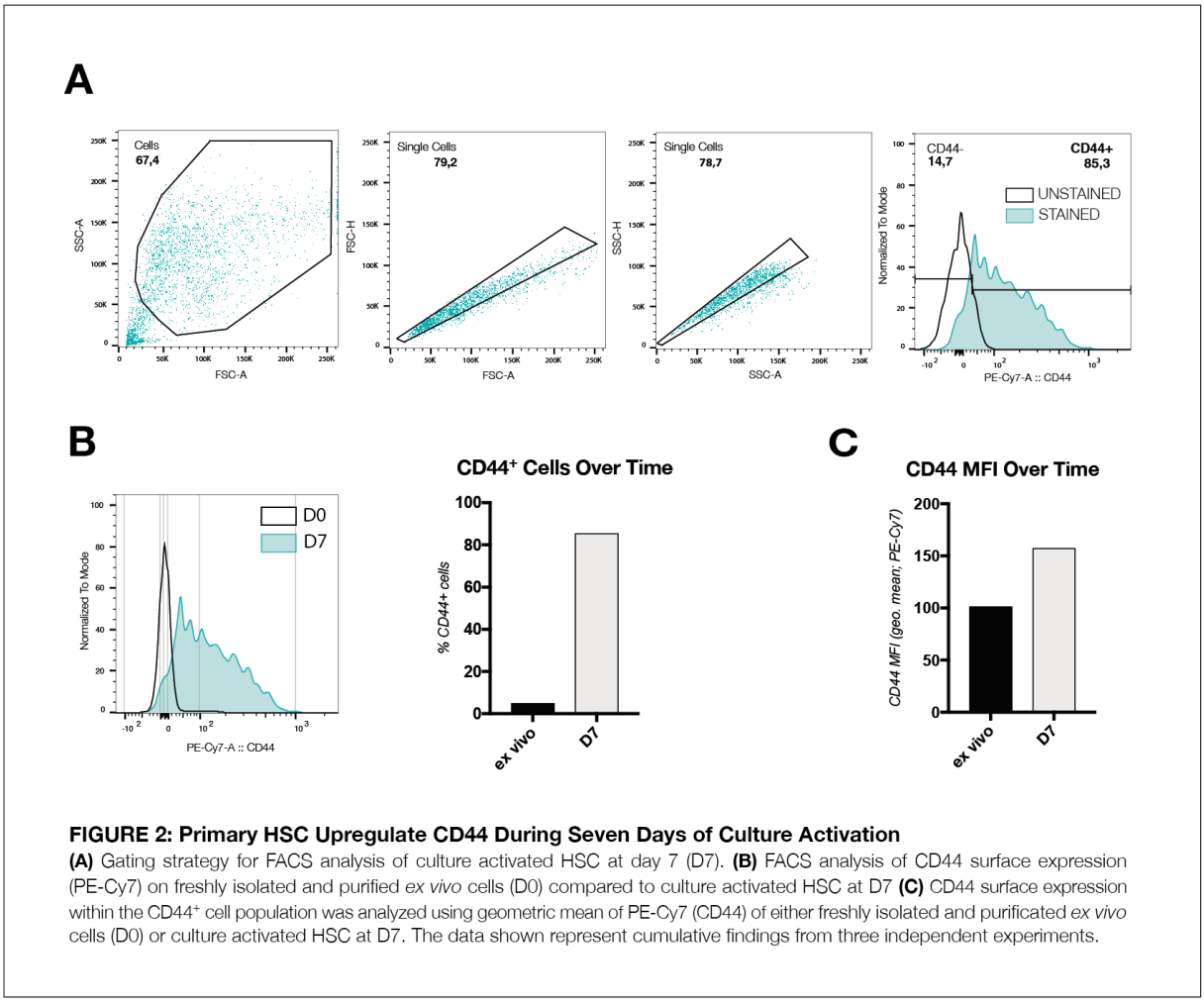

FIGURE 2: Primary HSC Upregulate CD44 During Seven Days of Culture Activation
(A) Gating strategy for FACS analysis of culture activated HSC at day 7 (D7). **(B)** FACS analysis of CD44 surface expression (PE-Cy7) on freshly isolated and purified *ex vivo* cells (D0) compared to culture activated HSC at D7 **(C)** CD44 surface expression within the CD44$^+$ cell population was analyzed using geometric mean of PE-Cy7 (CD44) of either freshly isolated and purificated *ex vivo* cells (D0) or culture activated HSC at D7. The data shown represent cumulative findings from three independent experiments.

2B), which increased to 80% of HSC during culture activation (Figure 2B). Not only did a larger proportion of HSC express CD44 after 7 days of culture, also the amount of CD44 per cell was increased as measured by the MFI within the CD44⁺ HSC using geometric mean (Figure 2C). During activation, the whole HSC population shifts in their PE-Cy7 intensity. CD44 expression was upregulated at D7 by a factor of 1,55 (D7:D0, MFI). Thus, isolated primary murine HSC upregulate CD44 expression over time and form a considerable CD44⁺ population at D7 of culture activation.

3.1.4 TGF-β1 Boosts CD44 Expression of Culture Activated HSC

TGF-β1 plays a key role in the wound healing process of injured livers, that are caused by viral infection, aflatoxins, chronic alcohol abuse but also in models of murine liver fibrosis, such as bile duct ligation (BDL) (Gressner et al. 2002; Breitkopf et al. 2005; Bissell et al. 1995). TGF-β1 secreted by LSEC, KC and activated HSC shape the inflammatory microenvironment and induces the production of various ECM components by HSC, such as collagen I, which leads to consecutive fibrotic remodeling of the liver (Friedman 2008) (U. E. Lee & Friedman 2011) (Troeger et al. 2012) (Inagaki & Okazaki 2007). While quiescent HSC express only small amounts of TGF-β1, it is increasingly expressed in activated HSC, further self-perpetuating their profibrotic functions via paracrine and autocrine patterns (Breitkopf et al. 2006; Friedman 2008). Given the essential role of TGF-β1 in HSC activation and its presence in the inflammatory microenvironment in the liver, we investigated whether CD44

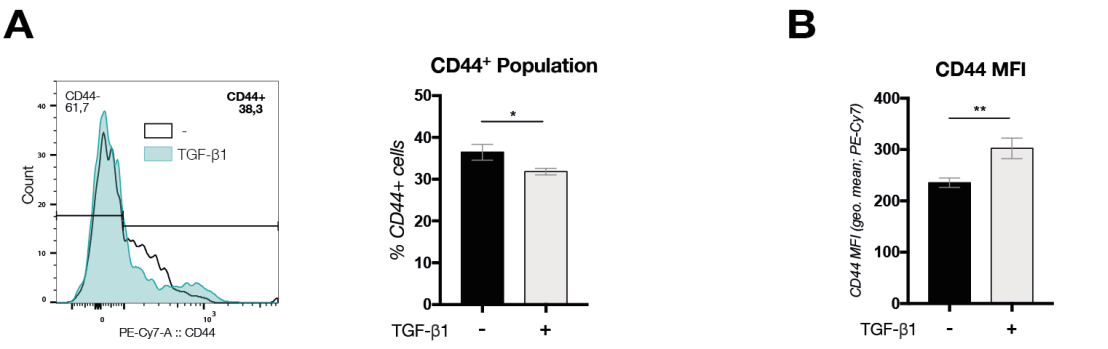

FIGURE 3: TGF-β1 Boosts CD44 Expression in Culture Activated HSC
(A) The amount of CD44⁺ within isolated primary murine HSC was FACS analyzed after seven days of culture activation. Cells were incubated with either complete medium only (-) or complete medium supplemented with 2 ng/ml TGF-β1 at D0. The data shown stem from one experiment with three technical replicates. Unpaired t-test; *p < 0.1 **(B)** CD44 surface expression within the CD44⁺ cell population was analyzed at D7 using the geometric mean of PE-Cy7 (CD44) fluorescence intensity. HSC were incubated with either complete medium only (–) or complete medium supplemented with 2 ng/ml TGF-β1 at D0. The data shown stem from one experiment with three technical replicates. Unpaired t-test; * p ≤ 0.05, ** p ≤ 0.01.

expression may additionally be affected by TGF-β1. As it has been shown that quiescent, but not activated myofibroblast-like HSC are sensitive to TGF-β1, we added TGF-β1 (2ng/ml) at D0 of cell culture (Dooley et al. 2001). CD44 expression was measured by flow cytometry. After 7 days, in two out of three experiments a greater amount of $CD44^+$ HSC developed within the TGF-β1 treated group (Figure 3A). These data will need further validation. However, in all three experiments, when analyzing the CD44 MFI within the $CD44^+$ HSC using geometric mean, TGF-β1 treated HSC were found to significantly upregulate CD44 expression (Figure 3B). Our data suggests that TGF-β1 potentiates CD44 upregulation on HSC after seven days of culture activation and promotes the formation of $CD44^+$ HSC cells.

3.1.5 HSC Dampen Bone Marrow Cell Maturation by Decreasing Dendritic Cell Formation and Promoting Myeloid-Derived Suppressor Cell Phenotypes

MDSC are thought to be comprised of immature myeloid progenitor cells (Hsieh 2015a). They are induced in situations of cancer, chronic inflammation and infections, trauma, transplantation and autoimmune disorders, exerting immunosuppressive functions (Greifenberg et al. 2009) (Höchst et al. 2015) (Dysthe & Parihar 2020). MDSC can be found in spleen, lymph nodes, tumors, blood and bone marrow (Lim et al. 2020). They are commonly but not exclusively produced in the bone marrow of people in pathological conditions (Gabrilovich & Nagaraj 2009) (Khaled et al. 2013). In murine *in vitro* models, they can be detected during maturation of bone marrow derived DC using GM-CSF (Höchst et al. 2015). MDSC generation was found to be mainly driven by GM-CSF (Chou et al. 2012) (Greifenberg et al. 2009) (Klotz et al. 2007) (Na et al. 2016) (Morales et al. 2010). Furthermore, addition of HSC to DC cultures promotes the expansion and differentiation of MDSC and inhibits the maturation to DC (Arakawa et al. 2014) (Chou et al. 2011) (Chou et al. 2012) (Hsieh et al. 2019) (Li et al. 2014). To find out whether CD44 expressed by HSC is responsible for facilitating expansion of MDSC by HSC presence, we initially cultured BMC either alone (monoculture) or on a confluent layer of D7 culture-activated primary HSC (coculture) (Figure 4B) for four days in medium supplemented with 30% supernatant of GM-CSF-producing cell line Ag 8653. Immature DC were gated for alive single cells, followed by cells positive for myeloid lineage marker CD11b and positive for dendritic cell marker

CD11c (Figure 4A). Granulocytic MDSC (gMDSC) - denoted H-gMDSC when derived from HSC coculture - were gated as $CD11b^{+}CD11c^{-}Ly6G^{+}Ly6C^{dim}$ cells. Monocytic

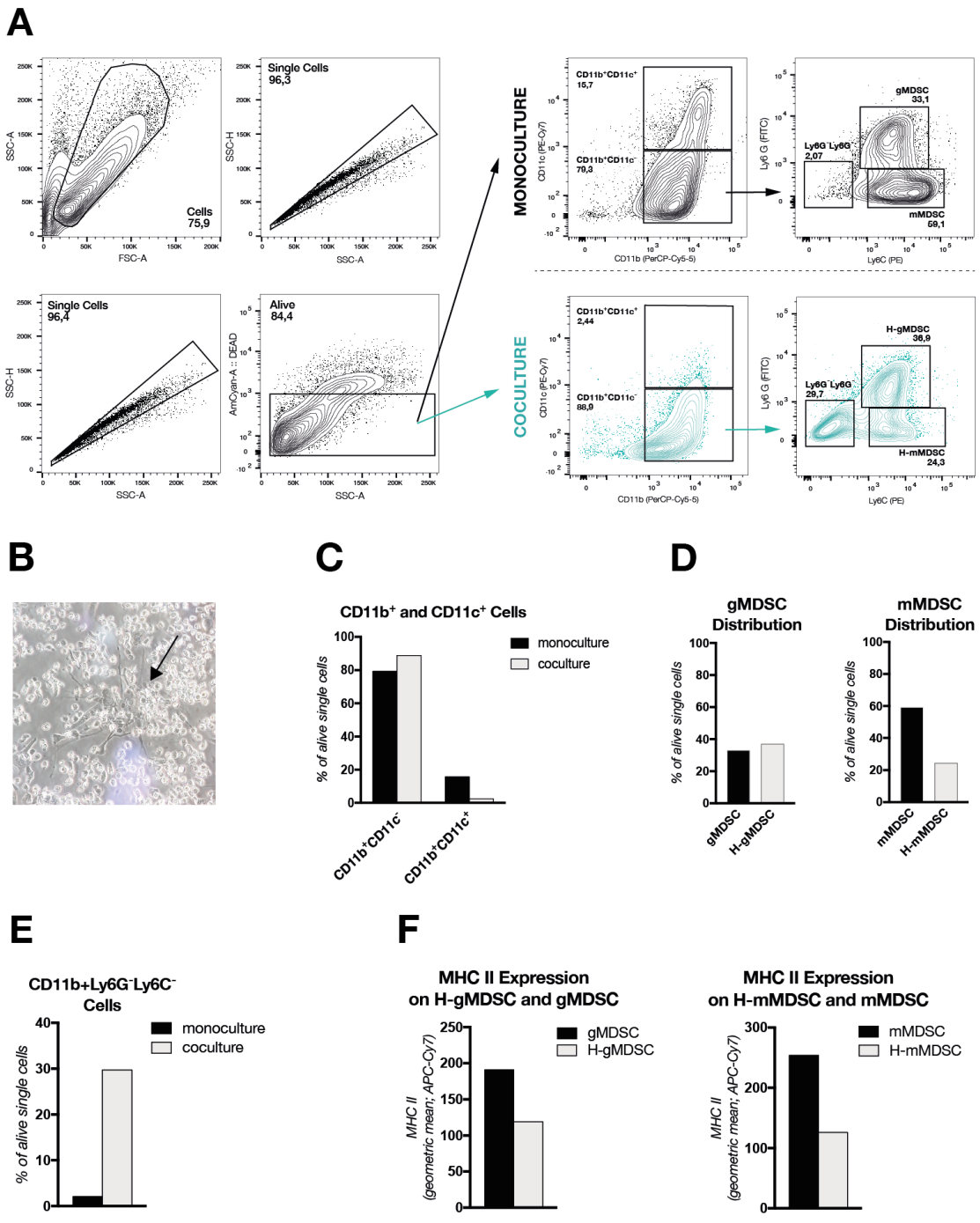

FIGURE 4: Coculture of BMC with HSC Dampens DC Maturation While Promoting the MDSC Phenotype
(A) Gating strategy of BMC after spending four days in culture either solely (monoculture) or with HSC in coculture (coculture). Cocultured cells within the MDSC phenotype gates were termed H-gMDSC and H-mMDSC. **(B)** Phase contrast microscopy images of culture activated, adherent HSC (black arrow) in coculture with BMC at day 2. **(C)** FACS-based analysis of CD11b and CD11c expression on BMC from monoculture compared to cocultured cells. **(D)** FACS-based analysis of mMDSC and gMDSC subsets either from monoculture (mMDSC & gMDSC) or coculture (H-mMDSC & H-gMDSC). **(E)** FACS analysis of $CD11b^{+}Ly6G^{-}Ly6C^{-}$ cells within monocultured or cocultured BMC. **(F)** Comparison of MHC II expression levels in MDSC subsets from either cocultured (H-mMDSC & H-gMDSC) or monocultured (mMDSC & gMDSC) BMC, using the geometric mean fluorescence intensity. The data shown are representative of three independent experiments.

MDSC (mMDSC) and H-mMDSC were gated as $CD11b^{+}CD11c^{-}Ly6G^{-}Ly6C^{+/hi}$ cells (Figure 4A). In presence of HSC, cocultured BMC showed about eightfold less $CD11b^{+}CD11c^{+}$ cells (2% vs. 16%) indicating a dampened formation of immature DC (Figure 4C). Accordingly, more monocytic $CD11b^{+}CD11c^{-}$ cells emerged in presence of HSC compared to monoculture (88% vs. 78%). In the MDSC subsets, cocultured BMC developed considerably less mMDSC and slightly more gMDSC (Figure D). Interestingly, we found a large population $CD11b^{+}Ly6G^{-}Ly6C^{-}$ cells formed almost exclusively in BMC cultured in presence with HSC (29,7% vs 2,3%) (Figure 4E). A further common and distinctive feature among murine MDSC (Chou et al. 2011) (Yang Zhao et al. 2015) is their low MHC II surface expression. Both, H-mMDSC and H-gMDSC show reduced MHC II expression compared to monocultured counterparts, thus being more congruent with the MDSC phenotype (Figure 4F).

3.1.6 The Presence of HSC Boosts Suppressive Capacity of MDSC Generated during BMC Maturation with GM-CSF

Next, we sought to confirm our phenotypical data, that suggest that HSC presence of boosts generation of MDSC from BMC, by assessing the suppressive function of the generated MDSC phenotypes. To this end, we performed suppression assays.

Suppression assays are a commonly performed assays, measuring the ability of suppressive cells (e.g. Tregs or MDSC) to suppress T cell proliferation *in vitro*. Therefore, we isolated splenic wild type polyclonal $CD4^{+}$ T cells from C57BL/6 mice, labeled them with CFSE and either activated them using CD3/CD28 dynabeads or left them untreated as a negative control. Unsorted MDSC from monoculture (MDSC) or from HSC coculture (H-MDSC) were added to the activated $CFSE^{+}$ $CD4^{+}$ T cells in 1:1, 1:2 and 1:4 ratios (MDSC:T cells). 72h later, proliferation of viable $CD4^{+}$ T cells was analyzed by flow cytometry (Figure 5A). H-MDSC showed significantly increased and more profound suppressive capacities towards T cell proliferation compared to monocultured counterparts (Figure 5B). The superior suppressive function of BMC cocultured in presence of HSC could be result from overall higher $CD11b^{+}CD11c^{-}$ cell numbers, indicating that more MDSC and less DC were present (Figure 4C) or from the induction of more efficient suppression mechanisms, reflected by the above mentioned more congruent MDSC phenotypical traits.

To compare suppressive capacities of monocytic and granulocytic MDSC subsets on

a cell to cell base, we sorted for H-mMDSC and H-gMDSC subsets as seen in Figure 4A. By sorting, we could further exclude any impact of the $CD11b^{+}Ly6G^{-}Ly6C^{-}$ subpopulation, that almost exclusively occurred within cocultured BMC. Hoechst et. al. reported that *in vivo* suppressive capacity can both reside in mMDSC and gMDSC, depending on the organ and chronic inflammatory settings. In bile-duct ligated mice, suppression was present in the hepatic mMDSC but not gMDSC subset (Höchst

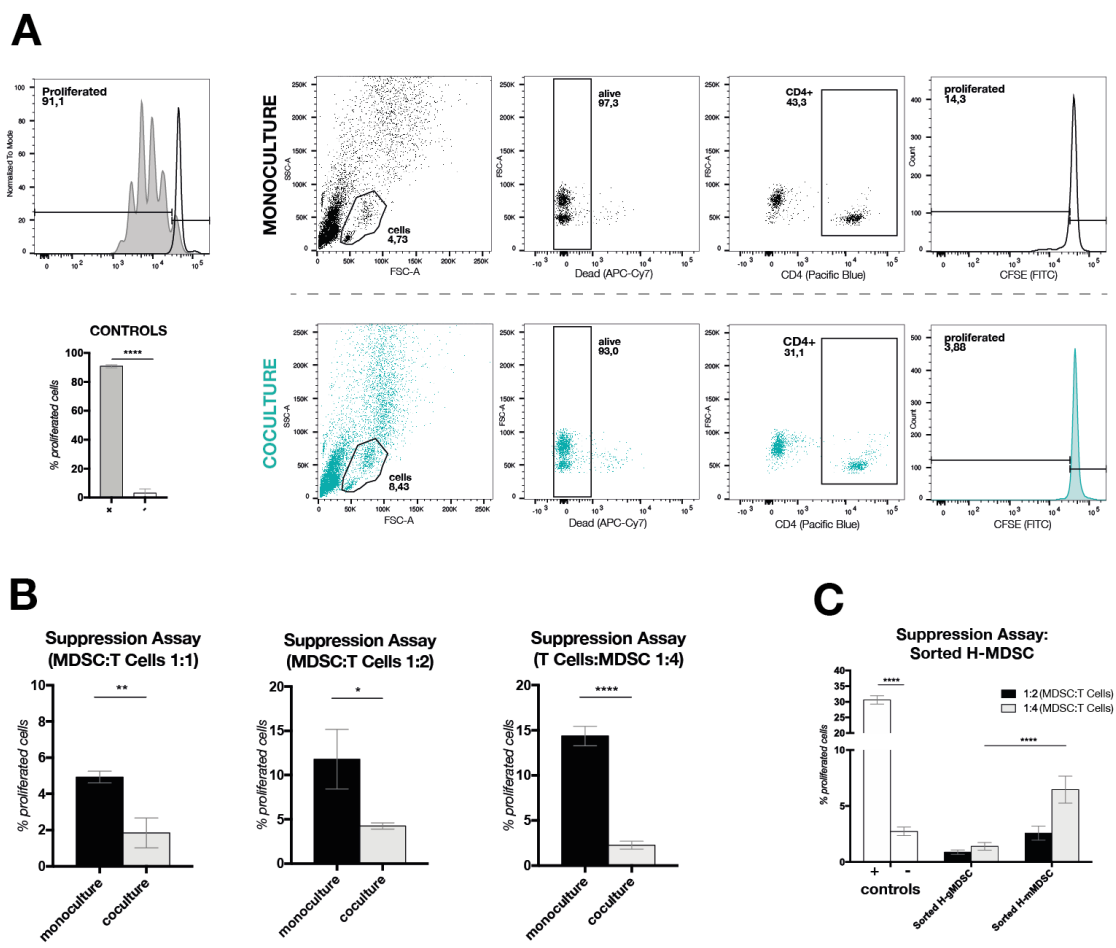

FIGURE 5: MDSC from HSC Coculture Show Increased Suppressive Capacity
(A) T cells were either stimulated (+) or left unstimulated as a negative control (–). After culturing BMC either alone (monoculture) or with HSC (coculture) for four days, we FACS-sorted $CD11b^{+}Ly6G^{+}Ly6C^{dim}$ (gMDSC) and $CD11b^{+}Ly6G^{-}y6C^{+}$ (mMDSC) cells. Coculture-derived MDSC were labelled H-mMDSC or H-gMDSC. These cells were then added to T cells in 1:1, 1:2, and 1:4 ratios (MDSC:T cells). $CD4^{+}$ T cell proliferation was assessed by FACS. Cells were gated by typical T cell size, viability, and CD4 expression. **(B)** Proliferated cells were measured as described and compared as indicated. Composite data are shown from two independent experiments. Unpaired t-test; * $p \leq 0.05$, ** $p \leq 0.01$, *** $p \leq 0.001$. **(C)** Cocultured BMC were sorted for $CD11b^{+}Ly6G^{+}Ly6C^{dim}$ (H-gMDSC) and $CD11b^{+}Ly6G^{-}Ly6C^{+}$ (H-mMDSC). One-way ANOVA was used; **** $p \leq 0.0001$.

et al. 2015). Surprisingly, both sorted H-gMDSC and H-mMDSC displayed profound suppression on 1:2 and 1:4 ratios (H-MDSC: T cells). Moreover, H-gMDSC were more profound suppressors compared to H-mMDSC (Figure 5C). Taken together our results

prove that the presence of HSC boosts the suppressive capacity of *in vitro* generated MDSC from BMC.

3.1.7 CD44 Deficiency of HSC Does Not Affect the Phenotype of Generated MDSC

It was previously shown by siRNA mediated knock-down of CD44 that the human HSC cell line LX2 utilizes CD44 to induce mMDSC from PBMC (Hoechst et al. 2013). To investigate whether CD44 has a similar role in murine HSC induced MDSC induction, we isolated primary HSC from $CD44^{-/-}$ mice (Schmits, Filmus, Gerwin, Senaldi, Kiefer, Kundig, Wakeham, Shahinian, Catzavelos, Rak, Furlonger, Zakarian, Simard, Ohashi, Paige, Gutierrez-Ramos & Mak 1997b).

First, we checked for CD44 expression on HSC during culture activation to validate the CD44 knock out in our animals. Neither CD44 wild type nor $CD44^{-/-}$ HSC expressed CD44 on D0 (Fig 6A). Furthermore, there was no upregulation of CD44 on $CD44^{-/-}$ HSC compared to high levels of CD44 expression found on wild type HSC (Figure 6A). Since CD44 plays an essential role in cell growth and motility (Ponta et al. 2003) we assessed HSC morphology using phase contrast microscopy during culture activation to exclude possible changes in cell-cell contact interactions. We did not observe morphological differences between HSC from either genotype (Figure 6B). Next, we cultured BMC in presence of D7 HSC isolated from wild type or $CD44^{-/-}$ mice as described above. CD44 deficiency did not affect the development of $CD11b^{+}CD11c^{+}$ and $CD11b^{+}CD11c^{-}$ populations, suggesting an unaltered, CD44 independent dampening of DC maturation (Figure 6C). CD44 deficiency of HSC did not alter the dampening of DC maturation or distribution of generated g-/mMDSC phenotypes (Figure 6D). Furthermore, the MHC II surface expression levels were not affected by the lack of CD44 expression on HSCs (Figure 6E). Upon analyzing MDSC typical surface markers, our data suggest that CD44 deficiency in HSC does not cause relevant phenotypic changes in *in vitro* generated MDSC from BMC.

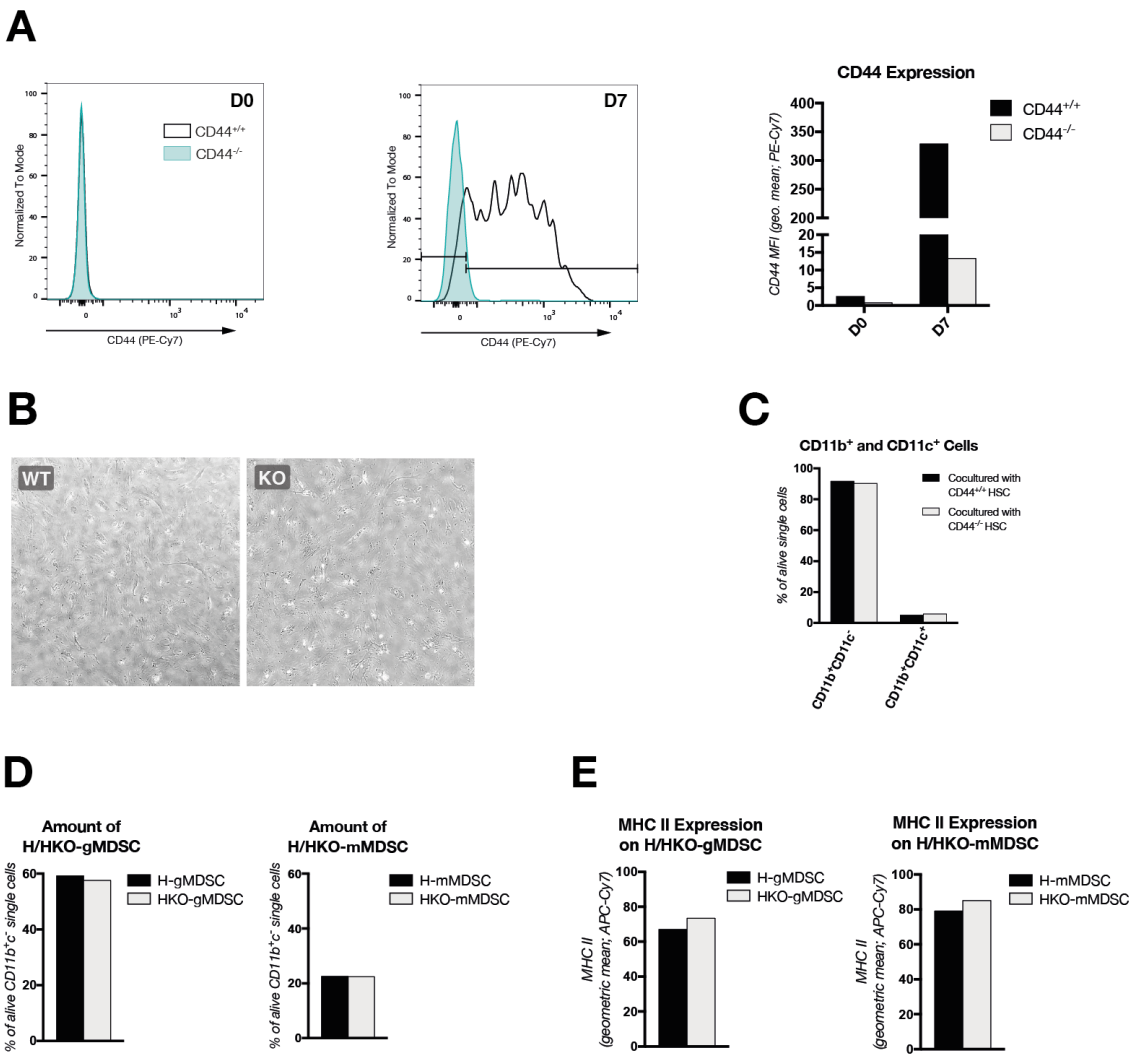

FIGURE 6: CD44 Knock Out on HSC Does Not Alter the Amount or MHC II Expression of Generated MDSC
(A) CD44 Expression on HSC isolated from $CD44^{+/+}$ and $CD44^{-/-}$ mice was measured using FACS. Measurements were taken ex vivo (D0) and after seven days in culture (D7). CD44 expression calculated using geometric mean fluorescence intensity. **(B)** Phase contrast microscopy images of isolated $CD44^{+/+}$ and $CD44^{-/-}$ HSC at day seven of culture activation. **(C)** FACS-based analysis of CD11b and CD11c expression on BMC after four days of coculture with either $CD44^{+/+}$ or $CD44^{-/-}$ culture activated HSC. **(D)** Comparison of $CD11b^{+}Ly6G^{+}Ly6C^{int}$ (H-gMDSC) and $CD11b^{+}Ly6G^{-}Ly6C^{+}$ (H-mMDSC) subsets within FACS analyzed BMC after four days of coculture with either $CD44^{+/+}$ (H-mMDSC/H-gMDSC) or $CD44^{-/-}$ (HKO-mMDSC/HKO-gMDSC) culture activated HSC. **(E)** FACS analysis of MHC II expression on H/HKO-gMDSC and H/HKO-mMDSC. Data shown are representative of two independent experiment.

3.1.8 CD44 Expressed by HSC Contributes to the Suppressive Capacity of MDSC Generated in Their Presence

Although the lack of CD44 expressed by HSC does not alter the expression of the typical surface marker MHC II or the proportion of Ly6G and Ly6C expressing cells, we subsequently analyzed the functional properties of the generated MDSC, by performing suppression assays. Due to different suppressive mechanisms of mMDSC

and gMDSC, we FACS-sorted for mMDSC and gMDSC as done before (Figure 4A). MDSC were taken from cocultures with CD44$^{+/+}$ HSC (H-MDSC) and compared to the ones generated in presence of CD44$^{-/-}$ HSC (H_{KO}-MDSC).

Gating strategy for FACS sorting was identical to phenotype gating used before (Figure 4A). At a 1:2 ratio (MDSC:T cells), mMDSC and gMDSC, regardless of independent from whether they were generated in presence of CD44$^{+/+}$ or CD44$^{-/-}$ HSC, appear to equally suppressive (Figure 7A). However, H-gMDSC were found to be significantly more suppressive than H_{KO}-gMDSC in a 1:4 ratio, suggesting a crucial role of CD44 in establishing profound suppression mechanisms within the gMDSC subset (Figure 7B). Unfortunately, FACS-based sorting resulted in relevant cell count losses so that we

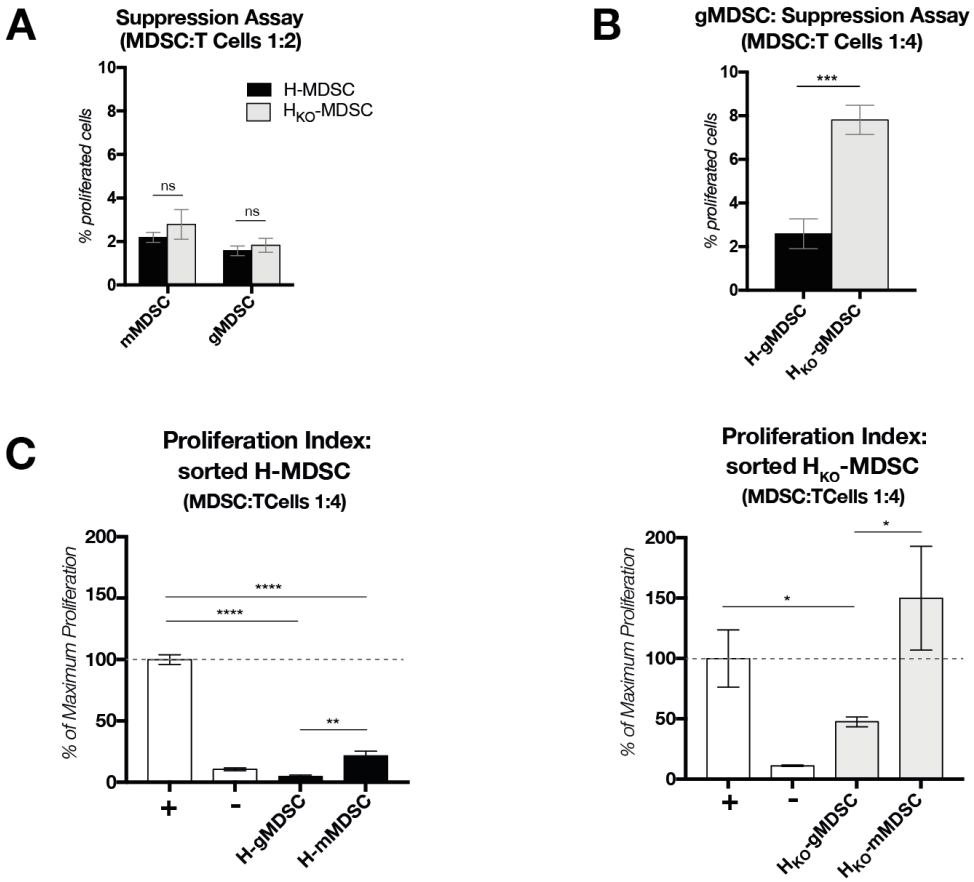

FIGURE 7: CD44 Expressed by HSC Contributes to the Suppressive Capacity of MDSC Generated in Their Presence **(A)** and **(B)** CD4$^+$ T cells were isolated and labelled with carboxyfluorescein succinimidyl ester (CFSE), then stimulated with anti-CD3/CD28 Dynabeads (+) or left unstimulated as a negative control (–). After coculturing BMC with either CD44 wild-type (CD44$^{+/+}$) or CD44 knockout (CD44$^{-/-}$) HSC for four days, we FACS-sorted CD11b$^+$Ly6G$^+$Ly6C^{int} (gMDSC) and CD11b$^+$Ly6G$^-$Ly6C$^{+/hi}$ (mMDSC) cells. BMC cocultured with CD44$^{+/+}$ HSC were labelled H-MDSC, or HKO-MDSC when cocultured with CD44$^{-/-}$ HSC, respectively. These MDSC were added to T cells in 1:2 and 1:4 ratios (MDSC:T cells). CD4$^+$ T cell proliferation was measured using flow cytometry. Data shown represent two independent experiments. Unpaired t-test; ***p<0.001. **(C)** Proliferation indices of sorted H/HKO-m/gMDSC were calculated by normalizing the positive control to 100% proliferation (maximum proliferation). Each graph represents one experiment. Unpaired t test; ****p<0.0001, **p<0.01, *p<0.1.

could not directly compare the monocytic MDSC on a 1:4 ratio within one experiment. The first experiment allowed us to analyze H-mMDSC, but not H_{KO}-mMDSC, and vice versa in the second experiment. Therefore, we calculated the proliferation indices to partly overcome the lack of direct comparability (Figure 7C). H-mMDSC were still strong suppressors at a 1:4 ratio while the presence of H_{KO}-mMDSC at a 1:4 ratio seemed to slightly promote and not inhibit the proliferation of T cells (Figure 7C). H_{KO}-gMDSC overall were more profoundly suppressive compared to H_{KO}-mMDSC in both experiments (Figure 7C), resembling the results we obtained with H-MDSC (Figure 5C). Taken together these results indicate that the development of profound suppressive capacities in both gMDSC and mMDSC to a relevant extent depends on HSC-expressed CD44.

3.2 The Role of CD44 in the Induction of Human Monocytic Myeloid-Derived Suppressor Cells

3.2.1 Introduction

CD44 was found to be essential for transdifferentiating $CD14^+$ PBMC into $CD14^+HLA\text{-}DR^{-/lo}$ mMDSC by HSC in a cell-cell contact dependent manner (Hoechst et al. 2013). CD44 is a widely expressed transmembrane glycoprotein involved in cell-cell adhesion and cell-matrix interactions (Turley et al. 2002; Yoo et al. 2016; Ponta et al. 2003). It mediates cellular homing, invasiveness, metastasis and angiogenesis (C. Chen et al. 2018) (Yoo et al. 2016) (Ponta et al. 2003). Additionally, CD44 can also function as receptor, a coreceptor and a signaling component (Ponta et al. 2003) (Turley et al. 2002). Given the heterogenicity of CD44's various functional traits, the exact mechanism by which CD44 promotes MDSC induction remains unclear. To gain more precise knowledge about its role in human MDSC induction, we aimed at assessing the effect of CD44 without its membrane-bound integrity to find out whether it would increase MDSC induction or their suppressive capacity by itself.

Therefore, we established a model of mMDSC induction *in vitro,* that could later be modified by adding recombinant CD44 protein. It has been shown that suppressive mMDSC can be effectively generated from human PBMC by redirecting DC maturation using GM-CSF in combination with IL-6 (Casacuberta Serra et al. 2017). GM-CSF is a

key factor in maintaining myeloid cell viability and promotes the formation of immature myeloid cells, like immature dendritic cells (iDC) (Ko et al. 2009; Lechner et al. 2010; Obermajer et al. 2011). It has also been described to be essential for inducing MDSC in human bone marrow (Marigo et al. 2010). Furthermore, GM-CSF was found to be solely sufficient for the induction of highly suppressive human MDSC from PBMC *in vitro* (Lechner et al. 2010). Additional cytokines, in particular TGF-β1 can expand mMDSC populations and enhance their ability to suppress $CD4^+$ T cells (C.-R. Lee et al. 2018).

3.2.2 Culture of $CD14^+$ PBMC with GM-CSF with and without TGF-β1 Effectively Generates Steady mMDSC Phenotypes *in vitro*

We isolated $CD14^+$ cells from PBMC from a healthy donor which routinely showed purity levels over 90% (96% ± 3,365 SD) (Figure 8A). We then cultured isolated $CD14^+$ PBMC either with GM-CSF or GM-CSF in combination with TGF-β1 for six days, after which cells were harvested and analyzed by flow cytometry. Dendritic cell–specific intercellular adhesion molecule-3-grabbing non-integrin (DC-SIGN) can be utilized as a surface marker to discriminate immature DC (iDC) from mMDSC (Obermajer & Kalinski 2018; An et al. 2018). DC-SIGN was not expressed by *ex vivo* PBMC (data not shown). Although iDC are described as $CD14^-DC\text{-}SIGN^+$ by Obermajer et al. (Obermajer & Kalinski 2018), a relevant proportion of our $DC\text{-}SIGN^+$ cells co-expressed CD14, resembling a subpopulation of inflammatory monocytic derived DC as described in recent literature (Marzaioli et al. 2020; Collin & Bigley 2018). Consequently, viable single cells were gated for $CD14^+DC\text{-}SIGN^-$ (mMDSC) and $DC\text{-}SIGN^+$ (iDC) (Figure 8B). We observed a distinct iDC formation within GM-CSF-only treated cells (64%) compared to substantially reduced iDC formation within cells treated with GM-CSF and TGF-β1 (15%) (Figure 8C). Reversely, we observed substantially higher amounts of mMDSC within GM-CSF and TGF-β1 treated PBMC, suggesting that in TGF-β1 presence iDC formation is inhibited and further shifted towards mMDSC phenotype expansion (Figure 8C).

CD14 expression is described to be downregulated by GM-CSF (Kruger et al. 1996) and TGF-β1 (Hamon et al. 1994). Furthermore, Casacuberta-Serra et. al. found downregulated CD14 surface expression on PBMC exposed to GM-CSF combined with IL-6 or TGF-β1 for six days. Indeed, we could detect CD14 downregulation on

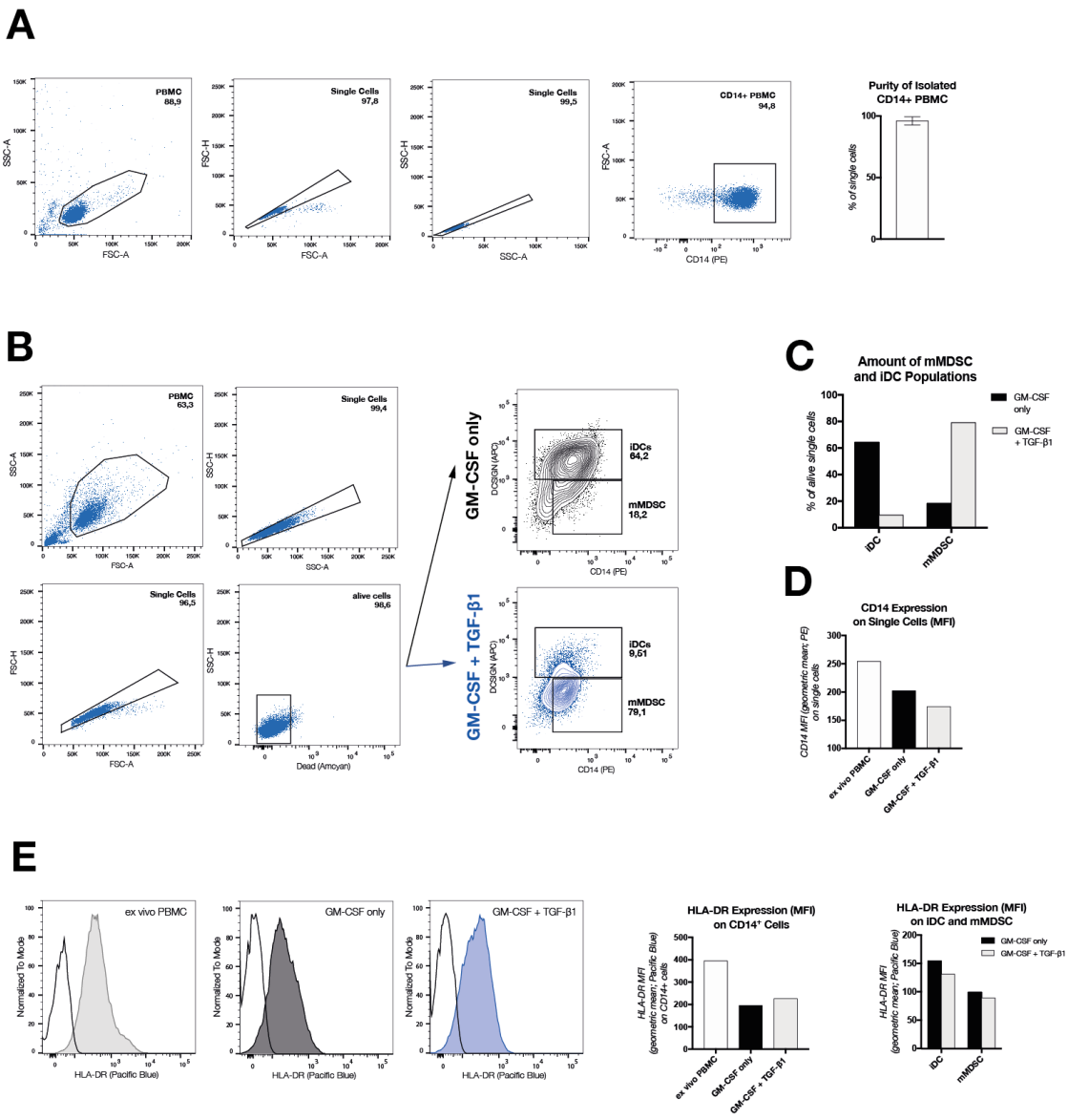

FIGURE 8: GM-CSF Alone and in Combination with TGF-β1 Induces a Stable mMDSC Phenotype from PBMC In Vitro
(A) Human PBMC were isolated from buffy coats of healthy donors and MACS-sorted for CD14. Purity was assessed by FACS gating as indicated. Data shown stem from three independent experiments. **(B)** MACS-purified CD14⁺ PBMC were cultured in either GM-CSF alone or in GM-CSF plus TGF-β1-containing medium. On day six, cultured cells were FACS-analyzed and gated as indicated. Viable single cells were further gated for DC-SIGN⁺ (iDC) and CD14⁺DC-SIGN⁻ (mMDSC). **(C)** Frequency of iDC and mMDSC in either GM-CSF only or GM-CSF plus TGF-β1 stimulated CD14⁺ PBMC. **(D)** CD14 expression was measured using the geometric mean of PE fluorescence (CD14). Pregate was set on CD14⁺ cells. **(E)** HLA-DR expression on *ex vivo* MACS-purified CD14⁺ PBMC and on CD14⁺ PBMC cultured for six days in either GM-CSF alone or GM-CSF plus TGF-β1. Pregating was performed on CD14⁺ cells. Data shown in B–E are representative of three independent experiments, including two different blood donors.

cells exposed to GM-CSF with or without TGF-β1, with lower levels of CD14 on cells that were additionally exposed to TGF-β1 (Figure 8D), matching Casacuberta-Serra's results (Casacuberta Serra et al. 2017). As human MDSC are also known to downregulated MHC class II expression, we analyzed HLA-DR expression on CD14⁺ cells after culture and compared them to *ex vivo* cells. HLA-DR expression was

downregulated on both GM-CSF treated cells and cells treated with GM-CSF combined with TGF-β1 (Figure 8E). Considering the reduced induction of HLA-DR expressing iDC and increased induction of mMDSC, which potentially downregulate HLA-DR, we expected CD14⁺ cells treated with GM-CSF and TGF-β1 to show a lower overall HLA-DR expression. Interestingly, we did not obtain consistent differences in HLA-DR expression. However, HLA-DR was less expressed on mMDSC compared to iDC in all three experiments (Figure 8E), indicating a more immature phenotype of mMDSC. Taken together, treatment of CD14⁺ PBMC with GM-CSF alone or combined with TGF-β1 effectively generated cells with an mMDSC phenotype.

3.2.3 Suppressive MDSC Are Generated by Treating CD14⁺ PBMC with GM-CSF and GM-CSF in Combination with TGF-β1

To confirm that the generated mMDSC not only possess the phenotype but also

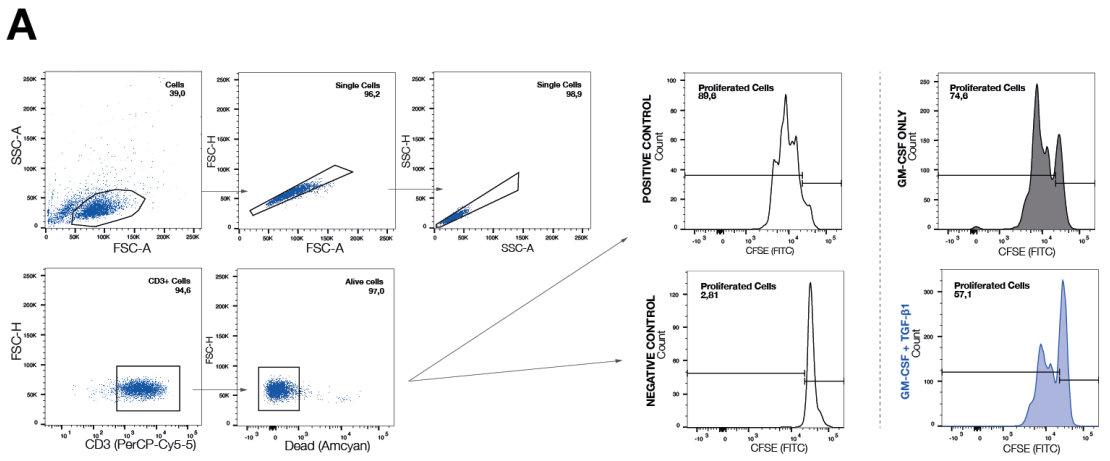

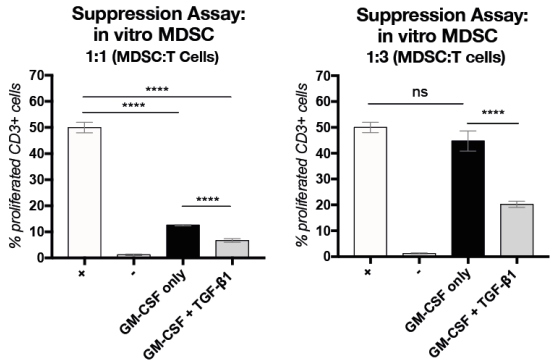

FIGURE 9: GM-CSF Alone and Combined with TGF-β1 Generates Suppressive Entities In Vitro

(A) Human CD8⁺ T cells were isolated and labelled with carboxyfluorescein succinimidyl ester (CFSE). T cells were either stimulated (+) or left unstimulated as a negative control (–). CD14⁺ PBMC were incubated with either GM-CSF (10 ng/ml) alone or GM-CSF combined with TGF-β1 (2 ng/ml) for six days. Cells were harvested, and activated T cells were added in various ratios. After 72 hours, cells were analyzed by flow cytometry. T cells were gated as viable single cells expressing CD3⁺. Proliferation of T cells was assessed by measuring CFSE fluorescence (FITC channel). **(B)** Proliferated cells were measured as described and compared across different ratios. Data shown are representative of three independent experiments. ANOVA; ns = not significant; *** $p \leq 0.001$.

suppressive function, we performed suppression assays. We added $CD14^+$ PBMC, after treatment with either GM-CSF only or GM-CSF combined with TGF-β1 for six days, to CFSE-labeled $CD8^+$ T cells. Proliferation of activated viable single $CD3^+$ cells was measured after 72 hours of incubation using flow cytometry (Figure 9A). Both, $CD14^+$ PBMC treated with GM-CSF and treated with GM-CSF plus TGF-β1 were capable of suppressing $CD8^+$ T cell proliferation (Figure 9B). At a 1:3 (MDSC:T cells) ratio, suppressive function started to decline, which might display a threshold area for the effective mMDSC number needed to counteract T cell proliferation (Figure 9B). PBMC cultured with GM-CSF and TGF-β1 were significantly more suppressive than PBMC cultured with GM-CSF only (Figure 9B), which is most likely explained by the larger amount of mMDSC phenotypes generated by the presence of TGF-β1 (Figure 8C-E). In summary, we established an *in vitro* model for generating human mMDSC from $CD14^+$ PDBMC by either using GM-CSF only or in combination with TGF-β1.

3.2.4 The CD44 Protein alone Does Not Affect the Phenotype or Amount of *in vitro* Generated Human mMDSC

In previous work of Hoechst et al., it has been shown that anti-CD44 blocking antibodies reduced the HLA-DR downregulation and the suppressive capacity of mMDSC induced from $CD14^+$ PBMC in presence of human HSC cell line LX2 in a dose-dependent manner (Hoechst et al. 2013). Furthermore, siRNA knock down of CD44 in LX2 cells led to their inability to facilitate HLA-DR downregulation of $CD14^+$ PBMC (Hoechst et al. 2013). As it has been demonstrated that the expression of CD44 on HSC is essential for inducing human mMDSC from $CD14^+$ PBMC by HSC, we wanted to elucidate whether the CD44 protein alone, i.e. without the cellular context of HSC, would increase mMDSC induction and/or promote their expansion or their functional traits.

Therefore, we conducted the induction of mMDSC as described above on culture dishes coated with either recombinant huCD44-Fc or as a control recombinant IgG1-Fc. We phenotypically analyzed the cells at day six using flow cytometry, with the gating strategy matching the one used above (Figure 8B). Initially we compared the amount of generated DC-$SIGN^+$ iDC and $CD14^+$DC-$SIGN^-$ mMDSC. Generating mMDSC from $CD14^+$ PBMC on recombinant CD44-Fc did not alter the amount of generated iDC or the mMDSC compared to cells cultured on the control

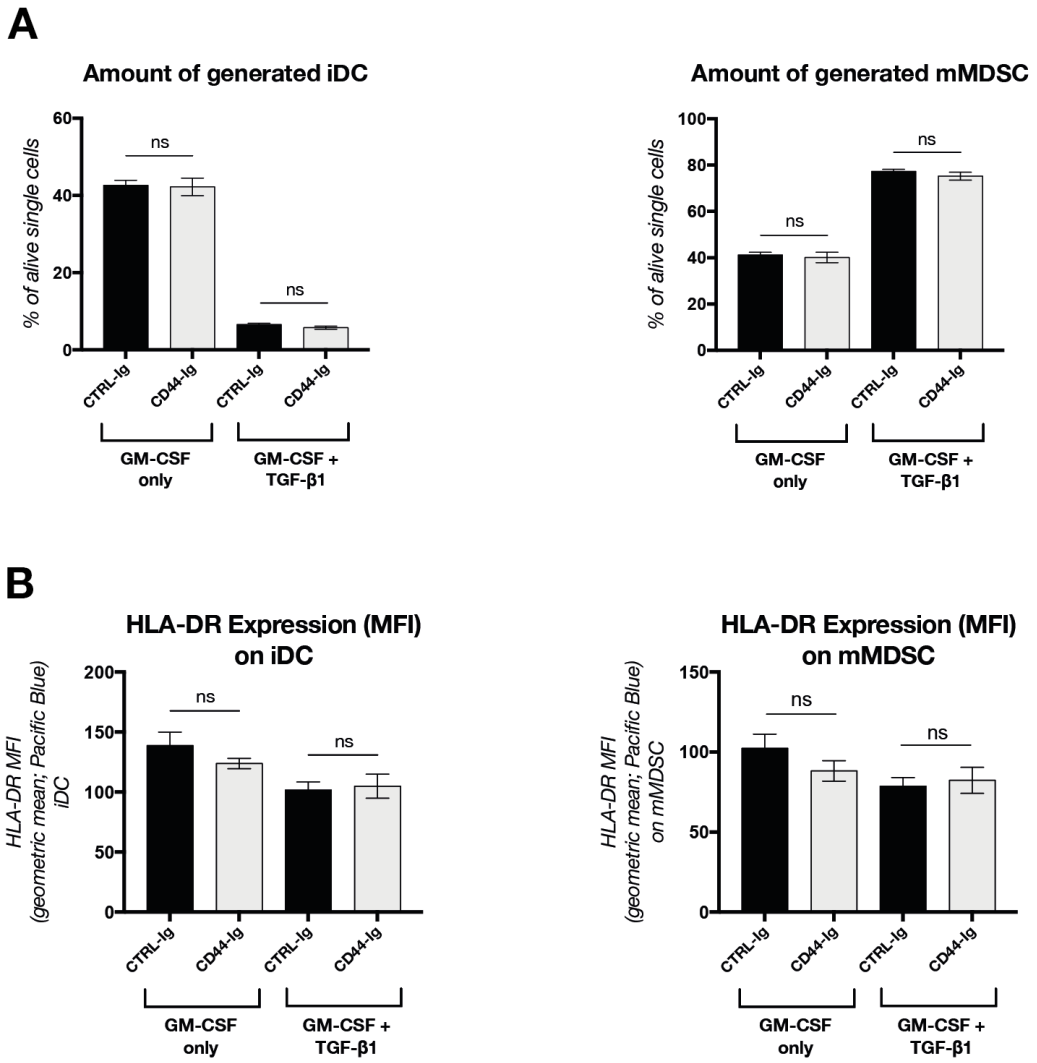

FIGURE 10: CD44 Does Not Alter the Phenotype or Frequency of In Vitro Generated Human mMDSC

(A) Human CD14⁺ PBMC were isolated and cultured in either GM-CSF (10 ng/ml) alone or GM-CSF combined with TGF-β1 (2 ng/ml) for six days. Prior to plating, culture dishes were coated with 1 µg/ml recombinant CD44-Fc (CD44-Ig) or recombinant IgG1-Fc (CTRL-Ig), respectively. Cells were harvested on day six and analyzed by flow cytometry. Viable single cells were gated for DC-SIGN⁺ cells (immature dendritic cells, iDC) and CD14⁺DC-SIGN⁻ monocytic MDSC (mMDSC). Triplicates were obtained from three independent wells. Data shown are representative of at least three independent experiments. Data were analyzed using ANOVA. ns = not significant. **(B)** HLA-DR expression on mMDSC and iDC was analyzed using the mean fluorescence intensity (MFI; Pacific Blue channel) in flow cytometry. Data shown are representative of at least three independent experiments. ANOVA test. ns = not significant.

IgG1-Fc (Figure 10A) in both GM-CSF only and GM-CSF plus TGF-β1 settings (Figure 10A). It is noteworthy, that culturing CD14⁺ PBMC on coated plates match the experiments with uncoated plates concerning the generated amount of iDC and mMDSC in comparison of the two treatment groups. Next, we compared the expression of HLA-DR on iDC and mMDSC. HLA-DR expression on both iDC and mMDSC was not altered after coculture in the presence of CD44-Ig Fc compared those

cultured on control IgG1-Fc (Figure 10B). Taken together, the presence of the CD44 protein solely does not alter the induction or expansion of mMDSC phenotypes in this model of human MDSC generation *in vitro*.

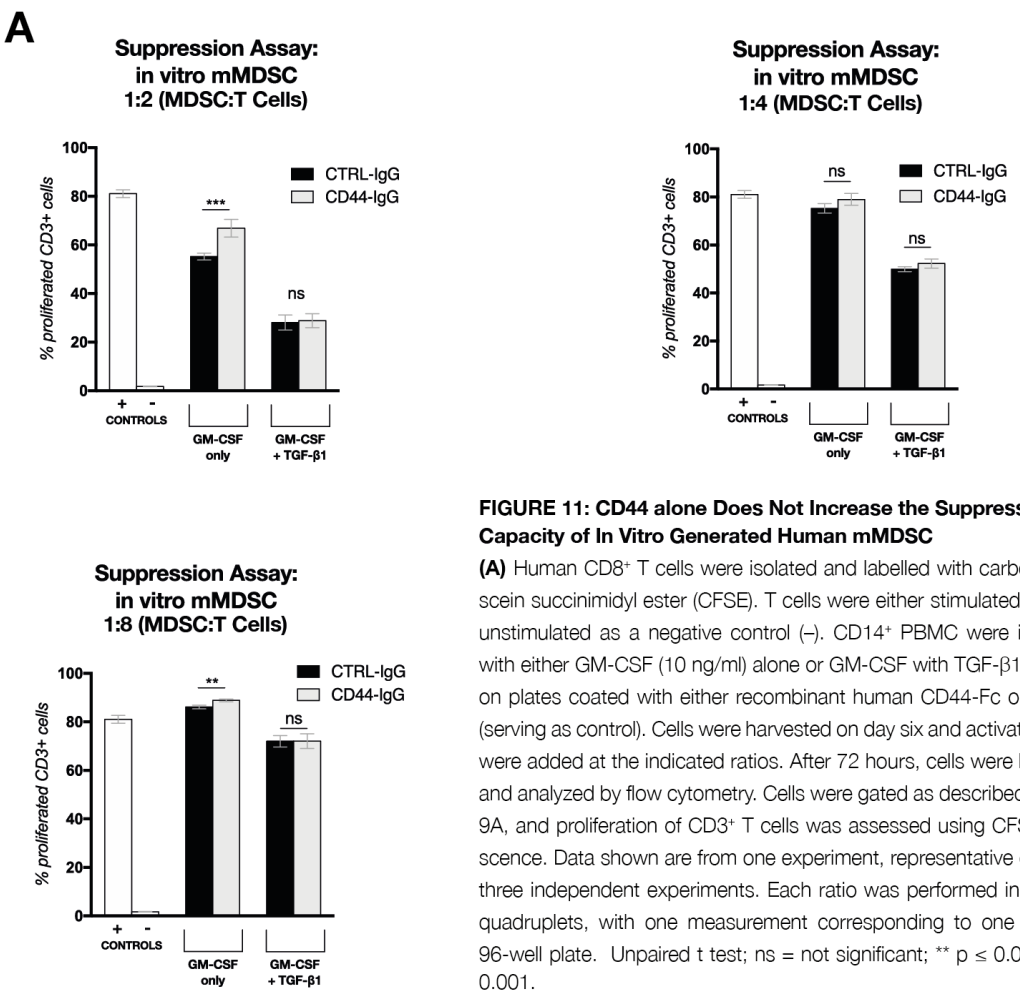

FIGURE 11: CD44 alone Does Not Increase the Suppressive Capacity of In Vitro Generated Human mMDSC

(A) Human $CD8^+$ T cells were isolated and labelled with carboxyfluorescein succinimidyl ester (CFSE). T cells were either stimulated (+) or left unstimulated as a negative control (–). $CD14^+$ PBMC were incubated with either GM-CSF (10 ng/ml) alone or GM-CSF with TGF-β1 (2 ng/ml) on plates coated with either recombinant human CD44-Fc or IgG1-Fc (serving as control). Cells were harvested on day six and activated T cells were added at the indicated ratios. After 72 hours, cells were harvested and analyzed by flow cytometry. Cells were gated as described in Figure 9A, and proliferation of $CD3^+$ T cells was assessed using CFSE fluorescence. Data shown are from one experiment, representative of at least three independent experiments. Each ratio was performed in technical quadruplets, with one measurement corresponding to one well of a 96-well plate. Unpaired t test; ns = not significant; ** $p \leq 0.01$, *** $p \leq 0.001$.

3.2.5 CD44 Does Not Increase the Suppressive Capacity of *in vitro* Generated Human mMDSC

Despite not phenotypically altering the cultured $CD14^+$ PMBC, CD44-Fc may still affect the suppressive capacity of the generated MDSC. Therefore, we performed suppression assays of cells cultured in either GM-CSF or GM-CSF with TGF-β1 containing medium that were plated on either huCD44-Fc or huIgG1-Fc as a control. The suppressive capacity of cells cultured on CD44-Fc was not significantly increased compared to their control groups (Figure 11A). This was found to be valid for GM-CSF

and GM-CSF with TGF-β1 treated cells. Interestingly, we unexpectedly measured a tendency of reduced suppressive capacities of cells cultured on CD44-Fc in the majority of our experiments, independent of TGF-β1 stimulation (Figure 11A).
In summary, CD44 without cellular context did not enhance suppressive capacity or expansion of human mMDSC generated from $CD14^+$ PBMC *in vitro*.

4 DISCUSSION

4.1 The Role of CD44 on Murine Hepatic Stellate Cells in Myeloid-derived Suppressor Cell Induction

4.1.1 Culture Activation and Expression of CD44 on HSC *in vitro*

After the successful establishment of the HSC isolation process, we focused on culture activation of isolated quiescent HSC. Our results show sufficient purity and successful HSC culture activation indicated by morphological aspects and measured Acta2 expression. Culture activation is by far the most commonly used model for primary murine HSC. They display a highly conserved activation process *in vivo*, mostly independent of the fibrogenic trigger, e.g. CCl4 or BDL (De Minicis et al. 2007). Although culture activation upregulates many key fibrotic genes, it does not reproduce the exact gene expression pattern associated with *in vivo* activation. Since physiological HSC activation is shaped by various hepatic cell types, which is difficult to reproduce in *in vitro, in vivo* activation should be considered gold standard. *In vivo*, HSC activation is influenced by complex interactions with other hepatic cell types, such as liver sinusoidal endothelial cells (LSEC) and Kupffer cells, as well as the ECM components (Mederacke et al. 2015). These interactions are not fully replicated in our current *in vitro* model. Therefore, while this *in vitro* system is crucial for studying HSC-specific CD44 dynamics, future studies should integrate co-culture systems or transition to *in vivo* models, such as BDL or CCl4-induced liver fibrosis, to confirm the

physiological relevance of these findings and gain deeper insights into HSC behavior in a more complex but physiologically relevant environment.

4.1.2 CD44: Regulation and Expression during HSC Activation

Upon culture activation, primary murine HSC show elevated mRNA levels of CD44 (De Minicis et al. 2007). Our data show that CD44 expression is significantly upregulated in murine HSC during culture activation, which aligns with findings in human HSC, reinforcing the conserved regulation of this marker across species. This observation is consistent with the literature that highlights CD44 as a key mediator in the activation of HSC and fibrogenic signaling (Hoechst et al. 2013). Interestingly, our study revealed a subset of $CD44^+$ quiescent HSC *ex vivo*, suggesting a potential pre-activated state in the absence of external stimuli. This finding aligns with reports of a pre-activated HSC population in older or metabolically compromised mice, which have been linked to conditions such as fatty liver disease and subclinical inflammation (Mederacke et al. 2015). Additionally, the progressive increase in both number of $CD44^+$ HSC and levels of CD44 expression during activation suggests a regulated and dynamic process. This mechanism may serve to amplify the fibrogenic and immunomodulatory functions of HSC over time, a concept that has been explored in several studies examining the role of CD44 in liver fibrogenesis (Friedman 2008).

4.1.3 TGF-β1 Boosts the Activation State of CD44-expressing HSC

TGF-β1 plays a pivotal role in wound healing process of the liver, thus in liver fibrosis. It is secreted by various resident hepatic cell types and profoundly influences the inflammatory microenvironment and HSC activation (Friedmann 2008; Troeger et al. 2012; Inagaki & Okazaki 2007). In order to gain deeper insight into the dynamics of CD44 regulation, we speculated, that adding TGF-β1 into culture might boost CD44 expression on culture activated HSC. Indeed, we observed significantly upregulated CD44 expression. Interestingly, TGF-β1 appears to increase CD44 expression only in already $CD44^+$ HSC, while it did not significantly expand the amount of surface $CD44^+$ HSC in our experiments. This suggests that TGF-β1 mainly amplifies the activation state of CD44-expressing HSC rather than inducing CD44 expression on CD44

negative HSC. The specificity of this effect may reflect a threshold-dependent mechanism, in which only fully activated HSC can respond to TGF-β1-mediated transcriptional changes. These findings have important implications for co-culture experiments aimed at studying HSC-driven MDSC induction. Since CD44 is implicated in MDSC differentiation, enhancing CD44 expression via TGF-β1 treatment could potentiate the immunosuppressive potential of HSC. Future studies should include functional assays, using TGF- β1-primed, culture activated HSC co-cultured with BMC for MDSC generation.

4.1.4 HSC Dampen BMC Maturation and Promote MDSC Phenotypes

MDSC can be generated during maturation of BMC using GM-CSF. Furthermore, HSC are shown to promote the expansion and differentiation of MDSC and further inhibit the maturation to DC within this process (Chou et al. 2012; Chou et al. 2011; Höchst et al. 2015). To gain more knowledge about the role of CD44 in this process we needed to establish a reliable *in vitro* model. Therefore, we cultured BMC either alone (monoculture) or on a confluent layer of culture activated primary HSC (coculture), both in GM-CSF containing media. Then we compared the emerging phenotypes.

Our findings align with previously published reports demonstrating the ability of HSC to inhibit the maturation of $CD11b^{+}CD11c^{+}$ dendritic cells from BMC and promote the expansion of MDSC (Arakawa et al. 2014; Chou et al. 2011; Hsieh et al. 2019). This inhibitory effect is indicative of the profound impact of HSC on the immunogenic microenvironment, particularly in its ability to skew the differentiation of immune cells towards a suppressive phenotype. Notably, we observed a phenotypic shift in MDSC subsets modulated by HSC, characterized by a reduction in monocytic MDSC (mMDSC) and stable levels of granulocytic MDSC (gMDSC). This seems to be contrary to the findings of Hoechst et al. who reported that upon liver inflammation *in vivo*, mMDSC accumulate instead of gMDSC, but matches the groups findings using BMC for MDSC *in vitro* generation (Höchst et al. 2015). This discrepancy highlights the complexity of MDSC biology, representing their phenotypic plasticity and partly limited comparability of the used *in vitro* model to *in vivo* models, as well as the need for an *in vivo* setting in future experiments.

The emergence of a subset of $CD11b^{+}CD11c^{-}Ly6G^{-}Ly6C^{-}$ cells typically resemble non-classical myeloid precursor cells (Damuzzo et al. 2015; Kong et al. 2013). Interestingly we found them to be predominantly promoted in presence of HSC. One possible Explanation is that a greater number of BMC myeloid progenitors remain in an immature state due to modulation by HSC. This reflects the dampening effects on cellular maturation by HSC. However, this population has not been described to this extent in comparable settings, suggesting that it may represent a novel or poorly characterized cell population, which should be considered for further investigation in this context.

While HLA-DR is commonly used to define human MDSC, MHC II surface proteins of murine MDSC are not part of the official phenotypical nomenclature. Nonetheless, reduced MHC II expression is a common and distinctive feature observed in murine MDSC, reinforcing their dampened maturation state (Chou et al. 2011; Yang Zhao et al. 2015). Therefore, we investigated the effects of HSC on MHC II expression patterns on the emerged myeloid subsets. In both gMDSC and mMDSC subtypes, MHC II expression on MDSC modulated by HSC was considerably lower than to those generated in monocultures. Taken together, these findings confirm HSC as potent inductors of MDSC phenotypes, highlighting the profound effects they can exert on cellular compositions of their immunological microenvironment.

4.1.5 Suppressive Capabilities of HSC-Modulated MDSC Subsets

To verify whether the found MDSC phenotypes did indeed exhibit functional characteristics of MDSC, we performed suppression assays comparing BMC cultured in presence or absence of HSC. Overall, BMC cultured in presence of HSC exhibited significantly increased suppressive capacities. This effect may be attributed to a higher amount of MDSC and less mature DC phenotypes (Figure 4C), or to the induction of more efficient suppression mechanisms in HSC modulated BMC. As our primary objective was to investigate the role of CD44 deficiency in HSC-mediated MDSC induction, we did not further explore the exact underlying mechanisms responsible for this enhanced suppressive phenotype. Nonetheless, studies conducted under comparable conditions have reported increased suppressive capacity on a per-cell basis (Hsieh et al. 2019; Chou et al. 2011). Both sorted g- and mMDSC generated in presence of HSC displayed suppression capabilities. Our data rendered gMDSC as

more profound suppressors of T cell proliferation. This contradicts the findings within livers of in BDL mice, where suppressive traits were exclusively associated with mMDSC phenotypes (Höchst et al. 2015). This again underscores the context-dependent plasticity and differentiation of MDSC subsets within the liver (Sehgal et al. 2021; Q. Sun et al. 2023).

4.1.6 CD44 Deficiency of HSC Functionally Affects *in vitro* Generated MDSC

To investigate the role of CD44 in MDSC induction by HSC we used primary HSC from CD44$^{-/-}$ mice. When comparing phenotypic subsets from HSC modulated BMC by flow cytometry, we did not observe any noticeable differences in amount of MDSC phenotypes or amount or MHC II surface expression (MFI) on generated MDSC. Thus, CD44 deficiency on HSC did not alter their ability to induce MDSC phenotypes from BMC *in vitro*. However, when comparing suppressive traits, we found that both mMDSC and gMDSC derived from BMC cultured with CD44$^{-/-}$ HSC exhibited a reduced capacity of suppressing T cell proliferation (Figure 7C). It should be noted, however, that due to the limited availability of CD44$^{-/-}$ mice, we were only able to perform two independent experiments. These preliminary results suggest a possible role for CD44 in murine MDSC induction by HSC *in vitro*, but further experiments are necessary to validate these findings.

Observed effects could be amplified overcoming mechanisms of functional molecular redundancy of CD44 within knock-out mice. ICAM-1 can act as co-receptor for c-Met, compensating for the loss of CD44. This has been demonstrated in liver regeneration models on hepatocytes, in which ICAM-1-specific antibodies inhibit liver cell proliferation and c-Met activation in CD44 knockout mice, indicating functional substitution (Olaku et al. 2011). This has not explicatively shown for HSC, but the molecular prerequisites - expression of ICAM-1 and c-Met - are given. Additionally, receptors for HA-mediated motility (RHAMM, CD168) were shown to compensate for the loss of CD44 in fibroblasts and mesenchymal progenitor cells by binding to HA, supporting cell migration and upregulating genes involved in inflammation. This effect is particularly pronounced in CD44$^{-/-}$ mice, in which RHAMM enhances signaling due to increased HA availability (Nedvetzki et al. 2004). Moreover, integrins such as avß3 and a5ß1 can play compensatory roles in processes such as cell migration and tissue

remodeling when CD44 is absent. This phenomenon is particularly relevant in liver fibrosis, where integrins partially substitute for CD44's function in HSC activation and migration (Satoh et al. 2000). To overcome possible functional redundancies in CD44$^{-/-}$ mice, siRNA-mediated knockdowns and CD44-blocking antibody experiments should be incorporated.

Recently published data from our research group has expanded the understanding of CD44-mediated immunoregulation through the use of CD44-blocking antibodies in HSC and BMC coculture (Hagenstein et al. 2024). These findings revealed a significant reduction in the suppressive capacity of both mMDSC and gMDSC subsets following CD44 blockade. Notably, hallmark immunosuppressive mediators typically produced by MDSCs, including inducible iNOS and TGF-β1 (in mMDSCs), as well as IL-10 (in gMDSC), were markedly downregulated at a transcriptional level in the presence of CD44 inhibition. While surface expression of MHC II remained unchanged, flow cytometric analysis uncovered distinct gene expression alterations that differed between MDSC subtypes. In mMDSCs, CD44 blockade led to upregulation of CD80, accompanied by increased T cell stimulation and reduced TGF-β1 expression, consistent with decreased suppressive function. In gMDSCs, the expression of CD80, CD86, and PD-L1 was concurrently upregulated, suggesting a complex regulatory shift. Based on recent literature, the balance between these molecules may reflect a functional neutralization of suppressive signaling. CD80 and PD-L1 are known to form heterodimers that can facilitate CD28-mediated T cell costimulation, while excess PD-L1 may engage PD-1 and induce inhibitory signaling. In this context, the simultaneous upregulation of co-stimulatory and co-inhibitory molecules may attenuate the net suppressive effect, especially given the accompanying increase in CD86, which is unaffected by CD80:PD-L1 dynamics (Yunlong Zhao et al. 2019). Taken together, these findings provide further mechanistic insight into the key role of CD44 as a regulatory node in HSC-mediated functional programming of MDSCs in chronic inflammatory and fibrotic liver disease (Hagenstein et al. 2024).

Another potential mechanism to be explored in the future involves the interaction of CD44 with soluble factors such as macrophage migration inhibitory factor (MIF), shown to enhances the differentiation of myeloid cells into MDSCs *in vitro*, but also acts as a chemotactic factor for MDSCs (Simpson et al. 2012). The interaction between CD44

and MIF has also emerged as a key regulatory mechanism in liver fibrosis. MIF primarily signals through its high-affinity receptor CD74. However, CD44 functions as a crucial co-receptor within the MIF/CD74 signaling complex, facilitating downstream activation of intracellular pathways such as ERK1/2 and MAPK. This axis plays a pivotal role in the pathogenesis of HBV-induced liver fibrosis. Recent studies have demonstrated that MIF and CD74 expression is markedly upregulated in HSC following exposure to HBV. Upon binding to CD74, MIF potentiates HSC activation and the upregulation of profibrotic markers, including a-smooth muscle actin (a-SMA) and TGF-β1 itself, thus MIF acting in a paracrine and possible autocrine perpetuator of MDSC generation. Pharmacological inhibition of MIF using small molecules has been shown to attenuate HSC activation and fibrogenesis. CD44 deficiency was shown to disrupt the MIF/CD74 signal transduction. However, evidence specifically addressing the role of this axis in HSC remains limited (Simpson et al. 2012; Cheng et al. 2025; Veillat et al. 2010).

It is important to consider that the use of GM-CSF-containing medium in our model may have masked more subtle effects of CD44 deficiency, as no reliable information was available regarding the GM-CSF concentration in our medium. GM-CSF is known to influence MDSC differentiation and function, and its concentration could significantly impact experimental outcomes (Triozzi et al. 2012). Triozzi et al. compared two dosing regimens of recombinant human GM-CSF in prostate cancer patients and found that higher, cyclic dosing promoted the expansion of MDSCs and regulatory T cells, whereas lower, continuous dosing favored dendritic cell activation and reduced the frequency of immunosuppressive cells. These findings highlight that GM-CSF dosing critically influences the balance between immunostimulatory and immunosuppressive effects (Triozzi et al. 2012). The generation and function of mMDSC from human PBMC is regulated in a dose-dependent manner by GM-CSF, with higher concentrations enhancing both their expansion and suppressive capacity (Lechner et al. 2010). Sun et al. demonstrated that low concentrations of GM-CSF promote granulopoietic differentiation, favoring the generation of granulocytes, whereas high concentrations favor monopoietic differentiation, leading to the expansion of monocytes and macrophages. These findings have direct implications for the development and function of MDSC subsets, which may arise under differing cytokine milieus (Y. Sun et al. 2018). Hence, the GM-CSF dose may directly shape MDSC

phenotype and could, at least in part, account for the phenotypic variability observed under different experimental or clinical conditions. Future studies should therefore incorporate precise recombinant GM-CSF titrations.

Future studies should also aim to validate our findings in *in vivo* fibrosis models, such as BDL or CCl4-induced liver injury. These models closely mimic the complexity of liver fibrosis and provide a more physiologically relevant setting for studying the role of CD44 in MDSC induction. By using *in vivo* systems, it would be possible to determine whether CD44 upregulation in HSC plays a similar role in MDSC induction as observed *in vitro*, and to assess the broader implications of these findings in liver disease progression.

As mentioned in 4.1.1, refining co-culture systems will be crucial for evaluating interactions between HSC and other important liver-resident cell types, such as KC or LSEC. Interactions between these cell types are integral to the fibrotic process and immune modulation in the liver, and their inclusion in *in vitro* co-culture models would provide a more accurate representation of the liver microenvironment (Kitto & Henderson 2021).

Finally, a comprehensive transcriptomic analysis comparing $CD44^{+/+}$ and $CD44^{-/-}$ HSC and the associated generated MDSC would yield valuable insights into differential gene expression related to the fibrotic and immune response. Such profiling could identify novel biomarkers or therapeutic targets that modulate HSC activation and MDSC differentiation, offering new strategies for managing liver fibrosis and improving treatment outcomes for patients suffering from chronic liver disease.

4.2 The Role of CD44 in the Induction of Human Monocytic Myeloid-Derived Suppressor Cells

Hoechst et al. have shown that human primary and LX2 cell-line HSC transduce $CD14^{+}HLA\text{-}DR^{+}$ PBMC into suppressive $CD14^{+}HLA\text{-}DR^{low/-}$ mMDSC in a CD44-dependent matter. They found this process to be contact-dependent (Hoechst et al. 2013). However, the exact underlying mechanisms of CD44 within this process remain

unclear. Moreover, it is not known whether MDSC-inducing mechanisms are triggered within PBMC by solely binding to CD44 or if they need cellular context of HSC. In our human work, we wanted to find out, whether CD44 alone is sufficient to induce mMDSC from $CD14^+$ PBMC. To this end, we initially established a model of *in vitro* mMDSC generation using GM-CSF and TGF-β1. Subsequently, we modified this model by adding recombinant CD44 protein and assessed its impact on phenotype and suppressive capacity of generated mMDSC.

We could show that treating $CD14^+$ PBMC with GM-CSF with or without additional TGF-β1 is an effective way to generate mMDSC *in vitro*. On a surface marker level, added TGF-β1 drastically expands the mMDSC population compared to GM-CSF treatment only. However, TGF-β1 treatment did not affect the overall HLA-DR expression on $CD14^+$ PBMC. In subset comparison of mMDSC and iDC, HLA-DR levels were consistently lower on mMDSC generated in GM-CSF with TGF-β1 cultures. However, the additional downregulation achieved by added TGF-β1 makes up only a marginally proportion of the total HLA-DR downregulation on treated compared to *ex vivo* cells. This qualifies rather GM-CSF to be a main driver of HLA-DR downregulation within this setting.

Both treatments produced highly suppressive mMDSC. Lechner et al. showed that treating $CD33^+$ PBMC with GM-CSF renders MDSC, but did not particularly focus on $CD14^+$ mMDSC (Lechner et al. 2010). We could confirm the findings of Casacuberta-Serra et al., that generated mMDSC by using GM-CSF and TGF-β1, but they did not compare them to GM-CSF only treated $CD14^+$ PBMC (Casacuberta Serra et al. 2017). Treatment with GM-CSF & TGF-β1 rendered cells with increased $CD8^+$ T cell suppressing capacities than GM-CSF only treated cells. Interestingly, Lechner et al. reported, that $CD33^+$ PBMC treated with GM-CSF and TGF-β1 did not show any suppressive traits and even stimulated T cell proliferation, while cells treated with GM-CSF only were found to be highly suppressive (Lechner et al. 2010). Since they used broader myeloid spectrum with $CD33^+$ PBMC, this could mean that additional TGF-β1 might only affect $CD14^+$ PBMC and $CD14^+$ mMDSC in that matter. We did not sort for the mMDSC phenotype before performing suppression assays, so it remains unclear whether TGF-β1 expands the mMDSC subset and/or boosts individual suppressive capacities within this model. Another possibility would be, that iDC among TGF-β1 treated cells became less effective in T cells stimulation while mMDSC suppressive functions remained unaltered by TGF-β1. Furthermore, we did not perform

suppression assays comparing sorted iDC with mMDSC phenotypes. Therefore, suppressive traits among iDC, like tolerogenic DC, cannot be ruled out entirely. Since Obermajer et al. used DC-SIGN within experiments using GM-CSF only or combined with PGE_2, it remains unclear to what extent it can be deployed as viable marker to delineate MDSC phenotypes in settings using TGF-β1 (Obermajer & Kalinski 2018). It is possible, that TGF-β1 is also reprogramming iDC into suppressive entities - tolerogenic DC - and therefore blurring phenotypical borders of iDC and mMDSC. Although our data support upholding on DC-SIGN as negative marker for mMDSC, further experiments should be made on that issue.

After successful establishment of an *in vitro* MDSC generation model, we proceeded to add CD44 protein. We compared mMDSC, that were generated on culture dishes coated with either recombinant human CD44-Fc or a control recombinant IgG1-Fc. We hypothesized, that presence of CD44 could trigger MDSC relevant pathways within $CD14^+$ PBMC and therefore enhance their phenotypical and/or functional aspects. However, we did not record any significant differences as far as the amount of iDC and mMDSC subsets are concerned. Neither did the presence of the cell-free CD44 lead to different HLA-DR expressions on iDC or mMDSC respectively. At a functional level, CD44 did not enhance suppressive functions of generated mMDSC. Interestingly, we observed a tendency of reduced suppressive capacities of cells cultured on CD44-Ig in GM-CSF only media. Taken together, the presence of CD44 without cellular context did not enhance *in vitro* mMDSC generation. These findings suggest the absence of pathways within $CD14^+$ PBMC, relevant for MDSC generation, that can be triggered by CD44 without its cellular context. However, since our model is based on soluble factors GM-CSF and TGF-β1, possible effects could be overshadowed as they might induce mMDSC via CD44-independent pathways. It is a commonly used model for *in vitro* mMDSC generation, in which the role of CD44 has not been examined yet. Since both GM-CSF and TGF-β1 are secreted by activated HSC, they at least partly reference to an actual *in vivo* situation (Hsieh 2015b; Friedmann 2008). Therefore, our experiments can be viewed as an initial approach, that should be subsequently further modified.

Höchst et al. showed that the induction of MDSC by primary human HSC and cell-line LX2 via CD44 was cell-to-cell contact dependent (Hoechst et al. 2013). It is still possible that HSC produce a so far unidentified soluble agent that creates specific preconditions necessary for the CD44-dependency and that this priming is not carried

out by recombinant GM-CSF or TGF- β1 respectively. Hence, experiments using conditioned media of primary or LX2 HSC instead of recombinant cytokines could overcome those limitations. In order to simulate a more realistic cellular integrity of CD44, without triggering possible signaling on the HSC site, $CD14^+$ cells could be cultured on fixated HSC.

There is still no full consensus of whether MDSC are present in a healthy state or remain fully absent until inflammational triggers arise. Though it is received, that circulating and resident MDSC expand in a pathological state (Veglia, Perego & Gabrilovich 2018a). We used $CD14^+$ of healthy donors only throughout our experiments. PBMC extracted from diseased or tumor bearing hosts might differ substantially in MDSC generation as far as their amount and biology are concerned. Future experiments using such PBMC could cast light on further not yet described facets of CD44 in the context of MDSC generation.

In summary, while CD44 appears crucial for MDSC induction via HSC, our findings suggest that its function is context-dependent, requiring cellular integrity or additional factors. Further experimental modifications, particularly incorporating elements from pathological contexts, are needed to delineate the precise mechanisms by which CD44 contributes to mMDSC generation.

5 ABSTRACTS

5.1 Abstract (English)

Title: The Role of CD44 in the Induction of Myeloid-Derived Suppressor Cells by Hepatic Stellate Cells

Chronic liver diseases are characterized by persistent inflammation and the development of a profibrotic microenvironment, ultimately leading to liver fibrosis. These processes are driven by dynamic interactions between immune and stromal cells. Myeloid-derived suppressor cells (MDSC) are key players in this context, arising in response to ongoing stimulation by pathological conditions such as infection, chronic

inflammation or cancer, exerting immunosuppressive traits and hence contributing both to hepatic stellate cell (HSC) activation and fibrogenesis, and, paradoxically, to protection against excessive immune-mediated tissue damage. HSC, recognized as central mediators of liver fibrosis and immune regulation, have been shown in studies such as those by Höchst et al. to induce monocytic MDSCs (mMDSC) from peripheral blood monocytes (PBMC) via CD44-dependent mechanisms. However, the precise mechanisms underlying this CD44-dependent induction remain poorly understood. This study further explores the role of CD44 in MDSC induction using both murine and human models.

To expand on current knowledge and gain deeper insights, we aimed to determine whether the role attributed to CD44 is maintained in a murine *in vitro* model of MDSC induction. Therefore, a HSC isolation protocol was established, involving enzymatic *in situ* liver perfusion, digestion, gradient purification, and finally, FACS-based sorting. Upon seven days of culture activation of primary quiescent *ex vivo* HSC, we observed a significant upregulation of surface CD44. MDSC can be generated *in vitro* by culturing isolated bone marrow cells (BMC) in GM-CSF-containing medium. HSC has been shown to crucially boost this MDSC induction. Therefore, as a model for HSC-mediated MDSC generation, we cultured BMC on a confluent monolayer of activated HSC in GM-CSF-supplemented medium. We then compared MDSC generated in the presence of HSC from CD44 wild-type mice to those generated in presence of HSC from CD44-deficient mice. The absence of CD44 on HSC did not change MDSC induction as assessed by typical MDSC surface marker expression. However, when assessing MDSC suppressive capacity, our preliminary data suggest that CD44 expression on HSC enhances the immunosuppressive function of MDSC. Moreover, these findings demonstrate the suitability of murine models for further investigating the role of CD44 in HSC-mediated MDSC induction.

The human model aimed to clarify the necessity of HSC as a cellular context in CD44-mediated MDSC induction and to determine whether recombinant CD44 alone could induce mMDSC from $CD14^+$ PBMC. To investigate the effects of CD44 on MDSC induction, an *in vitro* model was established by treating $CD14^+$ PBMC with GM-CSF with or without TGF-β1. It was demonstrated that GM-CSF primarily drives HLA-DR downregulation, whereas TGF-β1 expands the mMDSC population and enhances suppressive capacities. The experimental setup was then modified by using CD44-coated culture dishes, hypothesizing that CD44 could activate MDSC-relevant

pathways within $CD14^+$ PBMCs and thereby enhance their phenotypic and/or functional characteristics. However, flow cytometric analysis of *in vitro*-generated MDSCs in the presence of CD44 revealed no alterations in MDSC frequency or key surface markers. Furthermore, functional assessments using T cell suppression assays showed no enhanced suppressive properties in MDSC generated in the presence of recombinant CD44. Our *in vitro* findings indicate that CD44, in the absence of its cellular context, is insufficient to replicate the effects observed in HSC-dependent MDSC induction. These findings of our human model emphasize the essential yet context-dependent role of CD44 in MDSC induction by HSCs.

5.2 Abstract (German)

Titel: Die Rolle von CD44 in der Induktion myeloischer Suppressorzellen durch hepatische Sternzellen

Chronische Lebererkrankungen sind gekennzeichnet durch persistierende Inflammation mit Etablierung eines profibrotischen Mikromilieus, was letztlich zur hepatischen Fibrosierung führt. Diese Prozesse werden durch dynamische Wechselwirkungen zwischen Immun- und Stromazellen vermittelt. Myeloische Suppressorzellen (MDSC) spielen in diesem Kontext eine zentrale immunregulatorische Rolle. Sie entstehen infolge einer chronischen Stimulation im Rahmen von Pathologien wie Infektionen, chronische Inflammation oder Tumoren, entfalten immunsuppressive Eigenschaften und tragen so sowohl zur Aktivierung hepatischer Sternzellen (HSC) und damit zur Fibroseentwicklung als auch - paradoxerweise - zum Schutz vor überschießenden immunvermittelten Gewebeschäden bei. HSC, die als zentrale Vermittler fibrogener Prozesse sowie immunmodulatorischer Mechanismen gelten, wurden in Studien - u. a. von Höchst et al. - als Induktoren monozytärer MDSC (mMDSC) aus peripheren Blutmonozyten (PBMC) beschrieben. Dieser Prozess zeigte sich CD44-abhängig. Die zugrundeliegenden Mechanismen sind bislang jedoch nur unzureichend verstanden. Die vorliegende Arbeit untersucht daher weiterführend die Rolle von CD44 in der MDSC-Induktion in murinen und humanen Modellsystemen.

Zur Überprüfung der Übertragbarkeit bisheriger Erkenntnisse auf ein murines *In-vitro*-Modell wurde zunächst ein Protokoll zur Isolation primärer HSC etabliert, das auf enzymatischer *in situ* Leberperfusion, Dichtegradientenzentrifugation und

anschließender FACS-basierter Zellselektion beruht. Nach siebentägiger Kulturaktivierung zeigten die HSC eine progrediente Oberflächenexpression von CD44. Die Ko-Kultivierung aktivierter HSC mit murinen Knochenmarkzellen (BMC) in GM-CSF-haltigem Medium führte zur Induktion von suppressiven MDSC. Im Anschluss wurden MDSC aus Ko-Kulturen mit HSC von CD44 Wildtyp-Mäusen mit solchen aus CD44-defizienten Mäusen verglichen. Während die Abwesenheit von CD44 auf HSC die MDSC-Induktion - gemessen anhand von typischen MDSC-Oberflächenmarkern - nicht beeinflusste, deuten erste funktionelle Analysen darauf hin, dass CD44 entscheidend für die Entwicklung der immunsuppressiven Kapazität der MDSC ist. Diese Ergebnisse bestätigen nicht nur die fundamentale Rolle von CD44 auch im murinen Kontext, sondern auch die Eignung muriner Modelle zur weiteren Forschung an der CD44-vermittelten MDSC-Induktion durch HSC.

Im humanen Modellsystem wurde untersucht, ob CD44 allein - ohne zellulären Kontext von HSC - zur Induktion von mMDSC aus $CD14^+$ PBMC ausreicht. Hierfür wurde ein *in-vitro*-Modell etabliert, in dem $CD14^+$ PBMC mit GM-CSF - mit oder ohne Zugabe von TGF-β1 - behandelt wurden. Es zeigte sich, dass GM-CSF primär zur HLA-DR-Runterregulation führt, während TGF-β1 die Expansion und Suppressor Funktionen verstärkte. Anschließend wurde die Hypothese geprüft, ob rekombinantes CD44 - durch Beschichtung von Kulturplatten - MDSC-relevante Signalwege aktivieren und so deren Phänotyp oder Funktion modulieren könnte. Die Analyse mittels Durchflusszytometrie ergab keine Veränderungen in ihrer Häufigkeit oder Oberflächenmarkern der generierten MDSC. Auch funktionelle Suppressions-Assays zeigten keine veränderte immunsuppressive Funktion. Unsere Ergebnisse deuten darauf hin, dass CD44 allein - ohne zellulären Kontext - nicht ausreicht, um die beobachteten Effekte bei der HSC-abhängigen MDSC-Induktion zu reproduzieren. Die Daten aus dem humanen Modell deuten damit auf die stark kontextabhängige Rolle von CD44 in der MDSC-Induktion durch HSC hin.

6 REFERENCES

An, B. et al., 2018. CD1d is a novel cell-surface marker for human monocytic myeloid-derived suppressor cells with T cell suppression activity in peripheral blood after allogeneic hematopoietic stem cell transplantation. *Biochemical and Biophysical Research Communications*, 495(1), pp.519–525.

Arakawa, Y. et al., 2014. Cotransplantation With Myeloid-Derived Suppressor Cells Protects Cell Transplants. *Transplantation*, 97(7), pp.740–747.

Belladonna, M.L. et al., 2009. TGF-beta and kynurenines as the key to infectious tolerance. *Trends in molecular medicine*, 15(2), pp.41–49.

Bernsmeier, C. & Antoniades, C., 2017. myeloid-derived suppressor cells impair antimicrobial responses in patients with acute- on-chronic liver failure. pp.1–14.

Bissell, D.M. et al., 1995. Cell-specific expression of transforming growth factor-beta in rat liver. Evidence for autocrine regulation of hepatocyte proliferation. *Journal of Clinical Investigation*, 96(1), pp.447–455.

Bowen, D.G. & Walker, C.M., 2005. Adaptive immune responses in acute and chronic hepatitis C virus infection. *Nature*, 436(7053), pp.946–952.

Böttcher, J.P. et al., 2013. Liver-primed memory T cells generated under noninflammatory conditions provide anti-infectious immunity. *Cell reports*, 3(3), pp.779–795.

Böttcher, J.P., Knolle, P.A. & Stabenow, D., 2011. Mechanisms Balancing Tolerance and Immunity in the Liver. *Digestive Diseases*, 29(4), pp.384–390.

Brabletz, T. et al., 1993. Transforming growth factor beta and cyclosporin A inhibit the inducible activity of the interleukin-2 gene in T cells through a noncanonical octamer-binding site. *Molecular and cellular biology*, 13(2), pp.1155–1162.

Brandau, S. et al., 2016. Recommendations for myeloid-derived suppressor cell nomenclature and characterization standards. *Nature Communications*, 7, pp.1–10.

Brazil, J.C. et al., 2013. 3/4 Fucosyltransferase 3-Dependent Synthesis of Sialyl Lewis A on CD44 Variant Containing Exon 6 Mediates Polymorphonuclear Leukocyte Detachment from Intestinal Epithelium during Transepithelial Migration. *The Journal of Immunology*, 191(9), pp.4804–4817.

Breitkopf, K. et al., 2005. Anti-TGF-beta strategies for the treatment of chronic liver disease. *Alcoholism, clinical and experimental research*, 29(11 Suppl), pp.121S–131S.

Breitkopf, K. et al., 2006. TGF-β/Smad Signaling in the Injured Liver. *Zeitschrift für Gastroenterologie*, 44(01), pp.57–66.

Brenner, D.A., Kisseleva, T. & Cong, M., 2012. Myofibroblasts revert to an inactive phenotype during regression of liver fibrosis. pp.1–6.

Brocke, S. et al., 1999. Antibodies to CD44 and integrin alpha4, but not L-selectin, prevent central nervous system inflammation and experimental encephalomyelitis by blocking secondary leukocyte recruitment. *Proceedings of the National Academy of Sciences*, 96(12), pp.6896–6901.

Bunt, S.K., Sinha, P. & Ostrand-Rosenberg, S., 2017. Inflammation Induces Myeloid-Derived Suppressor Cells that Facilitate Tumor Progression. pp.1–7.

Calandra, T. & Roger, T., 2003. Macrophage migration inhibitory factor: a regulator of innate immunity. *Nature Reviews Immunology*, 3(10), pp.791–800.

Carriche, G.M. et al., 2021. Regulating T-cell differentiation through the polyamine spermidine. *The Journal of allergy and clinical immunology*, 147(1), pp.335–348.e11.

Casacuberta Serra, S. et al., 2017. Myeloid-derived suppressor cells can be efficiently generated from human hematopoietic progenitors and peripheral blood monocytes. *Immunology & Cell Biology*, 95(6), pp.538–548.

Cemerski, S. et al., 2002. Reactive oxygen species differentially affect T cell receptor-signaling pathways. *Journal of Biological Chemistry*, 277(22), pp.19585–19593.

Cemerski, S., van Meerwijk, J.P.M. & Romagnoli, P., 2003. Oxidative-stress-induced T lymphocyte hyporesponsiveness is caused by structural modification rather than proteasomal degradation of crucial TCR signaling molecules. *European Journal of Immunology*, 33(8), pp.2178–2185.

Chen, C. et al., 2018. The biology and role of CD44 in cancer progression: therapeutic implications. pp.1–23.

Chen, C.-H. et al., 2006. In vivo immune modulatory activity of hepatic stellate cells in mice. *Hepatology*, 44(5), pp.1171–1181.

Chen, D. et al., 2001. CD44-deficient mice exhibit enhanced hepatitis after concanavalin A injection: evidence for involvement of CD44 in activation-induced cell death. *The Journal of Immunology*, 166(10), pp.5889–5897.

Cheng, J.-Y. et al., 2025. MIF/CD74 axis in hepatic stellate cells mediates HBV-related liver fibrosis. *International immunopharmacology*, 147, p.113929.

Chikamatsu, K. et al., 2011. Immunoregulatory properties of CD44+ cancer stem-like cells in squamous cell carcinoma of the head and neck. *Head & neck*, 33(2), pp.208–215.

Chou, H.-S. et al., 2011. Hepatic stellate cells regulate immune response by way of induction of myeloid suppressor cells in mice. *Hepatology*, 53(3), pp.1007–1019.

Chou, H.-S. et al., 2012. Myeloid-Derived Suppressor Cells Protect Islet Transplants by B7-H1 Mediated Enhancement of T Regulatory Cells. *Transplantation*, 93(3), pp.272–282.

Collin, M. & Bigley, V., 2018. Human dendritic cell subsets: an update. *Immunology*, 154(1), pp.3–20.

Cotoi, C.G. & Quaglia, A., 2016. Normal Liver Anatomy and Introduction to Liver Histology. In S. Guandalini, A. Dhawan, & D. Branski, eds. *Textbook of Pediatric Gastroenterology, Hepatology and Nutrition: A Comprehensive Guide to Practice*. Textbook of Pediatric Gastroenterology, Hepatology and Nutrition: A Comprehensive Guide to Practice. Cham: Springer International Publishing, pp. 609–612.

Damuzzo, V. et al., 2015. Complexity and challenges in defining myeloid-derived suppressor cells. *Cytometry Part B: Clinical Cytometry*, 88(2), pp.77–91.

De Minicis, S. et al., 2007. Gene Expression Profiles During Hepatic Stellate Cell Activation in Culture and In Vivo. *Gastroenterology*, 132(5), pp.1937–1946.

Dhar, D. et al., 2018. Liver Cancer Initiation Requires p53 Inhibition by CD44-Enhanced Growth Factor Signaling. *Cancer cell*, 33(6), pp.1061–1077.e6.

Dolcetti, L. et al., 2010. Hierarchy of immunosuppressive strength among myeloid-derived suppressor cell subsets is determined by GM-CSF. *European Journal of Immunology*, 40(1), pp.22–35.

Dooley, S. et al., 2001. Expression of Smads during in vitro transdifferentiation of hepatic stellate cells to myofibroblasts. *Biochemical and Biophysical Research Communications*, 283(3), pp.554–562.

Dorhoi, A. & Plessis, Du, N., 2018. Monocytic Myeloid-Derived Suppressor Cells in Chronic Infections. *Frontiers in Immunology*, 8, pp.425–15.

Dropmann, A. et al., 2020. TGF-β2 silencing to target biliary-derived liver diseases. *Gut*, pp.gutjnl–2019–319091.

Dysthe, M. & Parihar, R., 2020. Myeloid-Derived Suppressor Cells in the Tumor Microenvironment. In *Tumor Microenvironment*. Hematopoietic Cells – Part A. Cham: Springer International Publishing, pp. 117–140.

Endo, K. & Terada, T., 2000. Protein expression of CD44 (standard and variant isoforms) in hepatocellular carcinoma: relationships with tumor grade, clinicopathologic parameters, p53 expression, and patient survival. *Journal of Hepatology*, 32(1), pp.78–84.

Fleming, V. et al., 2018. Targeting Myeloid-Derived Suppressor Cells to Bypass Tumor-Induced Immunosuppression. *Frontiers in Immunology*, 9, pp.11–11.

Friedman, S.L., 2008. Hepatic Stellate Cells: Protean, Multifunctional, and Enigmatic Cells of the Liver. *Physiological Reviews*, 88(1), pp.125–172.

Gabrilovich, D.I. & Nagaraj, S., 2009. Myeloid-derived suppressor cells as regulators of the immune system. *Nature Reviews Immunology*, 9(3), pp.162–174.

Gabrilovich, D.I. et al., 2007. The terminology issue for myeloid-derived suppressor cells. *Cancer research*, 67(1), pp.425–author reply 426.

Gargett, T. et al., 2018. GM-CSF signalling blockade and chemotherapeutic agents act in concert to inhibit the function of myeloid-derived suppressor cells in vitro. 5(12), pp.e119–12.

Geerts, A. et al., 1998. Purification of rat hepatic stellate cells by side scatter-activated cell sorting. *Hepatology*, 27(2), pp.590–598.

Geiger, R. et al., 2016. L-Arginine Modulates T Cell Metabolism and Enhances Survival and Anti-tumor Activity. *Cell*, 167(3), pp.829–842.e13.

Govindaraju, P. et al., 2019. CD44-dependent inflammation, fibrogenesis, and collagenolysis regulates extracellular matrix remodeling and tensile strength during cutaneous wound healing. *Matrix biology : journal of the International Society for Matrix Biology*, 75-76, pp.314–330.

Greifenberg, V. et al., 2009. Myeloid-derived suppressor cell activation by combined LPS and IFN-γ treatment impairs DC development. *European Journal of Immunology*, 39(10), pp.2865–2876.

Gressner, A.M. et al., 2002. Roles of TGF-beta in hepatic fibrosis. *Frontiers in bioscience : a journal and virtual library*, 7, pp.d793–807.

Grimm, M. et al., 2002. Inhibition of major histocompatibility complex class II gene transcription by nitric oxide and antioxidants. *Journal of Biological Chemistry*, 277(29), pp.26460–26467.

Groth, C. et al., 2019. Immunosuppression mediated by myeloid-derived suppressor cells (MDSCs) during tumour progression. *British journal of cancer*, 120(1), pp.16–25.

Hagenstein, J. et al., 2024. CD44 expression on murine hepatic stellate cells promotes the induction of monocytic and polymorphonuclear myeloid-derived suppressor cells. *Journal of leukocyte biology*, 116(1), pp.177–185.

Hammerich, L. & Tacke, F., 2015. Emerging roles of myeloid derived suppressor cells in hepatic inflammation and fibrosis. *World Journal of Gastrointestinal Pathophysiology*, 6(3), pp.43–9.

Hamon, G. et al., 1994. Transforming growth factor-beta 1 lowers the CD14 content of monocytes. *The Journal of surgical research*, 57(5), pp.574–578.

Han, J., Lee, C. & Jung, Y., 2024. Current Evidence and Perspectives of Cluster of Differentiation 44 in the Liver's Physiology and Pathology. *International Journal of Molecular Sciences*, 25(9).

Heine, A. et al., 2017. Generation and functional characterization of MDSC-like cells. *OncoImmunology*, 6(4), pp.e1295203–39.

Heymann, F. & Tacke, F., 2016. Immunology in the liver — from homeostasis to disease. *Nature Reviews Gastroenterology & Hepatology*, 13(2), pp.88–110.

Heymann, F. et al., 2015. Liver inflammation abrogates immunological tolerance induced by Kupffer cells. *Hepatology*, 62(1), pp.279–291.

Highfill, S.L. et al., 2010. Bone marrow myeloid-derived suppressor cells (MDSCs) inhibit graft-versus-host disease (GVHD) via an arginase-1-dependent mechanism that is up-regulated by interleukin-13. *Blood*, 116(25), pp.5738–5747.

Hoechst, B. et al., 2008. A New Population of Myeloid-Derived Suppressor Cells in Hepatocellular Carcinoma Patients Induces CD4+CD25+Foxp3+ T Cells. *YGAST*, 135(1), pp.234–243.

Hoechst, B. et al., 2013. Activated human hepatic stellate cells induce myeloid derived suppressor cells from peripheral blood monocytes in a CD44-dependent fashion. *Journal of Hepatology*, 59(3), pp.528–535.

Hoechst, B. et al., 2011. Plasticity of human Th17 cells and iTregs is orchestrated by different subsets of myeloid cells. *Blood*, 117(24), pp.6532–6541.

Höchst, B. et al., 2015. Differential Induction of Ly6G and Ly6C Positive Myeloid Derived Suppressor Cells in Chronic Kidney and Liver Inflammation and Fibrosis C. H. Kim, ed. *PLOS ONE*, 10(3), pp.e0119662–13.

Hsieh, C.-C., 2015a. Hepatic immune tolerance induced by hepatic stellate cells. *World Journal of Gastroenterology*, 21(42), pp.11887–7.

Hsieh, C.-C., 2015b. Hepatic immune tolerance induced by hepatic stellate cells. *World Journal of Gastroenterology*, 21(42), pp.11887–7.

Hsieh, C.-C. et al., 2019. Hepatic Stellate Cells Enhance Liver Cancer Progression by Inducing Myeloid-Derived Suppressor Cells through Interleukin-6 Signaling. *International Journal of Molecular Sciences*, 20(20), pp.5079–20.

Hu, H.-H. et al., 2018. New insights into TGF-β/Smad signaling in tissue fibrosis. *Chemico-biological interactions*, 292, pp.76–83.

Ibáñez-Vea, M., 2018. Myeloid-Derived Suppressor Cells in the Tumor Microenvironment: Current Knowledge and Future Perspectives. *Archivum Immunologiae et Therapiae Experimentalis*, 66(2), pp.113–123.

Inagaki, Y. & Okazaki, I., 2007. Emerging insights into Transforming growth factor beta Smad signal in hepatic fibrogenesis. *Gut*, 56(2), pp.284–292.

Jiang Y, Que W, Zhu P, Li XK. The Role of Diverse Liver Cells in Liver Transplantation Tolerance. Front Immunol. 2020 Jun 12;11:1203. doi: 10.3389/fimmu.2020.01203. PMID: 32595648; PMCID: PMC7304488.

Johnson, P. & Ruffell, B., 2009. CD44 and its Role in Inflammation and Inflammatory Diseases. pp.1–13.

Jordan, A.R. et al., 2015. The Role of CD44 in Disease Pathophysiology and Targeted Treatment. *Frontiers in Immunology*, 6, p.182.

Julia Schumann, K.S.U.S.C.A.B.S., 2015. Differences in CD44 Surface Expression Levels and Function Discriminates IL-17 and IFN-γ Producing Helper T Cells. pp.1–18.

Kallis, Y.N. et al., 2011. Remodelling of extracellular matrix is a requirement for the hepatic progenitor cell response. *Gut*, 60(4), pp.525–533.

Katoh, S. et al., 2003. A role for CD44 in an antigen-induced murine model of pulmonary eosinophilia. *Journal of Clinical Investigation*, 111(10), pp.1563–1570.

Khaled, Y.S., Ammori, B.J. & Elkord, E., 2013. Myeloid-derived suppressor cells in cancer: recent progress and prospects. *Immunology & Cell Biology*, 91(8), pp.493–502.

Kikuchi, S. et al., 2005. Role of CD44 in Epithelial Wound Repair. *Journal of Biological Chemistry*, 280(15), pp.15398–15404.

Kim, J. & Seki, E., 2023. Hyaluronan in liver fibrosis: basic mechanisms, clinical implications, and therapeutic targets. *Hepatology communications*, 7(4).

Kimura, K. et al., 2008. Critical role of CD44 in hepatotoxin-mediated liver injury. *Journal of Hepatology*, 48(6), pp.952–961.

Kimura, K. et al., 2009. Role of CD44 in CTL-induced acute liver injury in hepatitis B virus transgenic mice. *Journal of gastroenterology*, 44(3), pp.218–227.

Kitto, L.J. & Henderson, N.C., 2021. Hepatic Stellate Cell Regulation of Liver Regeneration and Repair. *Hepatology communications*, 5(3), pp.358–370.

Klotz, L. et al., 2007. Peroxisome proliferator-activated receptor gamma control of dendritic cell function contributes to development of CD4+ T cell anergy. *The Journal of Immunology*, 178(4), pp.2122–2131.

Knutson, J.R. et al., 1996. CD44/chondroitin sulfate proteoglycan and alpha 2 beta 1 integrin mediate human melanoma cell migration on type IV collagen and invasion of basement membranes. *Molecular biology of the cell*, 7(3), pp.383–396.

Ko, J.S. et al., 2009. Sunitinib Mediates Reversal of Myeloid-Derived Suppressor Cell Accumulation in Renal Cell Carcinoma Patients. *Clinical Cancer Research*, 15(6), pp.2148–2157.

Kong, Y.Y. et al., 2013. Myeloid derived suppressor cells and their role in diseases. *Current medicinal chemistry*, 20(11), pp.1437–1444.

Krishnamoorthy, M., Gerhardt, L. & Maleki Vareki, S., 2021. Immunosuppressive Effects of Myeloid-Derived Suppressor Cells in Cancer and Immunotherapy. *Cells*, 10(5), p.1170.

Kruger, M. et al., 1996. Granulocyte-macrophage colony-stimulating factor down-regulates CD14 expression on monocytes. *Immunology*, 89(1), pp.89–95.

Kumar, V. et al., 2016. The Nature of Myeloid-Derived Suppressor Cells in the Tumor Microenvironment. *Trends in Immunology*, 37(3), pp.208–220.

Lautt, W.W., 2009. Hepatic Circulation: Physiology and Pathophysiology

Lechner, M.G., Liebertz, D.J. & Epstein, A.L., 2010. Characterization of Cytokine-Induced Myeloid-Derived Suppressor Cells from Normal Human Peripheral Blood Mononuclear Cells. *The Journal of Immunology*, 185(4), pp.2273–2284.

Lee, C.-R. et al., 2018. Characterization of Multiple Cytokine Combinations and TGF-β on Differentiation and Functions of Myeloid-Derived Suppressor Cells. *International Journal of Molecular Sciences*, 19(3), pp.869–12.

Lee, U.E. & Friedman, S.L., 2011. Mechanisms of hepatic fibrogenesis. *Best Practice & Research Clinical Gastroenterology*, 25(2), pp.195–206.

Lee, Y.A. & Friedman, S.L., 2020. Stellate Cells and Fibrosis. In *The Liver*. John Wiley & Sons, Ltd, pp. 444–454.

Lerut, J. & Sanchez-Fueyo, A., 2006. An appraisal of tolerance in liver transplantation. *American journal of transplantation: official journal of the American Society of Transplantation and the American Society of Transplant Surgeons*, 6(8), pp.1774–1780.

Li, Y. et al., 2014. Myeloid-Derived Suppressor Cells as a Potential Therapy for Experimental Autoimmune Myasthenia Gravis. *The Journal of Immunology*, 193(5), pp.2127–2134.

Lim, H.X., Kim, T.S. & Poh, C.L., 2020. Understanding the Differentiation, Expansion, Recruitment and Suppressive Activities of Myeloid-Derived Suppressor Cells in Cancers. *International Journal of Molecular Sciences*, 21(10), pp.3599–13.

Lu, L. & Hsieh, C.-C., 2013. The role of complement component 3 (C3) in differentiation of myeloid-derived suppressor cells. pp.1–9.

Lutz, M.B. et al., 2000. Immature dendritic cells generated with low doses of GM-CSF in the absence of IL-4 are maturation resistant and prolong allograft survival in vivo. *European Journal of Immunology*, 30(7), pp.1813–1822.

Mandruzzato, S. et al., 2015. Toward harmonized phenotyping of human myeloid-derived suppressor cells by flow cytometry: results from an interim study. *Cancer Immunology, Immunotherapy*, 65(2), pp.161–169.

Marcellin, P. & Kutala, B.K., 2018. Liver diseases: A major, neglected global public health problem requiring urgent actions and large-scale screening. *Liver international : official journal of the International Association for the Study of the Liver*, 38 Suppl 1, pp.2–6.

Marigo, I. et al., 2010. Tumor-induced tolerance and immune suppression depend on the C/EBPbeta transcription factor. *Immunity*, 32(6), pp.790–802.

Marzaioli, V. et al., 2020. Monocyte-Derived Dendritic Cell Differentiation in Inflammatory Arthritis Is Regulated by the JAK/STAT Axis via NADPH Oxidase Regulation. *Frontiers in Immunology*, 11, p.1406.

Mazzoni, A. et al., 2002. Myeloid suppressor lines inhibit T cell responses by an NO-dependent mechanism. *The Journal of Immunology*, 168(2), pp.689–695.

McKallip, R.J. et al., 2005. Role of CD44 and its v7 isoform in staphylococcal enterotoxin B-induced toxic shock: CD44 deficiency on hepatic mononuclear cells leads to reduced activation-induced apoptosis that results in increased liver damage. *Infection and immunity*, 73(1), pp.50–61.

McKee, C.M. et al., 1996. Hyaluronan (HA) fragments induce chemokine gene expression in alveolar macrophages. The role of HA size and CD44. *Journal of Clinical Investigation*, 98(10), pp.2403–2413.

Mederacke, I. et al., 2015. High-yield and high-purity isolation of hepatic stellate cells from normal and fibrotic mouse livers. *Nature Protocols*, 10(2), pp.305–315.

Meschner, A. & Junqueira, L.C., 2013. Chapter 16: Organs Associated with the Digestive Tract. In *Junqueira's Basic Histology*. pp. 1–20.

Mikecz, K. et al., 1995. Anti-CD44 treatment abrogates tissue oedema and leukocyte infiltration in murine arthritis. *Nature medicine*, 1(6), pp.558–563.

Molon, B. et al., 2011. Chemokine nitration prevents intratumoral infiltration of antigen-specific T cells. *The Journal of Experimental Medicine*, 208(10), pp.1949–1962.

Morales, J.K. et al., 2010. GM-CSF is one of the main breast tumor-derived soluble factors involved in the differentiation of CD11b-Gr1- bone marrow progenitor cells into myeloid-derived suppressor cells. *Breast cancer research and treatment*, 123(1), pp.39–49.

Mougiakakos, D., Johansson, C.C. & Kiessling, R., 2009. Naturally occurring regulatory T cells show reduced sensitivity toward oxidative stress-induced cell death. *Blood*, 113(15), pp.3542–3545.

Na, Y.R., Jung, D. & Seok, H., 2016. GM-CSF Grown Bone Marrow Derived Cells Are Composed of Phenotypically Different Dendritic Cells and Macrophages. *Molecules and Cells*, pp.1–8.

Naor, D. et al., 2008. CD44 in Cancer. *Critical Reviews in Clinical Laboratory Sciences*, 39(6), pp.527–579.

Nedvetzki, S. et al., 2004. RHAMM, a receptor for hyaluronan-mediated motility, compensates for CD44 in inflamed CD44-knockout mice: a different interpretation of redundancy. *Proceedings of the National Academy of Sciences*, 101(52), pp.18081–18086.

Nepal, M.R., Shah, S. & Kang, K.-T., 2024. Dual roles of myeloid-derived suppressor cells in various diseases: a review. *Archives of pharmacal research*, 47(7), pp.597–616.

Obermajer, N. & Kalinski, P., 2018. Generation of myeloid-derived suppressor cells using prostaglandin E. pp.1–6.

Obermajer, N. et al., 2011. Positive feedback between PGE2 and COX2 redirects the differentiation of human dendritic cells toward stable myeloid-derived suppressor cells. *Blood*, 118(20), pp.5498–5505.

Olaku, V. et al., 2011. c-Met recruits ICAM-1 as a coreceptor to compensate for the loss of CD44 in Cd44 null mice. *Molecular biology of the cell*, 22(15), pp.2777–2786.

Orian-Rousseau, V., 2015. CD44 acts as a signaling platform controlling tumor progression and metastasis. pp.1–4.

Ouhtit, A. et al., 2013. TGF-β2: A Novel Target of CD44-Promoted Breast Cancer Invasion. *Journal of Cancer*, 4(7), pp.566–572.

Pallett, L.J. et al., 2015. Metabolic regulation of hepatitis B immunopathology by myeloid-derived suppressor cells. *Nature medicine*, 21(6), pp.591–600.

Parmiani, G. et al., 2007. Opposite immune functions of GM-CSF administered as vaccine adjuvant in cancer patients. *Annals of oncology : official journal of the European Society for Medical Oncology*, 18(2), pp.226–232.

Platten, M., Wick, W. & Van den Eynde, B.J., 2012. Tryptophan catabolism in cancer: beyond IDO and tryptophan depletion. *Cancer research*, 72(21), pp.5435–5440.

Ponta, H., Sherman, L. & Herrlich, P.A., 2003. CD44: From adhesion molecules to signalling regulators. *Nature Reviews Molecular Cell Biology*, 4(1), pp.33–45.

Protin, U. et al., 1999. CD44-deficient mice develop normally with changes in subpopulations and recirculation of lymphocyte subsets. *The Journal of Immunology*, 163(9), pp.4917–4923.

Racanelli, V. & Rehermann, B., 2006. The liver as an immunological organ. *Hepatology*, 43(2 Suppl 1), pp.S54–62.

Robinson, M.W., Harmon, C. & Farrelly, C.O.R., 2019. Liver immunology and its role in inflammation and homeostasis. pp.1–10.

Roman, G. et al., 2023. “iPSC-derived liver organoids and inherited bleeding disorders: Potential and future perspectives.” Frontiers in Physiology, 14, p.1094249. herited

Sancho-Bru, P. et al., 2005. Genomic and functional characterization of stellate cells isolated from human cirrhotic livers. *Journal of Hepatology*, 43(2), pp.272–282.

Satoh, T. et al., 2000. Interaction between hyaluronan and CD44 in the development of dimethylnitrosamine-induced liver cirrhosis. *Journal of gastroenterology and hepatology*, 15(4), pp.402–411.

Schmits, R., Filmus, J., Gerwin, N., Senaldi, G., Kiefer, F., Kundig, T., Wakeham, A., Shahinian, A., Catzavelos, C., Rak, J., Furlonger, C., Zakarian, A., Simard, J.J., Ohashi, P.S., Paige, C.J., Gutierrez-Ramos, J.C. & Mak, T.W., 1997a. CD44 regulates hematopoietic progenitor distribution, granuloma formation, and tumorigenicity. *Blood*, 90(6), pp.2217–2233.

Schmits, R., Filmus, J., Gerwin, N., Senaldi, G., Kiefer, F., Kundig, T., Wakeham, A., Shahinian, A., Catzavelos, C., Rak, J., Furlonger, C., Zakarian, A., Simard, J.J., Ohashi, P.S., Paige, C.J., Gutierrez-Ramos, J.C. & Mak, T.W., 1997b. CD44 regulates hematopoietic progenitor distribution, granuloma formation, and tumorigenicity. *Blood*, 90(6), pp.2217–2233.

Schober, A., Bernhagen, J. & Weber, C., 2008. Chemokine-like functions of MIF in atherosclerosis. *Journal of molecular medicine (Berlin, Germany)*, 86(7), pp.761–770.

Screaton, G.R. et al., 1993. The identification of a new alternative exon with highly restricted tissue expression in transcripts encoding the mouse Pgp-1 (CD44) homing receptor. Comparison of all 10 variable exons between mouse, human, and rat. *Journal of Biological Chemistry*, 268(17), pp.12235–12238.

Sehgal, R. et al., 2021. Immune surveillance by Myeloid derived suppressor cells (MDSCs) in liver diseases. *Digestive Diseases*.

Senoo, H. et al., 2010. Hepatic stellate cell (vitamin A-storing cell) and its relative – past, present and future. *Cell Biology International*, 34(12), pp.1247–1272.

Serafini, P. et al., 2008. Myeloid-derived suppressor cells promote cross-tolerance in B-cell lymphoma by expanding regulatory T cells. *Cancer research*, 68(13), pp.5439–5449.

Shi, C. & Pamer, E.G., 2011. Monocyte recruitment during infection and inflammation. *Nature Reviews Immunology*, 11(11), pp.762–774.

Simpson, K.D., Templeton, D.J. & Cross, J.V., 2012. Macrophage Migration Inhibitory Factor Promotes Tumor Growth and Metastasis by Inducing Myeloid-Derived Suppressor Cells in the Tumor Microenvironment. *The Journal of Immunology*, 189(12), pp.5533–5540.

Srivastava, M.K. et al., 2010. Myeloid-derived suppressor cells inhibit T-cell activation by depleting cystine and cysteine. *Cancer research*, 70(1), pp.68–77.

Stiff, A. et al., 2018. Nitric Oxide Production by Myeloid-Derived Suppressor Cells Plays a Role in Impairing Fc Receptor-Mediated Natural Killer Cell Function. *Clinical Cancer Research*, 24(8), pp.1891–1904.

Sun, L.K., Wahl, P.Wüthrich, 2001. CD44-mediated cyclooxygenase-2 expression and thromboxane A. pp.1–4.

Sun, Q. et al., 2023. Progress in research on the role played by myeloid-derived suppressor cells in liver diseases. *Scandinavian journal of immunology*, 98(4), p.e13312.

Sun, Y. et al., 2018. CD33 +CD14 +CD11b +HLA-DR −monocytic myeloid-derived suppressor cells recruited and activated by CCR9/CCL25 are crucial for the pathogenic progression of endometriosis. *American Journal of Reproductive Immunology*, 81(1), pp.e13067–10.

Takahashi, A. et al., 2005. Preferential cell death of CD8+ effector memory (CCR7-CD45RA-) T cells by hydrogen peroxide-induced oxidative stress. *The Journal of Immunology*, 174(10), pp.6080–6087.

Takeuchi, O. & Akira, S., 2010. Pattern recognition receptors and inflammation. *Cell*, 140(6), pp.805–820.

Talmadge, J.E. & Gabrilovich, D.I., 2013. History of myeloid-derived suppressor cells. *Nature reviews. Cancer*, 13(10), pp.739–752.

Tamadaho, R.S.E., Hoerauf, A. & Layland, L.E., 2018. Immunomodulatory effects of myeloid-derived suppressor cells in diseases_ Role in cancer and infections. *Immunobiology*, 223(4-5), pp.432–442.

Tcyganov, E. et al., 2018. ScienceDirect Plasticity of myeloid-derived suppressor cells in cancer. *Current Opinion in Immunology*, 51, pp.76–82.

Teder, P. et al., 2002. Resolution of lung inflammation by CD44. *Science (New York, N.Y.)*, 296(5565), pp.155–158.

Teye, K. et al., 2016. Isolation of All CD44 Transcripts in Human Epidermis and Regulation of Their Expression by Various Agents M. Blumenberg, ed. *PLOS ONE*, 11(8), pp.e0160952–21.

Thomas, D.A. & Massagué, J., 2005. TGF-beta directly targets cytotoxic T cell functions during tumor evasion of immune surveillance. *Cancer cell*, 8(5), pp.369–380.

Thomson, A.W. & Knolle, P.A., 2010. Antigen-presenting cell function in the tolerogenic liver environment. *Nature Reviews Immunology*, 10(11), pp.753–766.

Tiegs, G. & Lohse, A.W., 2010. Immune tolerance: what is unique about the liver. *Journal of autoimmunity*, 34(1), pp.1–6.

Triozzi, P.L. et al., 2012. Differential immunologic and microRNA effects of 2 dosing regimens of recombinant human granulocyte/macrophage colony stimulating factor. *Journal of immunotherapy (Hagerstown, Md. : 1997)*, 35(7), pp.587–594.

Troeger, J.S. et al., 2012. Deactivation of Hepatic Stellate Cells During Liver Fibrosis Resolution in Mice. *YGAST*, 143(4), pp.1073–1083.e22.

Tsuchida, T. & Friedman, S.L., 2017. Mechanisms of hepatic stellate cell activation. *Nature Reviews Gastroenterology & Hepatology*, 14(7), pp.397–411.

Turley, E.A., Noble, P.W. & Bourguignon, L.Y.W., 2002. Signaling Properties of Hyaluronan Receptors. *Journal of Biological Chemistry*, 277(7), pp.4589–4592.

Umansky, V. et al., 2016. The Role of Myeloid-Derived Suppressor Cells (MDSC) in Cancer Progression. *Vaccines*, 4(4).

Urashima, S. et al., 2000. Immunohistochemical Study of Hyaluronate Receptor (CD44) in Alcoholic Liver Disease. *Alcoholism, clinical and experimental research*, 24(S4), pp.34S–38S.

Vanhaver, C., van der Bruggen, P. & Bruger, A.M., 2021. MDSC in Mice and Men: Mechanisms of Immunosuppression in Cancer. *Journal of clinical medicine*, 10(13), p.2872.

Veglia, F., Perego, M. & Gabrilovich, D., 2018a. Myeloid-derived suppressor cells coming of age. *Nature Immunology*, 19(2), pp.108–119.

Veglia, F., Perego, M. & Gabrilovich, D., 2018b. Myeloid-derived suppressor cells coming of age. *Nature Immunology*, pp.1–12.

Veillat, V. et al., 2010. Macrophage migration inhibitory factor elicits an angiogenic phenotype in human ectopic endometrial cells and triggers the production of major angiogenic factors via CD44, CD74, and MAPK signaling pathways. *The Journal of clinical endocrinology and metabolism*, 95(12), pp.E403–12.

Vollmar, B. & Menger, M.D., 2009. The hepatic microcirculation: mechanistic contributions and therapeutic targets in liver injury and repair. *Physiological Reviews*, 89(4), pp.1269–1339.

Wang, Q. et al., 2002. CD44 deficiency leads to enhanced neutrophil migration and lung injury in Escherichia coli pneumonia in mice. *The American journal of pathology*, 161(6), pp.2219–2228.

Wasmuth, H. & Heinrichs, D., 2017. Macrophage migration inhibitory factor (MIF) exerts antifibrotic effects in experimental liver fibrosis via CD74. pp.1–6.

Weber, G.F. et al., 1996. Receptor-ligand interaction between CD44 and osteopontin (Eta-1). *Science (New York, N.Y.)*, 271(5248), pp.509–512.

Weiskirchen, R. & Gressner, A.M., 2018. Isolation and Culture of Hepatic Stellate Cells. pp.1–15.

Winau, F. et al., 2007. Ito Cells Are Liver-Resident Antigen-Presenting Cells for Activating T Cell Responses. *Immunity*, 26(1), pp.117–129.

Wu, P.-T. et al., 2019. Inhibition of CD44 induces apoptosis, inflammation, and matrix metalloproteinase expression in tendinopathy. *Journal of Biological Chemistry*, 294(52), pp.20177–20184.

Xu, Y. et al., 2020. <p>Activated Hepatic Stellate Cells (HSCs) Exert Immunosuppressive Effects in Hepatocellular Carcinoma by Producing Complement C3. *OncoTargets and Therapy*, Volume 13, pp.1497–1505.

Yaddanapudi, K., Mitchell, R. & Rendon, B., 2016. MIF Is Necessary for Late-Stage Melanoma Patient MDSC Immune Suppression and Differentiation. pp.1–13.

Yang, H.-R. et al., 2009. Mechanistic insights into immunomodulation by hepatic stellate cells in mice: a critical role of interferon-gamma signaling. *Hepatology*, 50(6), pp.1981–1991.

Yang, J. et al., 2018. Calcium-Binding Proteins S100A8 and S100A9: Investigation of Their Immune Regulatory Effect in Myeloid Cells. *International Journal of Molecular Sciences*, 19(7).

Yang, Z. et al., 2010. Mast cells mobilize myeloid-derived suppressor cells and Treg cells in tumor microenvironment via IL-17 pathway in murine hepatocarcinoma model. *PLOS ONE*, 5(1), p.e8922.

Yoo, S.-A. et al., 2016. MIFallele-dependent regulation of the MIF coreceptor CD44 and role in rheumatoid arthritis. *Proceedings of the National Academy of Sciences*, 113(49), pp.E7917–E7926.

Zhao, W. et al., 2011. Activated hepatic stellate cells promote hepatocellular carcinoma development in immunocompetent mice. *International Journal of Cancer*, 129(11), pp.2651–2661.

Zhao, W. et al., 2013. Hepatic stellate cells promote tumor progression by enhancement of immunosuppressive cells in an orthotopic liver tumor mouse model. 94(2), pp.0–0.

Zhao, Yang et al., 2015. Phenotype, development, and biological function of myeloid-derived suppressor cells. *OncoImmunology*, 5(2), pp.e1004983–12.

Zhao, Yunlong et al., 2019. PD-L1:CD80 Cis-Heterodimer Triggers the Co-stimulatory Receptor CD28 While Repressing the Inhibitory PD-1 and CTLA-4 Pathways. *Immunity*, 51(6), pp.1059–1073.e9.

7 ABBREVIATIONS

Arg – Arginase 1
AFLD – Alcoholic fatty liver disease
BDL – Bile Duct Ligation
BMC – Bone Marrow Cells
CCL – CC Chemokine Ligand
CCl4 - Carbon tetrachloride
CCR – CC Chemokine Receptor
CD – Cluster of Differentiation, e.g. CD44
CFSE - Carboxyfluorescein Succinimidyl Ester
cMoP common monocyte progenitors
CMP – Common myeloid progenitors
COX2 – Cyclooxygenase-2
D1/D2/Dx – Day 1, Day 2, Day x
DAMPs - Damage-associated molecular Patterns
DC – Dendritic Cells
DCSIGN - Dendritic cell–specific intercellular adhesion molecule-3-grabbing non integrin
ECM – Extra Cellular Matrix
EDTA - Ethylenediaminetetraacetic Acid
EGFR - Epidermal growth factor receptor
EGTA - Ethylene glycol-bis(β-aminoethyl ether)-N,N,N′,N′-tetraacetic acid
FACS – Fluorescence-Activated Cell Sorting
FCS – Fetal Calf Serum
G-CSF – Granulocyte Colony-Stimulating Factor
GAPDH – Glyceraldehyde 3-Phosphate Dehydrogenase
GBSS - Gey's Balanced Salt Solution
GFP – Green Fluorescent Protein
GM-CSF – Granulocyte-Macrophage Colony-Stimulating Factor
gMDSC – Granulocytic Myeloid-Derived Suppressor Cell, equals PMN-MDSC
H-gMDSC - gMDSC generated in wildtype HSC presence
H-mMDSC – mMDSC generated in HSC presence
HBV – Hepatitis B Virus

HCC - Hepatocellular Carcinoma

HCV – Hepatitis C Virus

HGF – Hepatocyte Growth Factor

HKO-MDSC – g-/mMDSC generated in presence of CD44 Knockout HSC

HLA – Human Leukocyte Antigen

HMGB1 - High Mobility Group Protein B1

HSC – Hepatic Stellate Cells

huCD44-Fc – Human recombinant CD44 on Fc Fragment of IgG

huIgG1-Fc - Human IgG1 Fc Fragment

IDO – Indoleamine 2,3-Dioxygenase

IFNγ – Interferon gamma

IL – Interleukin, e.g.: IL-1β – Interleukin-1 beta

IMDM Medium - Iscove's Modified Dulbecco's Medium

iMDSC – immature Myeloid-Derived Suppressor Cell

iNOS - Inducible Nitric Synthase

IRF – Interferon Regulatory Factor

IVC – Inferior Vena Cava

KC – Kupffer Cell

KO – Knock Out

LCK - lymphocyte-specific protein tyrosine kinase

Lin – Lineage

LPS - Lipopolysaccharide

LSEC – Liver Sinusoidal Endothelial Cells

M-CSF – Macrophage Colony-Stimulating Factor

MACS – Magnetic-Activated Cell Sorting

MASH - Metabolic Dysfunction-associated Steatohepatitis

MDSC – Myeloid-Derived Suppressor Cells

MHC – Major Histocompatibility Complex

MIF - Macrophage Migration Inhibitory Factor

mMDSC – monocytic Myeloid-Derived Suppressor Cell, equals M-MDSC

MMP – Matrix Metalloproteinase

MØ - Macrophages

mRNA – Messenger Ribonucleic acid

NAFLD – Non-Alcoholic Fatty Liver Disease

NF-kB - Nuclear factor kappa-light-chain-enhancer of activated B cells

NK – Natural Killer cells

NKT – Natural Killer T Cell

NO - Nitric Oxide

NOX2 - NADPH Oxidase

PAMPs - Pathogen-associated molecular pattern

PBMC – Peripheral Blood Mononuclear Cells

PBS - Phosphate-buffered saline

PD-1 – Programmed Death-1

PD-L1 – Programmed Death Ligand-1

PDGF – Platelet-Derived Growth Factor

PGE2 - Prostaglandin E2

qRT-PCR - Quantitative reverse transcription polymerase chain reaction

ROS - Reactive oxygen species

RPMI – Roswell Park Memorial Institute medium

STAT3 – Signal Transducer and Activator of Transcription 3

STAT5 – Signal Transducer and Activator of Transcription 5

TCR – T Cell Receptor

TGF-β – Transforming Growth Factor Beta

TLR – Toll-Like Receptor

TNFα – Tumor necrosis Factor alpha

Treg – T regulatory Cells

Th17 – T helper 17 cells

vCD44 – Variant Isoform of CD44

VEGF – Vascular Endothelial Growth Factor

8 LIST OF ILLUSTRATIONS & FIGURES

9 LIST OF TABLES

10 PUBLICATIONS

Journal Article:

Julia Hagenstein, Simon Burkhardt, Paulina Sprezyna, Elena Tasika, Gisa Tiegs, Linda Diehl. CD44 expression on murine hepatic stellate cells promotes the induction of monocytic and polymorphonuclear myeloid-derived suppressor cells.
In: Journal of Leukocyte Biology, 2024 Jun 28;116(1):177-185.
doi: 10.1093/jleuko/qiae053.

11 DECLARATION OF OWN CONTRIBUTION

This work was prepared during my research work at the Institute of Experimental Immunology and Hepatology of University Medical Center Hamburg-Eppendorf within the framework of the Graduate School of Collaborative Research Center SFB841. This thesis represents an original and independent scientific contribution. The conception of the project and the planning of the experiments were carried out in close consultation with my doctoral supervisor Prof. Linda Diehl, PhD.
Within this framework, I independently refined the research questions and developed the experimental approaches. The execution of the experimental work was largely my own responsibility and included the cultivation and treatment of human and murine cells, the performance of flow cytometry analyses and cell sorting, the execution and evaluation of quantitative real-time PCR, providing microscopic analyses, the documentation of experimental results and the analysis of the experimental data. For specific experimental steps, particularly the execution of extensive PCR experiments, I received technical assistance from medical-technical assistants. However, the responsibility for the design, execution, and interpretation of these experiments remained with me. The statistical evaluation of the data as well as the preparation of figures and tables were conducted independently. The writing of the dissertation, including the scientific discussion and contextualization of the results, was also

completed entirely under my own responsibility, which was subsequently reviewed by my doctoral supervisor.
In summary, my contribution comprises the conception of the main research questions together with Prof. Linda Diehl, the independent execution of the majority of the experimental work, the collection and analysis of the data, and the complete authorship of the dissertation. Contributions from others were limited to technical support in selected experimental steps and academic supervision provided by my doctoral supervisor within the usual scope of doctoral training.

12 EIDESSTATTLICHE VERSICHERUNG

Ich versichere ausdrücklich, dass ich die Arbeit selbständig und ohne fremde Hilfe, insbesondere ohne entgeltliche Hilfe von Vermittlungs- und Beratungsdiensten, verfasst, andere als die von mir angegebenen Quellen und Hilfsmittel nicht benutzt und die aus den benutzten Werken wörtlich oder inhaltlich entnommenen Stellen einzeln nach Ausgabe (Auflage und Jahr des Erscheinens), Band und Seite des benutzten Werkes kenntlich gemacht habe. Das gilt insbesondere auch für alle Informationen aus Internetquellen. Soweit beim Verfassen der Dissertation KI-basierte Tools („Chatbots“) verwendet wurden, versichere ich ausdrücklich, den daraus generierten Anteil deutlich kenntlich gemacht zu haben. Die „Stellungnahme des Präsidiums der Deutschen Forschungsgemeinschaft (DFG) zum Einfluss generativer Modelle für die Text- und Bilderstellung auf die Wissenschaften und das Förderhandeln der DFG“ aus September 2023 wurde dabei beachtet. Ferner versichere ich, dass ich die Dissertation bisher nicht einem Fachvertreter an einer anderen Hochschule zur Überprüfung vorgelegt oder mich anderweitig um Zulassung zur Promotion beworben habe. Ich erkläre mich damit einverstanden, dass meine Dissertation vom Dekanat der Medizinischen Fakultät mit einer gängigen Software zur Erkennung von Plagiaten überprüft werden kann.

13 ACKNOWLEDGMENTS

First and foremost, I would like to sincerely thank my doctoral supervisor, Prof. Dr. rer. nat. Linda Diehl, for giving me the opportunity to work and finally complete this thesis. This work would not have been possible without you and your unwavering support over the years through highs and lows.

I would also like express my gratitude to Prof. Dr. Gisa Tiegs for the opportunity to benefit from the valuable scientific guidance within the framework of the graduate program of SFB841 at the Institute of Experimental Immunology and Hepatology, University Medical Center Hamburg-Eppendorf.

Thanks to my lab peers for the shared stress, fun and making my lab time a time I will always miss. We laughed, we cried, we contaminated cell cultures and PCRs together - repeatedly.

I also would like to thank everyone who contributed to this thesis - either by offering advice, encouragement, or drying tears (both real and metaphorical). Especially to my friends and family - for their endless support and for always asking, "How's the thesis going?" even when the answer until today never changed. I'm genuinely looking forward to all the new questions you'll ask now that this one is finally answered.

And finally, I dedicate this work to future me - who hopefully won't read this and wonder what on earth they were thinking. But if you do: we made it! Eventually.